FREEZING PHYCOMYCES SPORANGIOPHORES IN SUPERFLUID HELIUM FOR ULTRASTRUCTURE STUDIES

Thesis by

Patricia Virginia Burke

In Partial Fulfillment of the Requirements

For the Degree of

Doctor of Philosophy

California Institute of Technology

Pasadena, California

1971

(Submitted August 17, 1970)

for Bill and Daddy Max

ACKNOWLEDGMENTS

First I wish to thank the Biology, Physics, and Aeronautics Departments for making such an interdisciplinary thesis possible.

Anthonie van Harreveld and Sudarshan Malhotra first introduced me to freeze-substitution. Oscar Kreutziger (Univ. of Calif. Berkeley) did the same for freeze-etching. Marko Zalokar taught me several things. Pat Koen and Josephine Pagano helped me with the technical details of electron microscopy and supplied materials when necessary.

The Low Temperature Physics Laboratory has provided me with office and laboratory space as well as equipment and fellow students to commiserate with while we were learning to be good plumbers. The advice and ideas of David Goodstein, Gene Gregory, John Andelin, Walter Ogier, Harris Notarys, James Mercereau, Steve Rockwood, John Wallace, and Ed Kelm have been valuable. Without the able technical assistance of Ed Boud, Sandy Santantonio, and Fred Wild, the apparatus used in these experiments would never have been designed or built. I've learned a lot from them.

Keith Matthews was always full of good ideas, even if I did waste too much time talking to him. I thank Don Skelton and the Freshman Physics Laboratory for good times, enjoyable students, and equipment to run my experiments. Jim Campbell of Electrical Engineering also supplied equipment and ideas. Bill Burke did most of the photography and drew most of the figures in this thesis.

Tom Harvey was ever present with interesting lecture demonstrations to amuse my husband, equipment, photographic assistance, and free meals. Dave Vail taught me the difference between a lathe and a mill, as well as how to use them.

The Fluid Mechanics Laboratory loaned me a vacuum evaporator and provided immediate assistance in setting it up. Gene Broadwell taught me how to make carbon film thermometers and a great deal about heat transfer. Hans Liepmann and Anatol Roshko provided some very enlightening discussions of this problem. Paul Demotakis and Garry Brown designed the overpressure flange.

I thank my fellow phycomycologists: Bill Goodell, Ken Foster, Igor Gamow, Ken Zankel, and Patty Reau and our able assistants Bertha Jones and Jeannette Navest for discussions, coffee, and birthday parties.

Ray Owen has come to my rescue many times. He also introduced me to Max.

I thank Max, Manny, Tobi, and Ludina for an enjoyable and sometimes exciting year.

The Physics Department and the Biology Division provided financial assistance through Graduate Teaching Assistantships and the USPHS Training Grant.

I would like to thank Barbara Sloan for assuring and reassuring me that somehow I would get this thesis written and she would get it typed. She and Max also corrected the spelling.

Finally, I would like to thank Max Delbrück for unstinting labor on this thesis. Ken Zankel once told me that Max really starts to teach when you start to write. It's true and the writing has been enlightening as well as hectic.

ABSTRACT

Knowledge of the ultrastructure of the growing zone of Phycomyces sporangiophores is a desirable adjunct to studies of their sensory physiology. This includes discovery of the type of organelles present and their spatial arrangement. Chemical fixation preserves some of the cell's organelles satisfactorily, but considerable disruption and dislocation occur. Physical fixation by freezing should preserve the spatial distribution of organelles within the cell if the freezing is rapid enough to prevent ice crystal formation. Ice crystal inhibitors do not penetrate the cell satisfactorily, so that crystal size is determined only by the freezing rate.

Liquid He II exhibits a quantum mechanical mechanism of heat transfer which is much more efficient than the normal, classical heat conduction in fluid. The heat transfer rate is qualitatively described by the Landau equations for liquid He II with additional terms (Gorter-Mellink mutual friction) to account for frictional forces within the liquid. For the case of a cylindrical heater, the maximum steady state heat transfer rate before film boiling occurs depends on the depth of the heater below the liquid surface (hydrostatic head), the pressure of the gas above the liquid, and the liquid temperature. For a gas pressure of 20 Torr or more in excess of the equilibrium vapor pressure, the appearance of the film boiling changes from a uniform gas film to a fine haze, presumably of tiny gas bubbles. If He^4 gas is used to pressurize the liquid, the temperature of

the liquid He bath rises to about 2 K and a layer of liquid He I forms at the gas-liquid interface. This layer of the He I grows at the expense of the bulk He II as heat is supplied by the warm gas. The phase boundary between the two liquid phases moves down through the liquid at about 5 cm/min. The conditions for optimal heat transfer occur immediately after the pressure increase. These conditions are a pressure excess of 20 Torr or more and a bath temperature of 1.9 - 2 K.

Sporangiophores are suspended by an iron filing from an electromagnet in a special chamber (room temperature) above a helium cryostat. As soon as the pressure excess in the cryostat exceeds 20-60 Torr they are released and fall freely into the superfluid helium through a tube of heated gas. The sporangiophores are collected in a plastic beaker at the bottom of the cryostat and transferred to a liquid nitrogen storage dewar. Frozen sporangiophores are prepared for electron microscopy using freeze-substitution and freeze-fracture techniques.

The thin sections and the freeze-fracture replicas show extensive ice crystal damage to stage IV sporangiophores which have a large central vacuole. Ice crystal damage is considerably less in stage I sporangiophores which have a much smaller vacuole. Presumably, the vacuole is responsible for the poor preservation of the ultrastructure.

TABLE OF CONTENTS

Chapter 1

Introduction

Chapter 2

Helium Experiments

Page

Page

Chapter 4

Concluding Remarks

Appendix

Chapter 1

INTRODUCTION

Phycomyces is a model system for sensory physiology (Bergman et al., 1969). A molecular description of the processes involved requires knowledge of the structures involved and their interrelationships. Electron microscopy can give this information. Previous work using chemical fixation preserved the various standard organelles well enough but disrupted the endoplasmic reticulum and destroyed the spatial relationships of the organelles. It has not shown any structures that might suggest a mechanism for the striking protoplasmic streaming or for the reception of light.

The problem is slow penetration into the cell of the chemicals used for fixation. One method of circumventing this is to fix the plant physically by freezing. If the cooling is fast enough, disruptive ice crystallization may be prevented or at least controlled. Such a method is used here. The coolant is liquid helium II, the so-called superfluid helium. This fluid has two mechanisms of heat transfer: conduction by diffusion and an unique, wavelike propagation of heat. The second mechanism makes superfluid helium the best thermal conductor known, however it is not easily utilized when large heat fluxes are required (of the order of 1 to 10 watts/cm^2).

The sporangiophore.

The giant sporangiophore (spph) of the fungus Phycomyces is shown in figure 1. The development of the spph is usually divided into five stages (Castle, 1942) of which only stages I and IV have

been used in these studies. The stage I spph grows up from the fungus' mycelium as a simple pointed tube. During stages II and III growth ceases and the sporangium is formed. Elongation begins again with stage IVa and its rate becomes constant in stage IVb. Both stage I and stage IV are light sensitive and have been studied extensively (Bergman et. al., 1969).

Figure 2 shows a longitudinal section of the top of a stage IV spph. The spph cell wall is about 0.6 μ thick and consists of a network of chitin micro-fibrils in a matrix of uncertain composition (Kreger, 1954). The wall of a stage I spph has a layer of randomly oriented microfibrils in the growing zone and below the growing zone an inner one in which most of the fibrils are transversely oriented (Frey-Wyssling and Muhlethaler, 1950). A membrane, the plasmalemma, separates the cytoplasm from the cell wall. Small, membranous vesicles resembling lomasomes (Moore and McAlear, 1961) occur between the plasmalemma and the cell wall (Thornton, 1966; Peat and Banbury, 1967; S. K. Malhotra unpublished). In a few sections an intriguing structure has been seen: a multifolded membranous structure resembling retinal rods, just inside the plasmalemma (Bergman et. al., 1969). The cytoplasm contains numerous nuclei, mitochondria, lipid droplets, glycogen granules, and other particles. There are bundles of endoplasmic reticulum and various other membranous vesicles in the growing zone of the spph (all growth occurs in this region of the spph which extends for 2 to 3 mm below the sporangium). Near the top of the vacuole, there are many vesicles, each containing regular cytoplasmic

constituents in various stages of disintegration. These vesicles, which presumably gradually merge with the vacuole, have been termed autophagic vesicles by Thornton (1968). The vacuole contains proteinaceous crystals, possibly a flavoprotein (Wolken, 1969), and cellular debris. It also contains an almost saturated solution of gallic acid (Dennison, 1959). The vacuole is surrounded by a membrane, the tonoplast. This membrane must be continuous in vivo but is frequently broken in electron micrographs (Thornton, 1966; Malhotra unpublished).

Fixation procedures.

Chemical fixation is hindered by the slow perfusion of fixatives through the cuticle and cell wall, and by a large, watery vacuole which is inherently unfixable and may interfere with the fixation of the cytoplasm. If this vacuole breaks before fixation is complete, the acid solution within the vacuole is released into the cytoplasm (McLean, 1960). This acid may destroy various cytoplasmic organelles or at least disrupt and rearrange them. If the spph is observed with a light microscope during fixation, considerable disruption and dislocation are seen. Microtubules and membranes may be especially susceptible to this disruption.

Thus very few microtubules or microfibrils have been seen (Thornton, 1966) -- an unlikely result if the streaming is mediated by the action of such organelles. The endoplasmic reticulum of

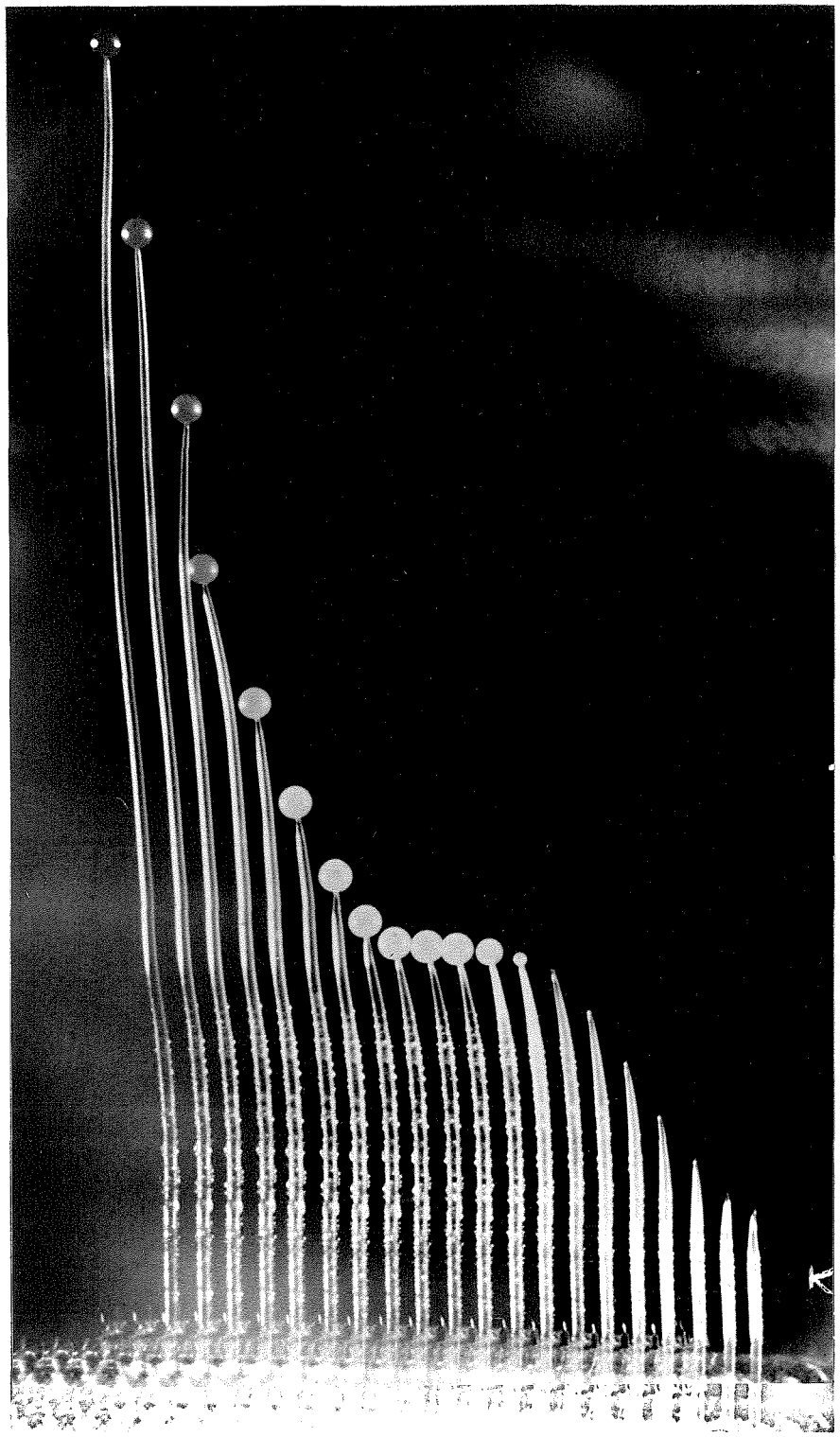

FIGURE 1. Stages of development of sporangiophores. Photographs of the same sporangiophore taken at 1 hour intervals. The sporangium is about .5 mm in diameter (Photo - Lois Edgar).

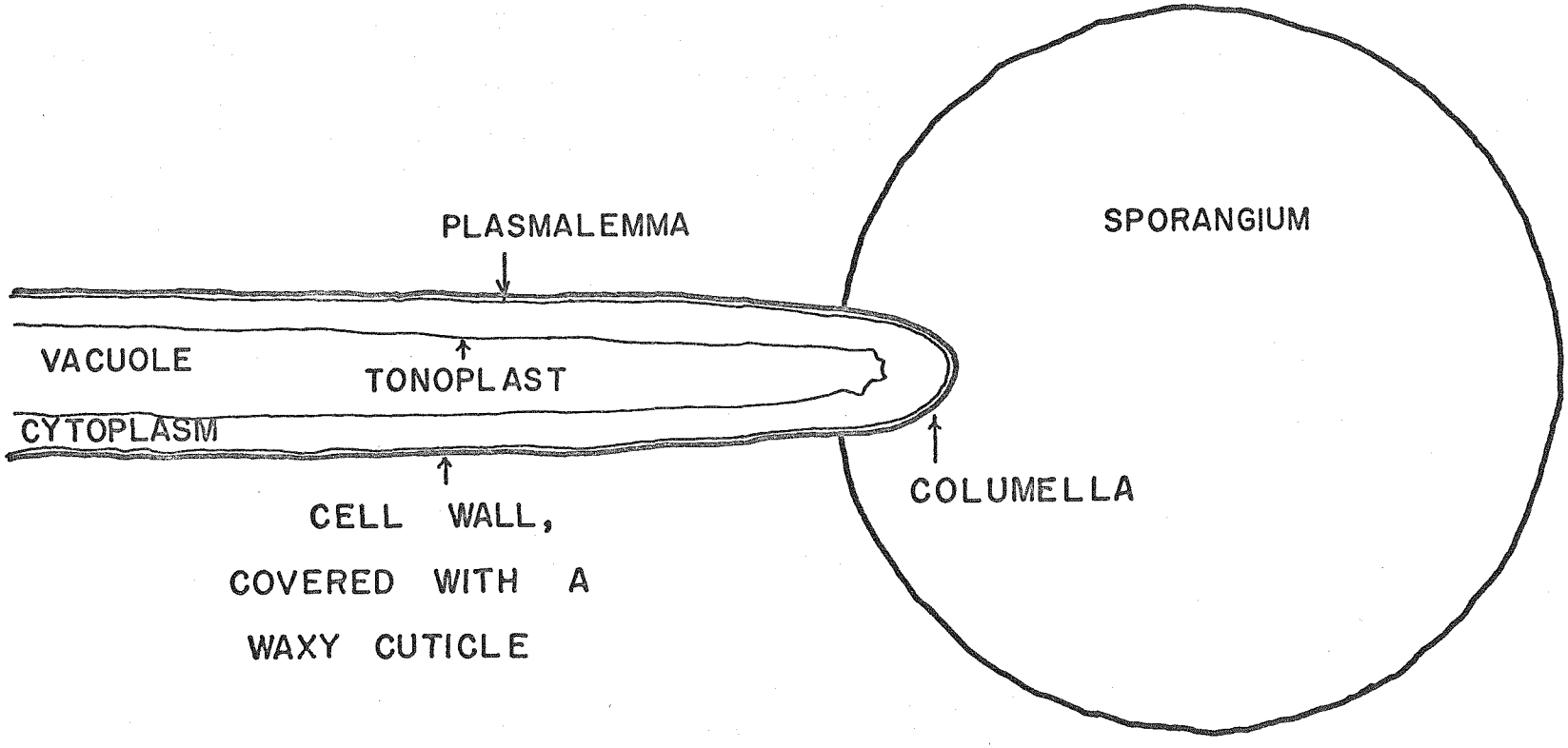

FIGURE 2. Longitudinal section of the apical end of a stage IV spph.

chemically fixed spphs takes on a disorganized appearance with many "pan scrubbers" and small vacuoles (Peat and Banbury, 1967). Further, the growing zone of stage IV spphs tends to collapse during the embedding procedure (Thornton, 1966).

Rapid freezing should not have these difficulties. It may preserve the spatial relationships between organelles for electron microscopic observation, and the morphology observed after freeze-fixation may be compared with that observed after chemical fixation.

Freezing was first used for thin sectioning in electron microscopy in the days before ultrathin sectioning was developed (Fernandez-Moran, 1950). It was abandoned with the advent of good ultramicrotomes and plastic embedding. Freeze-drying before embedding was then used by Sjøstrand and Baker (1958) as a check on the chemical methods. However, delicate structures tend to collapse in freeze-dried material during penetration of the plastic. Also, serious drying artifacts may occur if the Anderson critical point drying method is not used (Anderson, 1951). Freeze-substitution was developed to circumvent the problems of strong forces at the solid-gas interface (Fernandez-Moran, 1957). This is a low-temperature, dehydration technique in which an organic liquid is substituted for solid water within the frozen tissue. Here too the best results are obtained if the material is chemically fixed before embedding in plastic. There are still problems at the solid-liquid interface with its strong concentration gradients of water and organic solvent.

Finally, freeze-etching (Steere, 1957; Moor et. al.,1961) has been applied to biological specimens. This is a metal replica technique in which the replica is made of a frozen, fractured surface, after the material to be replicated has had some of its surface water removed by evaporation (the etching part of the procedure). This technique is complementary to the regular chemical ones and in some cases, where the freezing process is not lethal, should yield micrographs which correspond to the living structure.

Freezing procedures, boiling, and ice crystals.

In any of these techniques, adequate preservation for electron microscopy depends on the initial freezing. If a liquid coolant boils, an insulating gas film forms around the specimen. Such a film protects the specimen from the cold liquid and prevents rapid cooling. Since ice crystals will form and begin to grow as soon as the specimen temperature passes 0 C, cooling must be rapid to limit their growth and prevent dehydration and deformation of the cells. If the specimen is cooled at 100-1000 C/sec, numerous small ice crystals form which make the cells unsuitable for electron microscopy. If the cooling is very rapid (more than 10,000 C/sec) any ice crystals formed will be very small and should not interfere with electron microscopic observation. Many coolants have been used in attempts to freeze tissues very rapidly. The standard methods of rapid freezing include:

propane cooled with liquid nitrogen

isopentane cooled with liquid nitrogen

Freon 12 cooled with liquid nitrogen

solid nitrogen - liquid nitrogen slushes

brass or silver blocks cooled with liquid nitrogen.

The liquid hydrocarbons have large specific heats and large latent heats and may be cooled with liquid nitrogen to more than 100 degrees below their natural boiling points. Thus they can absorb a large amount of heat without boiling. Propane has been the most satisfactory of these coolants, presumably because it can be cooled more than the others (Propane freezes at 83 K; nitrogen boils at 77 K).

Nitrogen slushes (63 K) form only 14 K below liquid nitrogen's boiling point so they boil more easily than the hydrocarbons; however, the lower temperature of such slushes (63 K as opposed to about 120 K for the liquid hydrocarbons) favors stable glass formation (glassy water within the cell should be less destructive than small ice crystals).

The metal blocks have slightly more heat capacity per cc than the liquids and very much better thermal conductivity, so that they may be expected to cool specimens more efficiently. Their major drawback is deformation of the surface layer of cells from impact on the metal surface.

Slower methods of freezing which are satisfactory for storage but unsuitable for electron microscopy include:

liquid nitrogen

dry ice

various refrigerators.

In some cases the specimen is cooled to about -0.5 C and crystallization of the water is initiated in the extracellular spaces before cooling in a cryogen. This procedure dehydrates the cells and crystallizes the water outside the cells before they are put in the cryogen for storage.

In most cases the specimen is pretreated with a so-called cryoprotective agent - an ice crystal inhibitor. This may be: glycerol, ethylene glycol, propylene glycol, dimethylsulfoxide, or partial dehydration. This pretreatment does not work with Phycomyces spphs.

In a few cases chemical fixation has been used as an additional pretreatment. In such cases freezing is not used as the primary fixative but to obtain additional information with freeze-etching. More often chemical fixation is part of the post-freezing treatment (freeze-drying or freeze-substitution). A truly independent check on the results of chemical fixation requires a technique which avoids chemistry. Freeze-etching without any pre- or post-treatment offers this possibility. Usually this is not attempted. Historically the best results (lack of ice crystals) have been achieved with pretreatment which puts much less stringent requirements on the rate of freezing.

Early results of freeze-fixation.

Liquid helium II was first used as a fixative by Fernandez-Moran in 1959. Apparently most of his samples were pretreated with up to 60% glycerol. Preservation was said to be better than that obtained with liquid nitrogen and liquid nitrogen - freon coolants and to be independent of the pretreatment, but no convincing evidence has been presented. The freezing was done in 1 K liquid helium II which turns out to be a poor temperature choice for rapid freezing (see parts I and II) although convenient experimentally. Preparation for electron microscopy was by substitution and plastic embedment at temperatures between -120 and -30 C. Bullivant (1960, 1962) used this same basic freezing technique to prepare sections of mouse pancreas and retinal rods. He found it necessary to blow the tissue into the liquid to prevent slow freezing in the gas above the cryogen (van Harreveld, personal communication). Preparation for electron microscopy was by substitution for two weeks at -75 C followed by embedment at temperatures between -75 and -5 C. The preservation was comparable to that of glycerinated material frozen in propane at 98 K (-175 C).

Unfortunately, good preservation of frozen specimens is usually confined to the surface of the tissue block. This region is of the order of 10 microns thick regardless of the rapid freezing method employed. The remainder of the specimen shows more or less obvious ice crystal damage (Fernandez-Moran, 1959; Bullivant, 1960; van Harreveld and Crowell, 1964; Zalokar, 1966; Luyet and Menz, 1961;

Pease, 1967). This problem is not confined to untreated tissues but occurs in glycerinated ones as well, although the problem is less acute. Presumably it is related to the thermal conductivity of the tissue and the structure of the water in the cells.

Crystallization and the glassy state.

While very little is known about ice crystal formation and growth during rapid freezing of tissue, something is known about crystal formation and growth for pure water and its simple solutions.

If a liquid is cooled below its melting point, crystal growth occurs at a finite rate from a finite number of centers (nuclei). The critical size required for the formation of a stable crystal nucleus decreases rapidly with temperature. For water the probability of forming such a nucleus is very small near 0 C but increases exponentially as the temperature is decreased. This explains the supercooling of pure water to -35 to - 40 C. Once a nucleus is formed, crystal growth depends on diffusion to the crystal surface (viscosity limited) and rearrangement into the crystal lattice (limited by the ratio of bond strength to kT). Any foreign matter present may provide crystallization nuclei or restrict the mobility of the water molecules or both. If the liquid is cooled sufficiently rapidly, further rearrangement may not be possible and the liquid will form a glass.

Shepley and Bestul (1963) have discussed the glass transformation and its characteristic temperature as follows:

"A glass transformation temperature may be defined as a temperature below which a noncrystalline substance below its melting point no longer exists as an equilibrium supercooled liquid. Between T_g and the melting point a supercooled liquid is in equilibrium with respect to alternate liquidlike states, though not of course, in general, with respect to the crystalline state. At such temperatures the crystal has a still lower free energy, and is the ultimate equilibrium physical state. If a substance does not crystallize on cooling to such temperatures it must be because of prohibitive crystallization kinetics or cooling procedures. On cooling below T_g an uncrystallized substance departs from supercooled liquid equilibrium. This is thought to be because at such temperatures the removal of energy from a system to effect cooling on any ordinary time scale does not allow sufficient time for the equilibrium redistribution of the remaining energy over all degrees of freedom.

The distinction between the equilibrium supercooled liquid and the glass is thus based on kinetics. Nevertheless, even though T_g is not inherently a uniquely defined quantity ..... [it is] useful to indicate the general location of a glass transformation."

The glassy state of water.

In the case of water, on the one hand the viscosity is extremely low (glasses have viscosities of the order of 10^{13} poise) and the melting point is anomalously high. (If one extrapolates from similar hydrides one expects T_{fusion} = 170 K and $T_{boiling}$ = 190 K.) Both the low viscosity and the high melting point favor rapid crystal growth. On the other hand the water structure, with many hydrogen bonds, favors glass formation, thus stable glasses have been formed when the freezing point is reduced by making binary mixtures (with H_2O_2, LiCl, HCl, H_3PO_4, ethanol, glycerol).

The glass of pure water can be made by depositing water vapor on a cold surface (temperature less than 113 K). Such glasses have been studied using X-ray diffraction and differential thermal analysis.

Upon warming, this glass transforms irreversibly to ice Ic (the cubic form of ice I) at about 134 K (130 - 145 K) and gives off a small quantity of heat. There is some variation in the numbers quoted in the literature and T_g has not been observed, apparently because the glass is extremely unstable and T_g is very close to the crystallization temperature for ice Ic (near 140 K).

Glass formation of water in tissues.

Although vitreous water, formed by cooling bulk water samples, has only been reported in two cases (Pryde and Jones, 1952, and Staronka, 1939; not reproducible), several calculations have been made of the cooling rates necessary for its formation in tissue.

Stephenson (1956) froze pieces of guinea pig liver in liquid propane at 120 K. He found that the nucleation rate was higher than that for water, but that T_g was also higher (about 170 K). He estimated the critical cooling velocity for glass formation to be 5000 K/sec (or that the temperature of the sample must be lowered below 170 K within 20 msec). This estimate comes from cooling curves of pieces of guinea pig tissue and from calculations of crystallization rates in water assuming that a glass phase can be formed around 170 K (-100 C). The sample must be sufficiently small that any temperature gradients within the sample are negligible and do not limit the heat transfer.

Menz and Luyet (1961), too, has estimated the necessary cooling rates. He froze single muscle fibers in propane at 120 K. Such fibers

show good preservation and lack of ice crystals for the first micron beneath the surface. Similar limits for good preservation have been found by others, notably van Harreveld and Crowell (1964) and Bullivant (1962). This limit may be imposed by the thermal conductivity of the tissue.

Bullivant (1965) and Rebhun (1965) have measured cooling rates for thermocouples embedded in copper or stainless steel. They find that propane cooled with liquid nitrogen is the best of the conventional coolants and that dT/dt is one or two thousand degrees per second. Van Harreveld has estimated the cooling time for the first 10μ of tissue specimens striking a cold silver mirror (temperature 66-77 K) as at least 8 msec.

We estimated conservatively that glass formation would occur or, at least, that the ice crystals formed would be very small (on the order of hundreds of Ångstroms) if a spph was cooled from room temperature to 77 K within 10 msec (compare the 20 msec time of Stephenson and the 8 msec or more of van Harreveld). This rate is equivalent to 20,000 K/sec. Since a spph contains 0.06 j/cm with a surface area of 0.03 cm^2/cm, this rate corresponds to 200 watts/cm^2 heat flux at the spph surface.

Superfluid helium as a coolant.

Superfluid helium is a unique fluid with remarkable heat transfer properties. If defined in conventional terms, its apparent thermal conductivity may be 1000 times larger than that of copper. Thus

liquid helium might be an ideal coolant for the preparation of specimens for electron microscopy. However a careful study of the properties of liquid helium is required to make use of this apparent thermal conductivity.

Liquid helium exists in two phases called helium I and helium II. Helium I is a conventional fluid, albeit somewhat unusual and gas-like. Helium II is a "quantum fluid," that is, the temperature is sufficiently low and the forces between molecules are of such a magnitude that the quantum mechanical effects of a system with Bose statistics dominate the behavior of this fluid.

The He^4 atom is a light spherically symmetric particle which obeys Bose-Einstein statistics. Because of its small mass, its "zero point energy" is large and because of its spherical symmetry, the attractive forces between atoms are very small. These effects conspire to yield the low density and gas-like nature of the liquid in general.

A non-interacting gas of Bose particles (liquid helium I is a strongly interacting system of Bose particles) undergoes a phase transition near 0 K in which some of the particles start to "condense" into the lowest energy state (ground state) of the system. At zero degrees Kelvin all the particles of a non-interacting Bose gas will occupy this same ground state. For non-interacting helium atoms the condensation temperature would be about 3 K at the density of liquid He^4. This is close to the λ temperature (T_λ = 2.17 K) at which the transition from liquid helium I to liquid helium II occurs

in the real fluid (see figure 3 for the phase diagram). These two phenomena are closely related, although the transition from He I to He II is not very well understood.

The two fluid model.

There exists another way to describe helium II which has led to a very successful set of phenomenological equations and explains a large number of the strange properties of the fluid. This approach was first developed by Landau (1941).

Liquid helium II near absolute zero may be thought of as a bulk system, "at rest" in the ground state, plus some thermal excitations. This model is analogous to the Debye theory of solids in which there is a crystal lattice and all thermal energy is localized in vibrations of the lattice, called phonons, which travel through the lattice. The energy spectrum of these thermal excitations (quasi-particles) is shown in figure 4. It contains two major types of excitations or quasi-particles: (1) the phonons ($\varepsilon = u_I p$, where u_I is the velocity of sound in the liquid), which have the same energy-momentum relationship as phonons in a crystal lattice and are associated with density fluctuations in the real fluid; (2) the rotons ($\varepsilon = \Delta + \frac{(p-p_o)^2}{2\mu}$, where Δ, p_o, and μ are experimentally measured constants), which were so named because originally they were thought to be associated with vortex motions in the real fluid.

Since there is a momentum flux associated with motions of these thermal quasi-particles, it is possible to assign a density

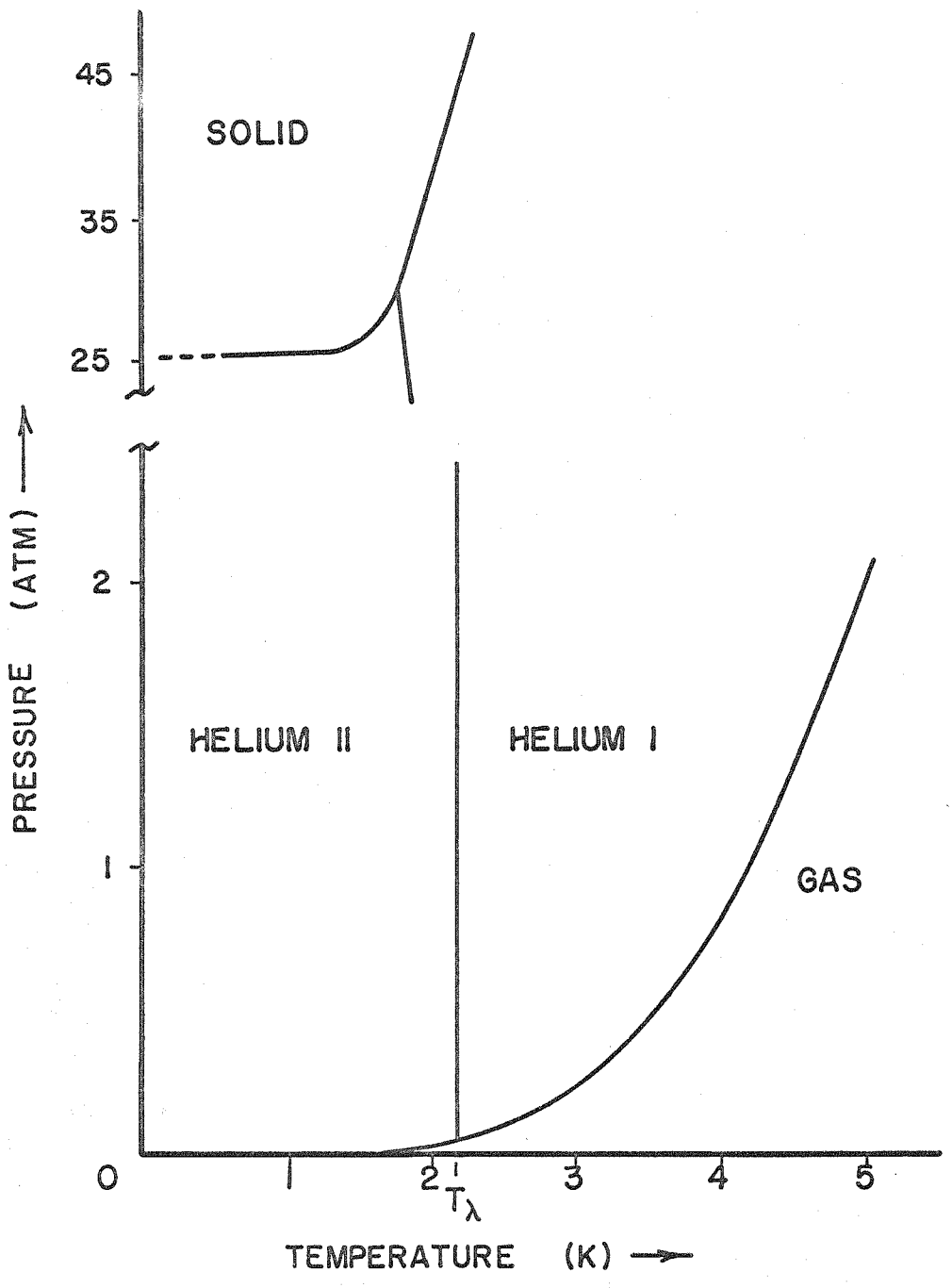

FIGURE 3. He^4 phase diagram.

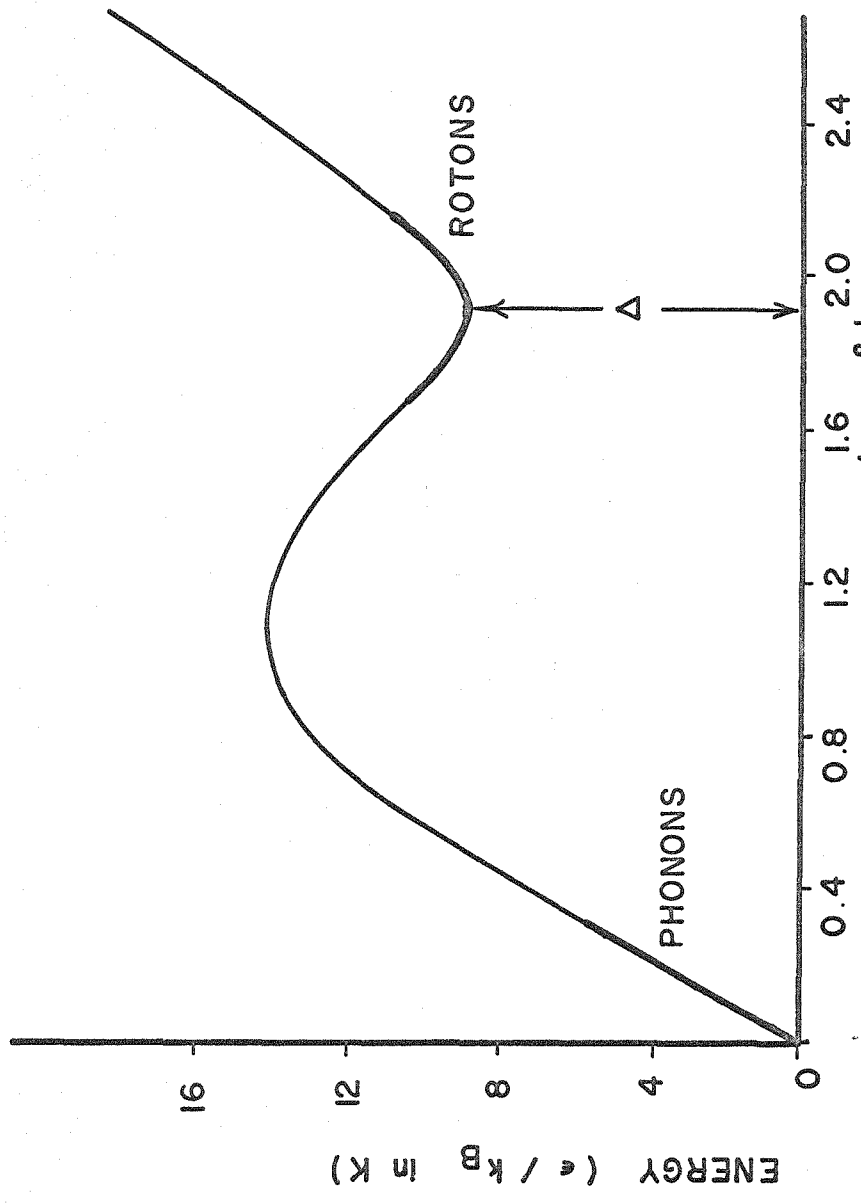

FIGURE 4. Landau's energy spectrum for excitations in helium II. Energy is measured in units of Boltzmann's constant, momentum in units of h.

and a velocity field to them. This is the "normal fluid" part of liquid helium II. This fluid has all the characteristics of a normal classical fluid (viscosity, entropy, thermal conductivity, etc.). The remainder of the liquid helium II is assigned to the "superfluid" part. It also has a density and a velocity field. Its characteristics are those of a perfect classical fluid because its viscosity and entropy are assumed to be zero in keeping with its association with the ground state of the fluid. The superfluid and the normal fluid are the components of the "two-fluid model" for liquid helium II. At low temperatures and low relative velocities ($\vec{v}_n - \vec{v}_s$) these two fluids are non-interacting and are coupled only through the total density

$$\rho = \rho_n + \rho_s \tag{1}$$

and the total mass flux of liquid helium II

$$\vec{j} = \rho_n \vec{v}_n + \rho_s \vec{v}_s \tag{2}$$

(Throughout the remainder of this thesis the subscripts n and s will refer to the normal and superfluid component of liquid helium II, respectively.)

The equations of the two-fluid model predict two types of wave motion. The first is a density (pressure) wave corresponding to ordinary sound because $\vec{v}_n \simeq \vec{v}_s$ and the two fluids oscillate together. The second is an entropy (temperature) wave called second sound, which can be thought of as a sound wave in the quasi-particle gas. In second sound there is no net mass flow ($\vec{j} = 0$)

and the two fluids flow through each other, the normal fluid carrying entropy, the superfluid not. This counter flow also occurs whenever there is a temperature gradient in the liquid. It is the special mechanism of heat transfer in He II and accounts for its amazing thermal conduction.

Experiments measuring heat transfer through liquid helium II in capillaries of diameter d give a heat current, $\vec{q}$, related to the temperature gradient as

$$\nabla T = \frac{-12\eta}{d^2(\rho S)^2 T}\vec{q} \qquad (3)$$

In this equation η is the normal fluid viscosity, ρ is the fluid density, and S is the entropy per gram of liquid (ρS is the entropy per unit volume). This relation holds at low relative velocities, $(\vec{v}_n - \vec{v}_s)$, and small temperature differences, ΔT. It is predicted by the two fluid model, and it would lead to enormous heat transfers at large values of ΔT. However, in larger capillaries or for $\Delta T > 10^{-2}$ K, a cubic term appears which limits the heat transfer,

$$\nabla T = \frac{-12\eta}{d^2(\rho S)^2 T}\, q - \frac{A(T)\rho_s\rho_n}{(\rho_s S T)^3}\, q^3 \qquad (4)$$

where A(T) is an empirical parameter called the Gorter-Mellink coefficient. This cubic term is attributed to dissipation caused by an interaction of the normal fluid and the superfluid (called "mutual friction"). It dominates the heat transfer from the spph to the liquid, and is responsible for the observed

maximum in the heat transfer around 1.9 - 2.0 K (see figure 6).

Source of the heat transfer limitation.

At low relative velocities $(\vec{v}_n - \vec{v}_s)$ there is not expected to be any interaction between the superfluid and the normal fluid because it is difficult to excite the superfluid. For example, thermal excitations may be created which increase the density of the normal fluid, but these thermal excitations are difficult to excite mechanically because the energy-momentum relationship must be satisfied for each thermal excitation created. This last idea is the source of the Landau explanation of superfluidity (Landau, 1941). He considered the excitation of phonons and rotons within pure superfluid flowing through a capillary. The fluid flowing in such a tube will slow down by exciting thermal motions in the liquid layer near the wall.

Consider helium flowing through a tube in a coordinate system where the liquid is at rest and the tube moves with velocity $\vec{v}$. The tube is constrained to move only in the direction of $\vec{v}$. If the relative motion creates in the liquid excitations of energy ε and momentum $\vec{p}$, the conservation of energy and momentum give

$$E_1 - E_2 = \Delta E_{tube} = \varepsilon \qquad (5)$$

$$P_1 - P_2 = \Delta P_{tube} \leqslant (p) \qquad (6)$$

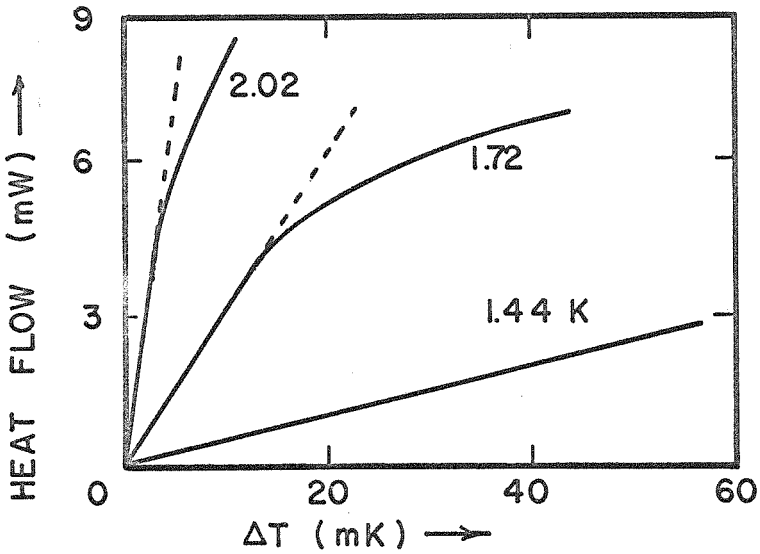

FIGURE 5. Heat flow through liquid helium II in a slit of width 2.4μ as a function of the temperature difference ΔT across the slit (Winkel, Groenou, and Gorter, 1955).

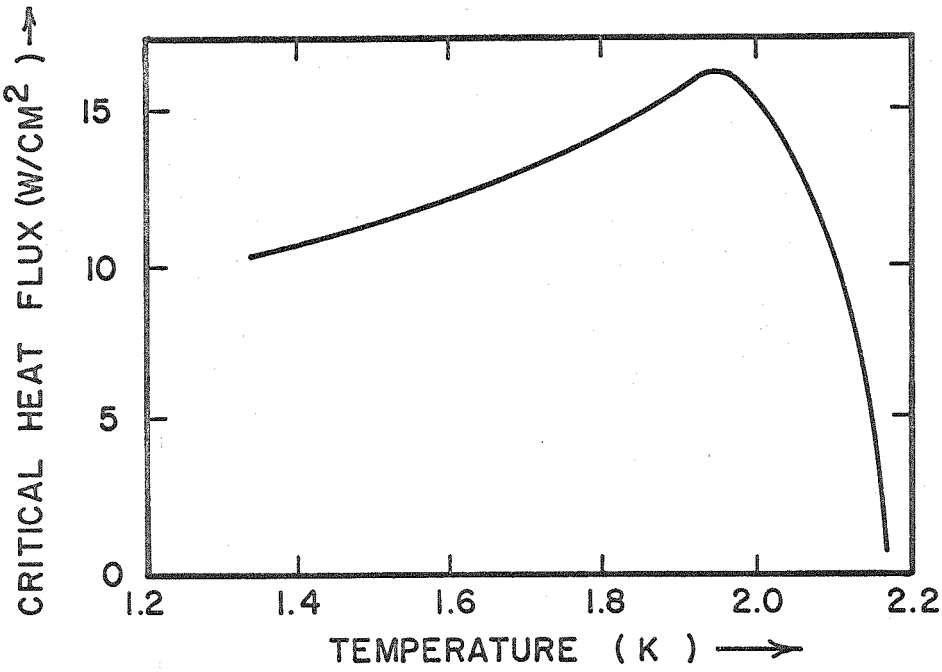

FIGURE 6. Maximum heat flux from a 76.2μ wire as a function of bath temperature at a depth of immersion of 30 cm (Lemieux and Leonard, 1968).

where E_1 and E_2 are the initial and final energies and P_1 and P_2 are the initial and final momenta of the tube. (The equality in equation 6 holds if the excitation has its momentum along the direction of $\vec{v}$.) Now

$$E_1 - E_2 = \frac{P_1^2}{2M} - \frac{P_2^2}{2M} = \frac{P_1 \Delta P}{M} + 0(\Delta P^2) \tag{7}$$

where M is the mass of the tube, $\sim P_1/v$

therefore $\varepsilon \leqslant v\Delta P \leqslant vp.$ (8)

An excitation may only be created if

$$v_c \geqslant \varepsilon/p)_{min} \tag{9}$$

where ε and p are determined by the energy spectrum of the excitations. The critical velocity to excite a phonon is u_I, the velocity of first sound, which is 2×10^4 cm/sec ($\varepsilon = u_I p$ for phonons). The critical velocity to excite a roton is Δ/p_o which is 6×10^3 cm/sec, where Δ and p_o are parameters of the roton energy-momentum relationship shown in figure 4. Unfortunately the experimental critical velocity is orders of magnitude less than this value and its source must be sought in other modes of fluid motion.

Onsager suggested and Feynman developed quantized vortices as excitation of the superfluid which are difficult to excite thermally but may be excited mechanically. There is considerable experimental evidence for the existence of quantized vortices and quantized vortex rings in liquid helium II (Rayfield and Reif, 1963, 1964).

The exact form these vortices assume and their interaction with the thermal excitations and with themselves is uncertain, but the data on ions in He II and the observed critical velocities agree best with classical vortex rings (John Andelin, personal communication).

If the relative velocity of the two fluids is not small, dissipative processes appear which limit the fluid flow and the heat transfer. This breakdown of superflow can be accounted for by adding non-linear, frictional terms to the equations of motion. Experimentally these terms have the form

$$\vec{F}_{sn} = A(T)\ \rho_n \rho_s \left(\vec{v}_n - \vec{v}_s\right)^3 \tag{10}$$

where A(T) is the Gorter-Mellink coefficient which varies slowly with temperature. This force of mutual friction between the two fluids is usually attributed to some sort of interaction between the vortices and the phonons and rotons. The equations of motion (modified Navier-Stokes equations) are

$$\rho_n \frac{d\vec{v}_n}{dt} = -\frac{\rho_n}{\rho} \nabla p - \rho_s S \nabla T + \eta \nabla^2 \vec{v}_n + \vec{F}_{sn} \tag{11}$$

$$\rho_s \frac{d\vec{v}_s}{dt} = -\frac{\rho_s}{\rho} \nabla p + \rho_s S \nabla T - \vec{F}_{sn} \tag{12}$$

where p is pressure. Since heat transport is entirely by the normal fluid we have

$$\vec{q} = (\rho S)\ T\ \vec{v}_n \quad . \tag{13}$$

For small relative velocities here $F_{sn} \sim 0$, $dv/dt \sim 0$ (steady state), and no net mass flow, $\langle \vec{j} \rangle = 0$, the equations of motion yield our first equation for heat transfer (3). If the relative velocities are not small, but accelerations, ∇p, and $\eta \nabla \vec{v}_n$ are assumed small, the equations of motion yield the cubic term in the second equation for heat transfer (4).

Maximal heat transfer rate.

There is an upper limit to the heat transfer rate beyond which the liquid boils and a gas layer forms around the heater. Since this critical heat flux, q_c, is of considerable interest to engineers designing superconducting magnets, a fair amount of data is available. For single, horizontal wires in a bath of He II, this critical flux depends on the bath temperature, wire diameter, depth of the wire below the liquid surface (pressure), and "dewar geometry" (Frederking, 1968). q_c increases as wire diameter decreases. This increase is probably due to the difficulty of forming a gas bubble on the curved surface. The other dependencies of q_c may be explained by examining the equations of motion (11 and 12). For wires about .01 cm in diameter, the critical heat fluxes are of the order of 1 to 10 watts/cm^2, the higher values corresponding to depths of about 10 cm beneath the liquid surface (figure 6). Much larger values have been reported, notably 80 watts/cm^2 at depth of 70 cm

beneath the liquid surface (Coulter et al, 1968).

No one seems to observe nucleate boiling, although the film is not necessarily steady. A distinction is made between film boiling with and without noise (hiss). That with noise is more violent and frequently has a greater heat transfer (the bubbles may build and collapse). Schlieren photography has not shown any optical inhomogeneities (the index of refraction is proportional to the liquid density which is proportional to the temperature) around the wire even at fluxes of 8.6 watts/cm^2 just before film boiling occurred. The apparatus used was capable of detecting a thermal gradient of 3.55 mK/cm (Coulter et al., 1968).

Broadwell and Liepmann (1969) have investigated the heat transfer in a vertical tube closed at the bottom by a flat heating element. The tube has a constriction such that large values of $(\vec{v}_n - \vec{v}_s)$ occur only in the neighborhood of the constriction. They find that the critical heat flux (boiling) occurs when the temperature near the heater reaches the saturation temperature corresponding to the local pressure. This finding explains the depth effect (increase of the critical heat flux with depth). The heat flux at which the local temperature reaches this saturation temperature is determined by the cubic term in the heat transfer equation (4).

Critical heat flux for a model spph.

The critical heat flux from a horizontal wire heater in a bath of liquid helium II may be estimated from the equations of motion (11 and 12). If $\vec{v}_n$ and $\vec{v}_s$ are approximately zero at the liquid surface (far from the wire), and if $\vec{v}_n$ is given by equation (13) near the wire and $\vec{v}_s$ is then given by the requirement of no net mass flow, $\langle\vec{j}\rangle = 0$, the temperature at the wire is

$$T_2 - T_1 = \frac{-1}{S}\left(\frac{\rho_n}{\rho_s}\,\frac{q}{\rho ST}\right)^2\Bigg|_1^2 + \frac{A(T)\rho_n}{S}\int_1^2\left(\frac{q}{\rho_s ST}\right)^3 dz \qquad (14)$$

where the subscripts 1 and 2 refer to the liquid surface and the wire surface, respectively, and z is the vertical dimension. Boiling occurs when

$$T_2 - T_1 = \left.\frac{dT}{dp}\right)_{sat}\left(\rho gh + p_o\right) \qquad (15)$$

where $dT/dp)_{sat}$ is the slope of the vapor pressure curve (figure 3), $h = z_2 - z_1$, and p_o is any excess gas pressure (greater than the P_{sat} which corresponds to T_1) above the liquid. Therefore, the critical heat flux, q_c, is given by

$$\left.\frac{dT}{dp}\right)_{sat}\left(\rho gh + p_o\right) = -\frac{1}{S}\left(\frac{\rho_n}{\rho}\,\frac{q}{\rho_s ST}\right)^2 + \frac{A(T)\rho_n}{S}\int_1^2\left(\frac{q}{\rho_s ST}\right)^3 dz \qquad (16)$$

The integral in equation (16) may be estimated by making the substitution

$$q^* = \rho S T \, v_n \frac{A(z)}{A^*} \tag{17}$$

where q^* is the heat flux per unit area at the wire, A^* is the surface area of the wire, and $A(z)$ is the area over which the heat flux spreads (Broadwell and Liepmann, 1969). Then

$$\left(\frac{dT}{dp}\right)_{sat} (\rho g h + p_o) = -\frac{1}{S}\left(\frac{\rho_n}{\rho}\frac{q^*}{\rho_s S T}\right)^2 + \frac{A(T)\rho_n}{S}\left(\frac{q^*}{\rho_s S T}\right)^3 \int_1^2 \left(\frac{A^*}{A(z)}\right)^3 dz \tag{18}$$

The integral $\int_1^2 \left(A^*/A(z)\right)^3 \, dz$ is a geometric factor which decreases from unity at the wire to small values near the liquid surface. Near the wire, it may be approximated by

$$\int_a^h \left(\frac{a}{z}\right)^3 dz = \frac{a}{2} - \frac{a^3}{2h^2} \tag{19}$$

where a is the radius of the wire. Once z becomes greater than the dewar diameter, the geometrical factor approaches a constant, the heat transfer approximates that in a capillary tube, the depth effect exhibited in equation (18) disappears.

Figure 7 shows the temperature and depth dependence of q^* computed with equation (18). The calculations were done for a wire .001 cm in diameter and 1 cm long (dimensions appropriate to a spph).

Calculations for p_o equal to 40 Torr and 80 Torr are also included, since these excess pressures are frequently used when freezing spphs.

The calculated values of q* in figure 7 are lower than those for a measured critical heat flux in horizontal wires of similar size shown in figure 6. However, the temperature dependence is the same and the calculations show that the heat transfer increases with depth and excess pressure.

The calculated depth effect disappears at high (near T_λ) and low (below 1.5 K) temperatures, as observed experimentally. In freezing experiments the liquid temperature and pressure are adjusted to obtain as large a critical heat flux as possible.

Freeze-fixation of Phycomyces.

Chapter 2 of this thesis describes experiments performed on gaseous and liquid helium in the search for an optimal freezing procedure. These experiments suggested the actual procedure described in chapter 3. The frozen spphs were prepared for electron microscopy by freeze-substitution or freeze-etching. The micrographs obtained from these preparations are discussed and compared with micrographs of chemically fixed spphs in chapter 3. The results of the various experiments on liquid helium and Phycomyces spphs are summarized in chapter 4.

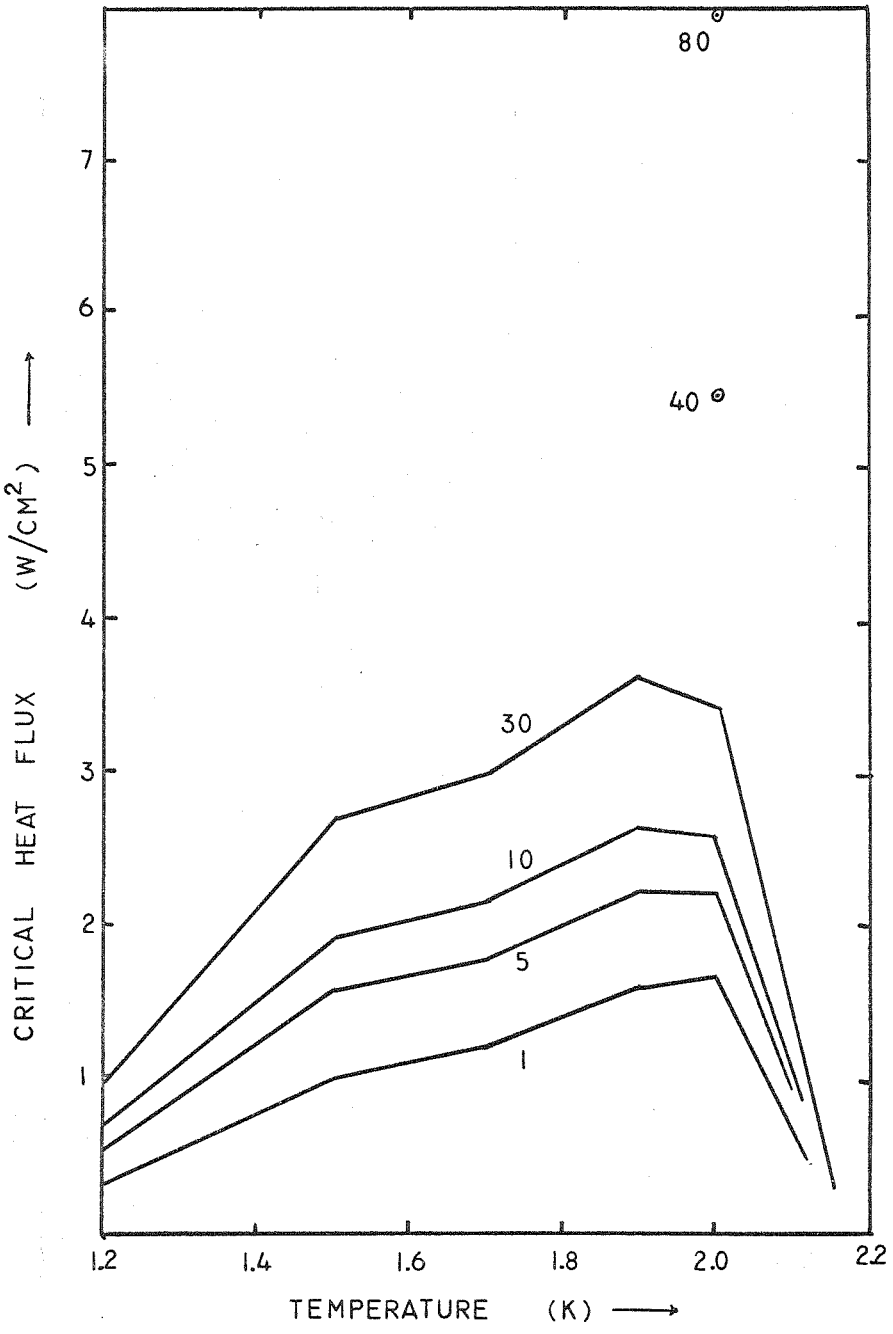

FIGURE 7. Critical heat flux for a .01 cm wire calculated with equations (18) and (19) for wire depths of 1,5,10, and 30 cm, and for dewar overpressures of 40 and 80 Torr.

Chapter 2

HELIUM EXPERIMENTS

There are two major problems encountered when using cryogens to freeze specimens for electron microscopy: cooling in the gas phase and cooling in the liquid phase. The cryogen is usually contained in a dewar vessel with cold liquid at the bottom and cold gas above the liquid. The specimen falls through this gas before reaching the liquid. For electron microscope specimens very rapid freezing is necessary as soon as the specimen temperature passes 0 C; therefore, cooling in the gas must be sufficiently slow to avoid freezing before the specimen enters the liquid, and cooling in the liquid must be maximized.

I have done several model experiments to find these conditions: a) measurements of the temperature gradient in the gas above the liquid and calculations of the cooling of a spph falling through it; b) direct measurements of the cooling of a carbon film as it is lowered into the dewar; c) measurement of the liquid temperature during transient supersaturation (gas pressure increased manyfold over the equilibrium value); d) measurements of the transient heat transfer to the liquid under various conditions.

Simple calculations of spph cooling in the gas and a literature search for cooling in the liquid were done first. A basic freezing and preparative procedure was then devised. Since the results were

not satisfactory, experiments were done to find conditions that would maximize heat transfer to the liquid. Further unsatisfactory results led to detailed calculations of cooling in the gas. These calculations were done in hopes of locating our problems and devising means of minimizing the heat transfer in the gas phase. A final set of spphs was then prepared for electron microscopy.

The following sections will describe the problem of a freely falling spph and present the estimates of spph cooling in the gas and liquid phases.

Fall of a spph through the gas above the liquid and through the liquid helium itself.

Viscous drag is negligible on a spph falling through gaseous helium. If the spph falls 60 - 80 cm before reaching the gas-liquid interface (figure 8), elementary kinematics gives the velocity at the interface as 340 to 395 cm/sec and the time spent in the gas phase as .35 to .40 sec. Because this time is long, considerable cooling occurs and the problem of whether or not this cooling may cause freezing must be examined in detail. After entering the liquid there is some viscous drag and a small buoyancy force on the spph. That these forces are very small can be seen from the spph's terminal velocity in the liquid

$$v_t = \frac{V(\rho_{spph} - \rho_{He})g}{f} \gtrsim 4500 \text{ cm/sec} \qquad (20)$$

where f is the frictional coefficient[1], V is the spph volume, ρ_{spph} is the spph density, ρ_{He} is the liquid density, and g is the acceleration due to gravity. Since the time constant for approaching this velocity (1.6 sec) is large compared with the time for the spph to fall through the liquid (.1 - .15 sec), the spph velocity is still very close to the free fall velocity.

The experimentally determined fall times from the magnet to any point in the dewar were very close to the free fall time plus a constant .15 sec. The delay occurs in the release of the iron filing from the magnet. It was determined by taking pictures of a small piece of paper, which had been attached to the magnet with a small iron filing, at known times after the magnet was turned off.

---

[1]The frictional coefficient, f, has been evaluated using a formula for a prolate ellipsoid with random orientation (Tanford, 1962). Since the spph is aligned with the flow, the actual value will be less than this.

$$f < 6\pi\eta a \frac{\sqrt{1-(b/a)^2}}{\ell n \left\{ \left(1 + \sqrt{1 - (b/a)^2}\right)/b/a \right\}}$$

For a spph a = 2 cm, b = .005 cm, this formula reduces to

$$f \lesssim 6\pi\eta a/\ell n(2a/b) \sim 6\pi\eta(.3 \text{ cm}).$$

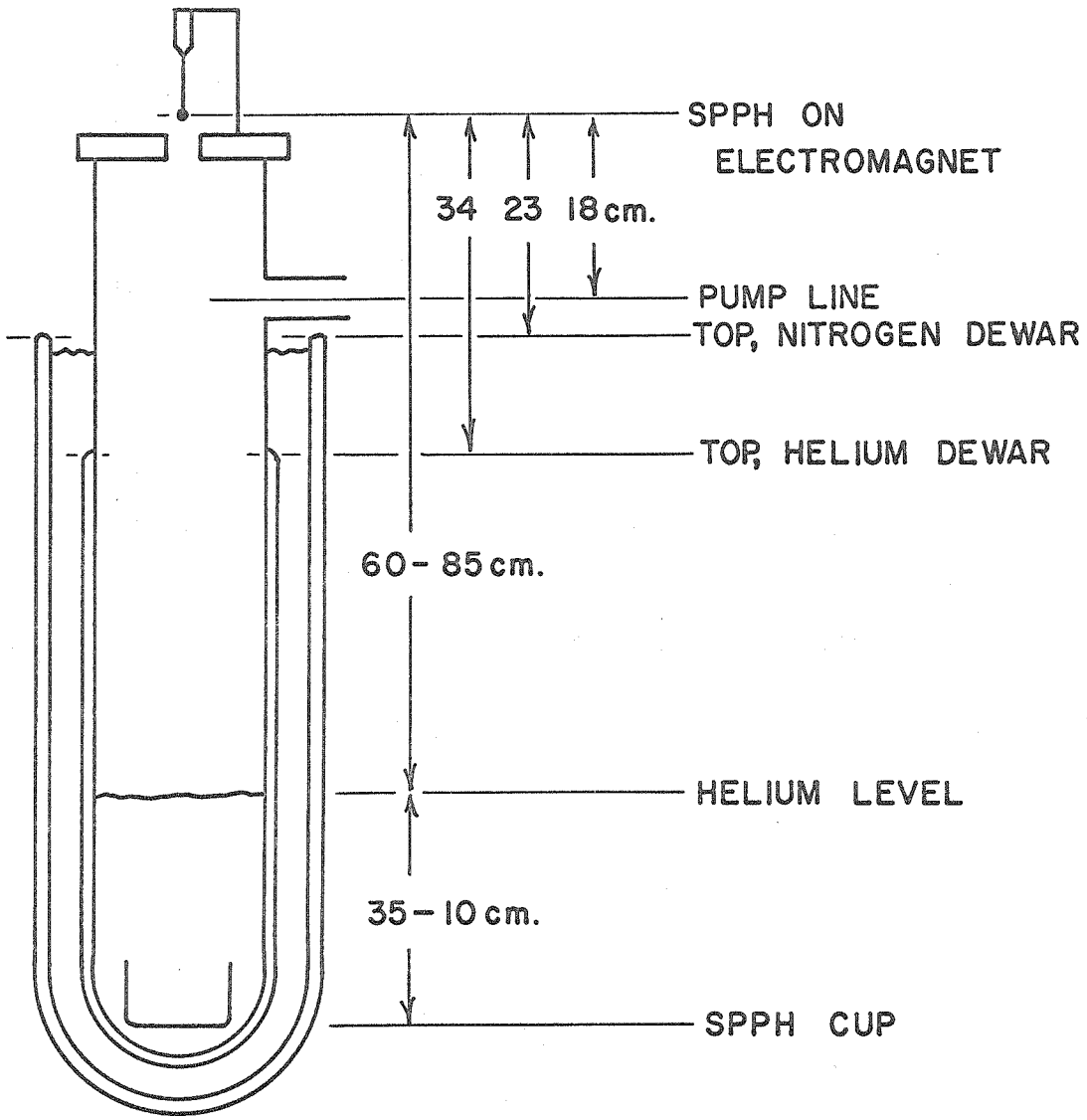

FIGURE 8. Sketch illustrating the helium cryostat dimensions and the free fall distances for a spph. All distances are measured from the sporangium.

We require heat transfer rates of about 200 w/cm^2 for about 10 msec to remove 0.06 joules (.015 calories) per cm spph. This rate is an order of magnitude larger than the steady state critical heat flux case. However, our heat transfer problem is far removed from the case of steady state heat transfer from horizontal cylinders.

There probably is some gas formation as the spph plus iron filing enters the liquid helium, because this entry is frequently accompanied by a hiss or a whistle. The noise is probably caused by the formation of many small bubbles in the helium (Broadwell and Liepmann, 1969). We hope that the high velocity of the spph prevents a stable gas film from forming around the spph. Such a gas film would limit the heat transfer.

A. Estimates of spph cooling in the gas phase.

The spph loses thermal energy by: radiation, evaporation, conduction, and convection. The first two are easily estimated, the last two are not.

The radiation heat loss rate is

$$q = \sigma \left(T^4_{spph} - T^4_{environment} \right) A \mathcal{F} \qquad (21)$$

where σ is the Stephan-Boltzmann constant, A is the spph area, and $\mathcal{F}$ is a factor which accounts for the geometry and the emissivity of the surface ($\mathcal{F} \sim .9$). This heat loss rate is about 1.3×10^{-3} watts with a corresponding temperature drop during free fall of about 2 C

for a 1 cm spph.

The evaporative heat loss is estimated at $.38 \times 10^{-4}$ watts/cm spph at 20 C and 75% relative humidity. This calculation is based on a measured transpiration rate of 1 nliter/min-cm spph (Bergman et al., 1969). In dry helium gas the transpiration rate and hence the heat loss is approximately double. Under these conditions a 1 cm spph will loose heat approximately at a rate of $.75 \times 10^{-4}$ watts with a corresponding temperature drop of 0.1 C during free fall.

Both these cooling rates are much too low to cause freezing in the gas phase.

Conduction and convection heat losses.

Conduction and convection heat losses may be calculated using the Newtonian heat transfer equation

$$q = hA(T_{spph} - T_{\infty}) \tag{22}$$

where T_{spph} is the surface temperature of the spph and T_{∞} is the temperature of the gas far from the spph. The heat transfer coefficient, h, has been calculated for some geometries and measured for others. For forced convection on a flat plate

$$h_{fp} = .664k \sqrt[3]{P} \sqrt{R_{\ell}/\ell} \tag{23}$$

where k is the thermal conductivity, P is the Prandtl number = $\eta c_p/k$, and R is the Reynolds number = $u\ell\rho/\eta$; η is the viscosity, c_p is the specific heat, u is the gas velocity in the dewar or the velocity of the spph in our case, ℓ is the length of the spph, and ρ is the gas density. Estimates of the heat transfer using this formula will be low because the spph is a long, slender cylinder ($r << \ell$) so that the curvature of the spph surface affects the heat transfer. In general the heat transfer from a cylinder is about twice that for a flat plate and is insensitive to the actual value of r/ℓ.

Preliminary calculations were done using heat losses 1, 2, and 3 times the flat plate heat transfer to calculate the spph temperature as it falls through the helium gas. Table 1 gives T_{spph} as it reaches the surface of the liquid helium for several of these calculations.

For the 0.85 Torr (1.2 K) case such a calculation is sufficient to show that the freezing point is not reached. It is not sufficient for the other cases. Therefore additional calculations were done using a heat transfer formula derived by Liepmann (1958)

$$q = \frac{.524}{p^{2/3}} (\eta\rho)^{1/3} C_p (T_{spph} - T_{gas}) \cdot \pi d \int_0^{\ell} \frac{\sqrt{\tau_\omega}\, dx}{\left(\int_0^x \sqrt{\tau_\omega}\, d_x \right)^{1/3}} \tag{24}$$

where d is the spph diameter, x is the distance from the spph tip, τ_ω is the wall stress $\left(\tau_\omega = \eta\frac{\partial u}{\partial y}\right)$ on the spph, and y is the distance from the spph surface. This last equation is a real measure of the heat transfer from a constant temperature cylinder, but since the expression for τ_ω is not a simple, closed, analytical function, the solution is tedious. τ_ω was calculated using the formulae suggested by Glauert and Lighthill (1955) for long, thin cylinders. The relevant dimensions are shown in figure 9. These calculations are also summarized in Table 1.

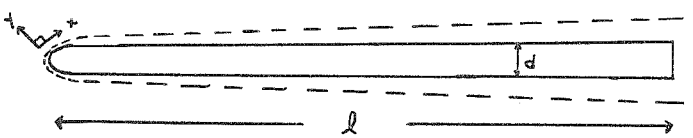

FIGURE 9. Diagram of model spph used in the heat transfer calculations. The dashed line shows the boundary layer thickness which increases with x.

Comparison of the heat transfer from stage I and stage IV spphs.

All the calculations are for stage I spphs. Analytical calculations for stage IV spphs are not possible because the gas flow pattern around the spph is not known. In both cases the heat transfer depends on the conditions in the "boundary layer"[2]. This layer may be thick or thin, and the flow within it may be laminar or turbulent, subsonic or supersonic. If the velocity field within the boundary layer is known, the heat transfer may be calculated. This has been done for the stage I spph which has a laminar, subsonic boundary layer.

The behavior of the boundary layer of a stage IV spph may be conjectured from analogous situations to behave as follows: it separates from the spph near the midpoint of the sporangium and

---

[2]The boundary layer is a relatively thin layer of fluid near the cell wall, in which viscous forces dominate the fluid flow. The fluid velocity, u, changes from zero at the wall to the free stream value, u_∞, at the edge of the boundary layer. This velocity profile, u(y), for the apical end of a stage I spph is shown in the accompanying figure. δ is the boundary layer thickness.

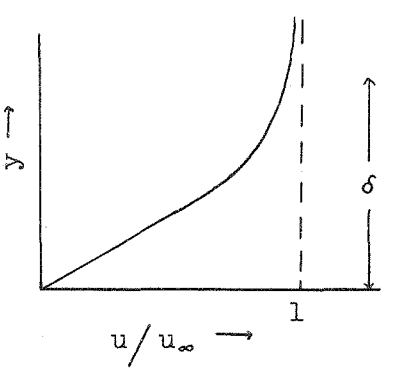

FIGURE 10.

Pressure (Torr)	Bath temperature (K)	Spph temperature calculated using: flat plate (C)	2x flat plate (C)	3x flat plate (C)	cylinder (C)
.85	1.2	25	23	21	---
17.5	1.9	18	8	≤ 0	1
40	---	17	7	≤ 0	2
80	---	13	~ 0	< 0	< 0
120	---	10	< 0	< 0	< 0

TABLE 1. Temperature of a spph at the gas-liquid interface of the helium dewar.

reattaches to the spph about two sporangium diameters, 2D, behind the sporangium. At distances of 8-10D (well beyond the growing zone) the flow is again like that around a stage I spph. Between the separation and reattachment points there is a region of reverse flow (figure 11). The mixing that occurs between this back flowing fluid and the boundary layer above it determines the heat transfer in this region. The character of the boundary layer is very important in determining this mixing (Fletcher et al., 1970).

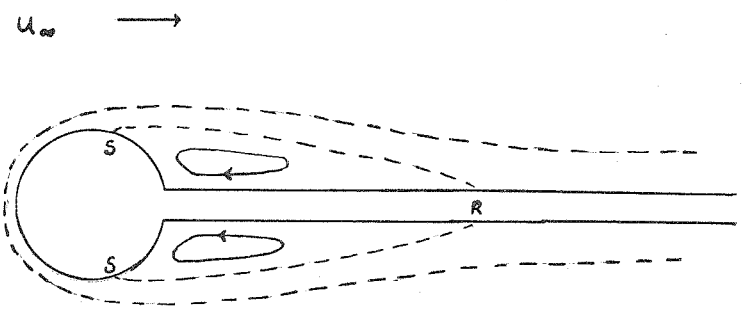

FIGURE 11. Schematic of the boundary layer separation showing the separation, S, and reattachment, R, points and the region of reverse flow.

There are no papers (that I can find) on the heat transfer from such a geometry with a laminar, subsonic boundary layer. There is one paper on the heat transfer from a spherical protuberance in a flat plate with a turbulent, subsonic boundary layer (Seban and Caldwell, 1968). They find that the heat transfer is increased immediately behind the sphere and then approaches the values found for a flat plate. However, the thermal resistance near the wall is not changed much by the presence of the sphere and they attribute the increased heat transfer behind the sphere to an enlargement of the turbulent boundary layer and an alteration of the mixing. Since for the spph's laminar boundary layer, the heat transfer might be expected to decrease with increased thickness rather than increase (flat plate results), we might expect a decrease in heat transfer immediately behind the sporangium (the spph falling head first) as compared with the stage I spph case. Roshko[3] (personal communication) believes that the heat transfer from a stage IV spph will be reduced somewhat immediately behind the sporangium and then, at greater distances from the sporangium, return to the values found for a stage I spph.

---

[3]Anatol Roshko, Professor of Aeronautics, Graduate Aeronautical Laboratories, California Institute of Technology.

Spph heat shield.

Figures 12 a,b, and c give the measured values of $T_{gas}(z)$ and the calculated values of $T_{spph}(z)$ as it falls through this gas. The spph temperature starts to drop when the temperature difference between the spph and the helium gas reaches 100 K and thereafter it is approximately linear in z. At z = 0 the spph temperature curves all come close to or fall below the freezing point (the .85 Torr (1.2 K) case excepted). Thus a shorter dewar or a spph heat shield is desirable. These graphs show that the spph gun (used to shoot spphs into the liquid in one freezing experiment) is of little value because the spph looses a minute amount of energy in the first 20 cm of free fall while attaining a higher velocity (200 cm/sec) than that imparted to the spph by the spring gun (150 cm/sec).

After these calculations were completed an additional, electrically heated tube was added to the dewar flange. This tube extends 60 cm below the sporangium when the spph is suspended from the electromagnet as shown in figure 8. The helium gas within the tube can be maintained at 250 K or more to within 5 cm of the tube end under all conditions. Since the heat loss from the spph is negligible for temperature differences less than 100 K, spph cooling will not be appreciable until the spph leaves the tube. Thereafter the temperature drop is at most 13 C (2 C/10 msec

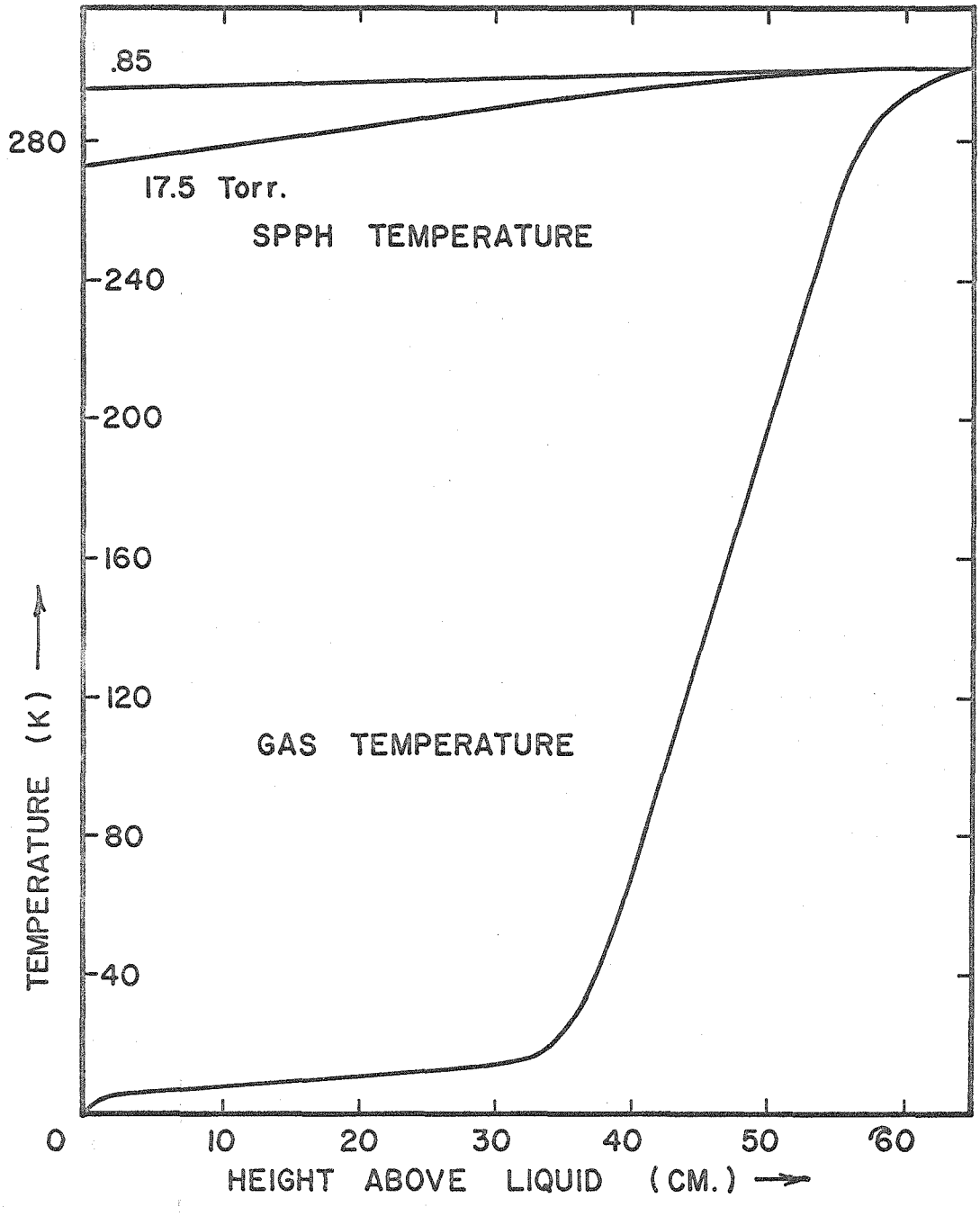

FIGURE 12a. Temperature gradient in the helium dewar at saturation and the calculated temperature of a spph as it falls through this gradient for dewar pressures equal to: 0.85 Torr (1.2K) and 17.5 Torr (1.9 K).

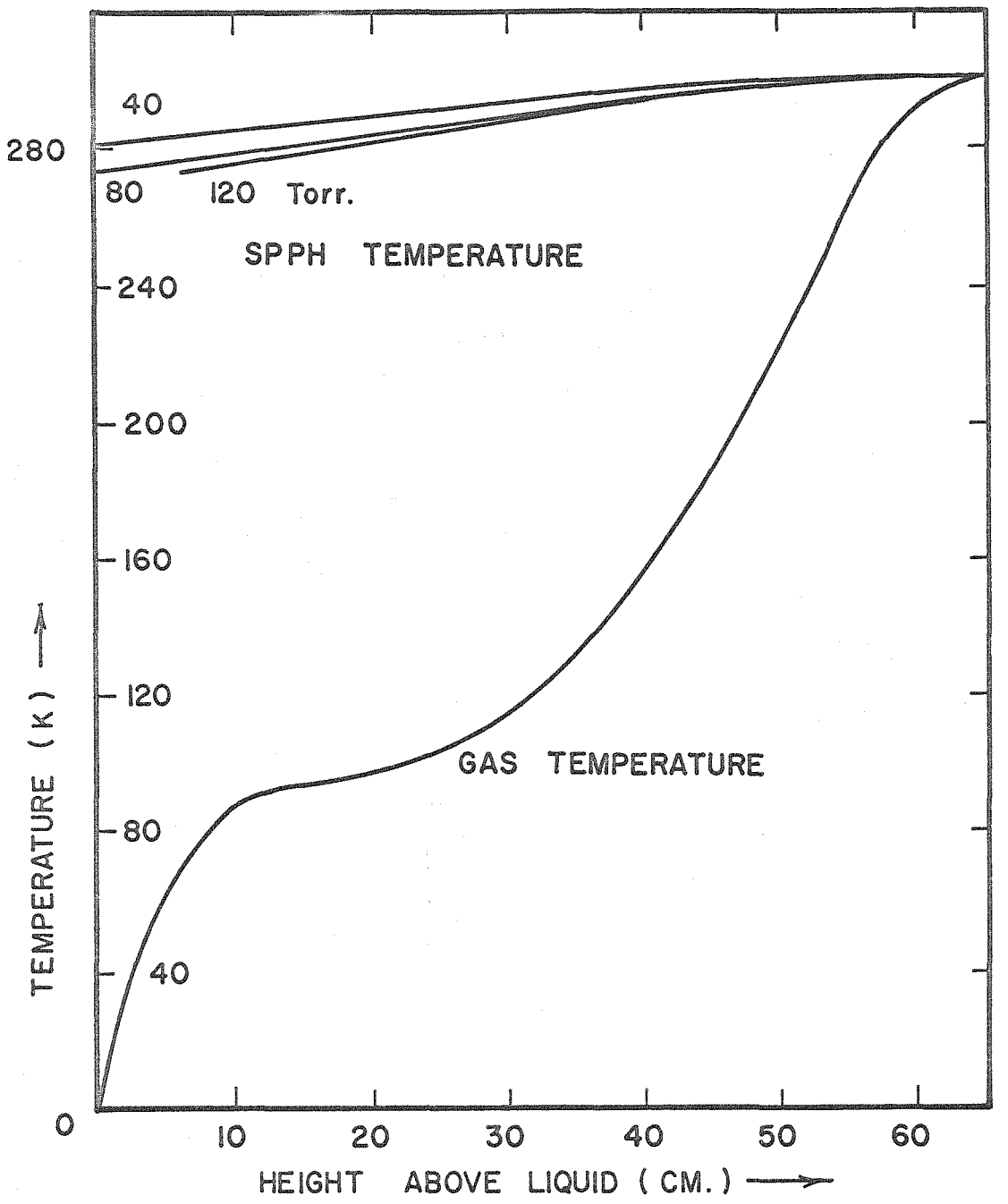

FIGURE 12b. Temperature gradient in the helium dewar when supersaturated and the calculated temperature of a spph as it falls through this gradient for dewar pressures equal to: 40 Torr, 80 Torr, and 120 Torr.

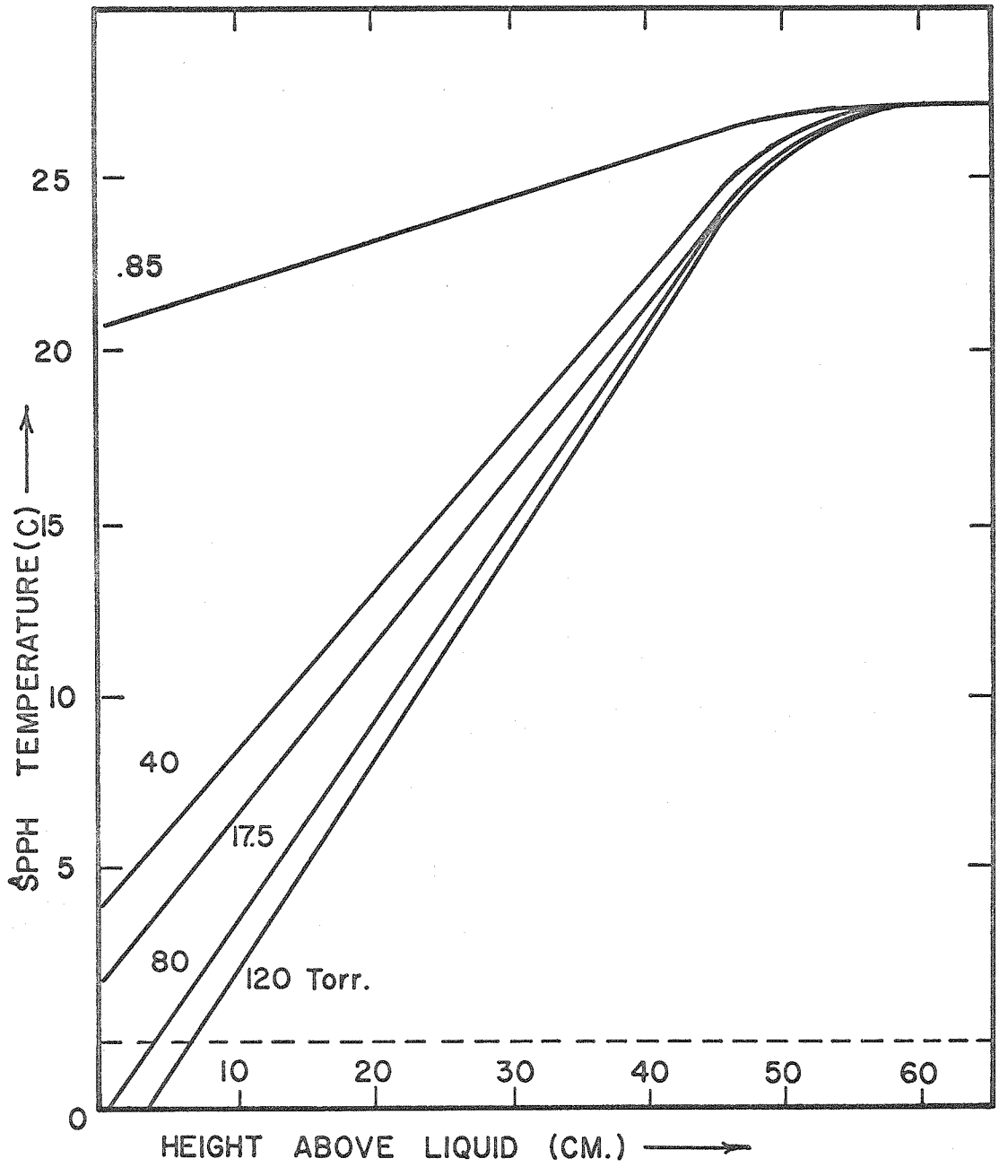

FIGURE 12c. Calculated temperature of a spph as it falls through the helium gas in the dewar for the gas at various pressures.

for at most 66 m sec). Therefore, such spphs will be well above the freezing point as they enter the liquid.

Numerical calculations.

Heat transfer from the spph to the gas is limited by the heat transfer coefficient h. At the spph wall the heat outflow per unit area is

$$k \frac{\partial T_{spph}}{\partial r}\Bigg)_a = h \left(T_{spph} - T_\infty \right) , \qquad (25)$$

where k is the thermal conductivity of the spph and a is its radius. If h is very small or k is very large, the temperature gradient within the spph will approach zero. Bi = ha/k is a measure of the ratio of the thermal impedance within the spph to the thermal impedance at the spph wall. In our case, $ha/k \leq 10^{-2}$ and the spph temperature may be assumed uniform.

Another measure of the temperature distribution within the spph is the thermal diffusion time. This is approximately 4 msec (see equation 27, page 60 , and the comments following it), therefore the spph temperature may be assumed constant in space if times of the order of 10 msec are used.

The spph temperature was assumed to be uniform when calculating the heat loss of the spph to the gas. The heat loss calculations were done for equal time intervals as the spph progressed down the

dewar. The results are presented in terms of $T_{spph}(z)$.

The heat loss, $q\Delta t$, is calculated for 10 msec intervals using equations (22) and (23) or equation (24). The new spph temperature is

$$T_{spph_2} = T_{spph_1} - q\Delta t/mc_p \qquad (26)$$

where T_{spph_1} and T_{spph_2} are the initial and final temperatures of the spph, m is the mass of the spph, c_p is its specific heat, and Δt is 10 msec. Heat loss in the next 10 msec interval is then calculated using T_{spph_2} as the spph temperature. For example, with the helium bath at 1.9 K and 17.5 Torr: at t = 210 msec, the spph has fallen 21.61 cm, the gas temperature at this height is 178 K and the spph temperature at 200 msec was 299 K; therefore, the heat loss calculated with equation (24) is 1.46×10^{-4} joules/10 msec, and the new spph temperature is 298 K.

All temperature dependent parameters (density, viscosity, and thermal conductivity of the gas) were evaluated at T_{spph} because the heat transfer is determined by conditions near the cell wall. The change in T_{spph} was never more than 2 C/10 msec. Over so small an interval the temperature dependent parameters vary little. Both u (the free fall velocity of the spph) and the gas temperature change rapidly with z, but the spph heat loss per unit time is relatively insensitive to the variation. Since both u and the gas temperature are evaluated at the end of the time interval, Δt, the

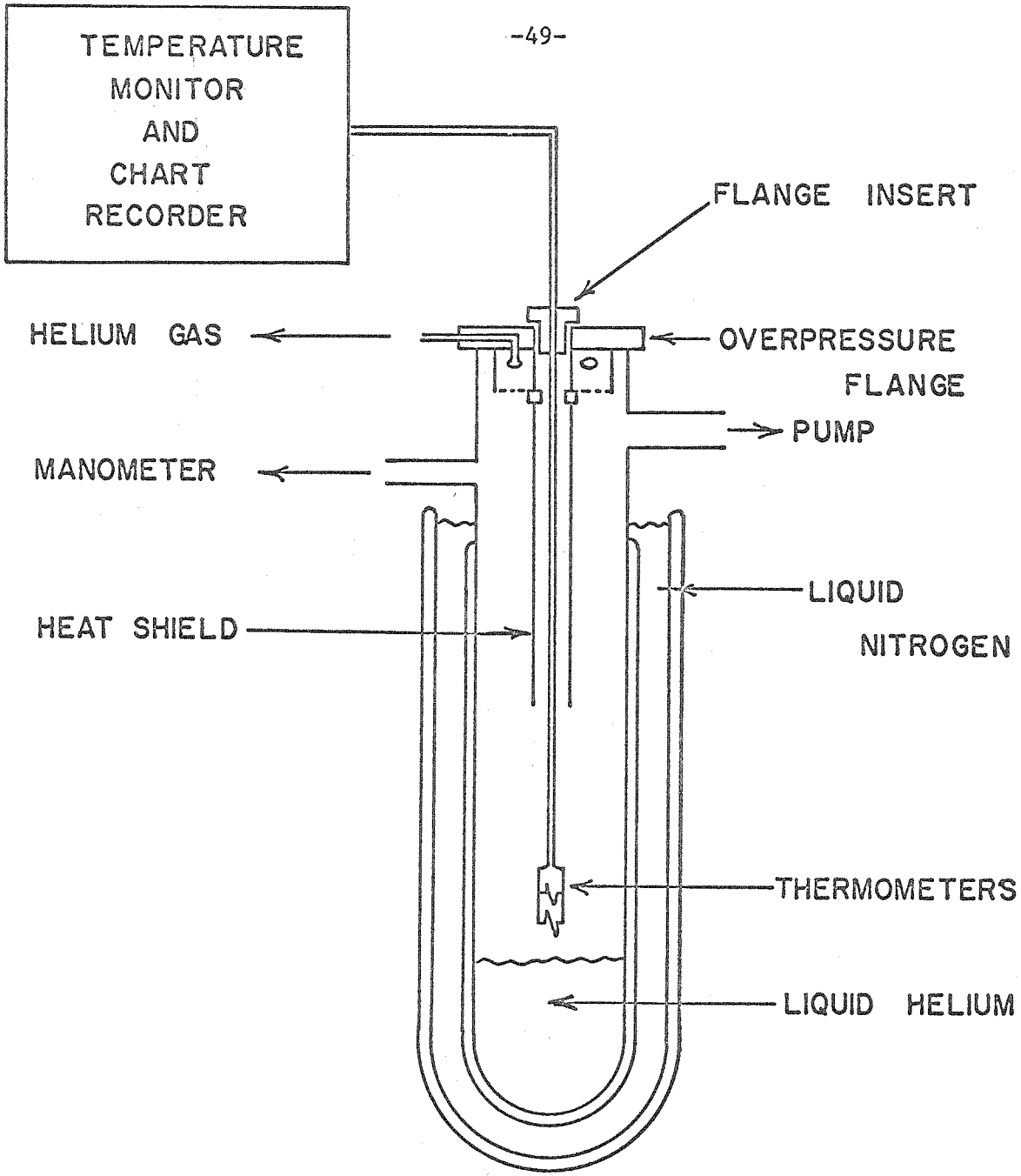

FIGURE 13. Apparatus for measuring the temperature gradient in the helium gas.

heat loss may be overestimated but not underestimated.

Measurement of the temperature gradient in the helium gas in the dewar.

The temperature gradient in the helium gas in the dewar was measured with the apparatus shown in figure 13. A small flange with two thermometers was inserted into the overpressure flange used when freezing spphs. The thermometers could be located at any height in the dewar; the temperature could be read directly or recorded (as a function of time) with a Hewlett-Packard Model 7000A X-Y chart recorder with a Model 17007A chart drive. Between room temperature and 77 K the temperature was measured with a copper-constantan thermocouple with reference junction at 0 C. Below 77 K the thermometer was a Speer 100 Ω, 1/2 watt (grade 1002) carbon resistor (Speer Carbon Co., Bradford, Pa.).

The temperature gradient in the dewar is independent of the liquid helium level down to the top of the helium double dewar (see figures 8 and 12). Below this point the curves are similar and depend on the relative distance to the liquid surface. The temperature gradient is nearly independent of pressure under equilibrium conditions. A representative curve for the temperature gradient is given in figure 12a. (The temperature gradient is a violent function of the pumping speed, but this is zero during spph freezing experiments.) At greater pressures (supersaturated) the

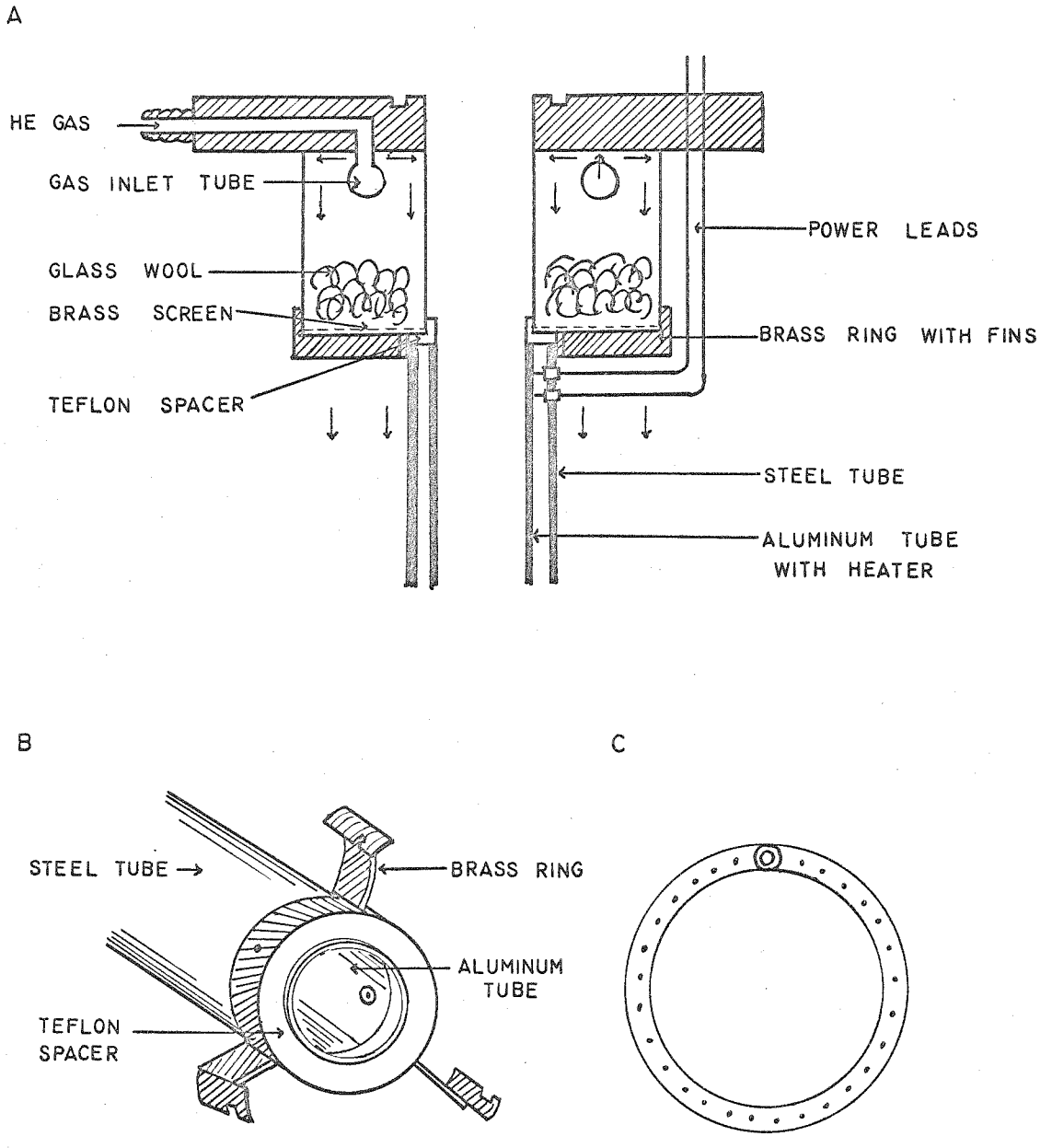

FIGURE 14. Detail of overpressure flange: a) overpressure flange with heat shield showing the construction of the gas nozzle and heat shield; arrows show the helium gas flow; b) heat shield; c) gas inlet tube for overpressure flange nozzle; small holes have .023" diameter.

temperature gradient depends on the pressure. The pressure depends on the amount of warm gas added to the dewar. The calculations show that these two effects on spph cooling (temperature rise and pressure rise) nearly balance one another. Once the pressure has reached 80 Torr the temperature gradient ceases to change enough to affect the heat transfer calculation. The temperature gradient in figure 12b is representative of the temperature gradient in the gas under supersaturation conditions. It is for a pressure of 80 Torr which was a common supersaturation pressure in the freezing experiments.

Construction and use of the spph heat shield.

The heated tube added to the dewar flange is actually two concentric tubes separated by teflon spacers at top and bottom. The outer tube is made of stainless steel which is a poor thermal conductor and shields the inner tube from the helium gas in the main part of the dewar. The inner tube is made of aluminum, a good thermal conductor, which is wound with 1200 Ω of Evanohm wire. A teflon spacer separates the tubes from the dewar flange so that they may be cooled to 4 or 77 K while the flange remains at room temperature. The heat shield is held in a brass ring with three radiating fins (see figure 14) by three teflon coated steel pins; the heat shield is suspended from the overpressure flange by

the brass ring.

When the heat shield is used the helium dewar is precooled to liquid nitrogen temperature at follows. A small amount of air is let into the helium dewar vacuum jacket (this air freezes out and has a negligible vapor pressure at 4 K). The helium dewar is filled with helium gas and the nitrogen dewar is filled with liquid nitrogen. When the helium gas inside the heat shield reaches 95-100 K (about 1 hour) the flange insert with thermometers is removed and liquid helium is transferred into the dewar. The transfer is stopped when thermal oscillations begin in the heat shield tube. These thermal oscillations of the liquid and gaseous helium make further liquid transfer wasteful. They begin after the liquid level has risen 1 to 10 cm up the heat shield. The flange insert is returned to the dewar and the liquid helium is pumped down to 1.2 K. As soon as the liquid level is below the heat shield, the heater is turned on. The gas temperature at the bottom of the shield rises to 250 K within 50 minutes if the power input is 33 watts. The gas temperature may be held nearly constant with a power input of 25 watts or allowed to continue rising slowly toward 0 C.

During transient pressure increases in the dewar, the gas within the tube remains undisturbed except near the bottom of the tube

and the temperature remains nearly constant. Temperature fluctuations at the bottom of the tube are of the order of 10 K for a pressure increase of 80 Torr. The fluctuations disappear about 5 cm above the bottom of the tube.

B. Cooling of a carbon film as it is lowered into the helium dewar.

Earlier, some experiments were done to measure the cooling of a thermometer probe as it was lowered through the dewar into the liquid. The results are not immediately applicable to spph cooling because, although the geometry was the same, the velocity was less (about 20 cm/sec) and the enthalpy, H(T), was different. However, the T(t) curves do show that the cooling rate in the gas phase decreases if the temperature of the liquid (pressure of the gas) is lowered by pumping to a lower equilibrium state. The cooling is also less if the gas pressure is raised by admitting warm gas, causing supersaturation. The cooling of the probe in the liquid improves under both these conditions, that is, He II is a better coolant than He I and supersaturated He II is better still. These data were substantiated and superseded by the heat transfer calculations of section A. Therefore, they are not reported in detail.

C. Overpressure experiment.

If liquid helium II at 1.2 K (equilibrium vapor pressure of .625 Torr) is suddenly brought to one atmosphere pressure (760 Torr) by the addition of warm helium gas to the dewar, the temperature of the liquid helium rises rapidly (about 5 sec) to about 2 K, and then slowly (about 3 min) approaches T_λ (figure 15). Thermal conduction measurements show that the fluid maintains its enormous heat transfer capabilities as long at $T < T_\lambda$ (Liepmann, Broadwell, and Dimotakis, personal communication).

This effect may be understood as follows. As the gas pressure increases the liquid departs from equilibrium with the gas phase and becomes supersaturated (supercooled). As soon as the pressure exceeds 37.94 Torr, He I is the stable phase,[4] therefore the liquid will go from He II to He I as fast as energy is supplied to warm the liquid above 2.172 K (T_λ).[5] The speed of the conversion depends on the specific heat of He II and on the three heat sources available: the radiation heat leak (about 300 mw), the spph heat content (0.06 j/cm spph), and the heat of vaporization of the

---

[4]The phase boundary between He I and He II on the P-T diagram (figure 3) is nearly vertical (73.5 atm/K) so that it is nearly impossible to make the phase transition from He II to He I by increasing the pressure.

[5]There is no latent heat for the transition He II → He I, therefore, at equilibrium the phases can not coexist and the transition must occur as soon as the temperature reaches T_λ.

the helium gas condensing into the liquid (23 j/gm). This last is the major heat source and it introduces heat at the liquid surface.

$C_{sat}(T)$, the specific heat of liquid helium, is shown in figure 16. It rises logarithmically near T_λ. This fact explains the findings, mentioned above, that for a constant heat flux, the liquid temperature climbs very rapidly to about 2 K and then slowly approaches T_λ. At the liquid surface the heat flux is sufficient to change a thin layer of liquid to He I. This layer acts as an insulator because He I can maintain a temperature gradient and is a rather poor thermal conductor (classical fluid). Thus we find that in this non-equilibrium situation, a phase boundary between the He I and the He II does form. It propagates downward through the liquid bath as heat is supplied (through the He I phase) to raise the temperature of the liquid at the interface above T_λ.

If the gas pressure is raised to one atmosphere and held there, the phase boundary propagates downward about .07 cm/sec. In spph freezing experiments the gas pressure was raised only to 40-80 Torr and reduced again immediately after the spph entered the liquid. This procedure limits formation of He I by introducing a smaller quantity of gas over a shorter period of time (about 10 sec). At the same time it increases the pressure at any depth in the liquid ($\rho gh + p_o$, where p_o = 40-80 Torr - p_{sat} and ρgh = .012 Torr/cm liquid helium). Since the critical heat flux at which boiling occurs

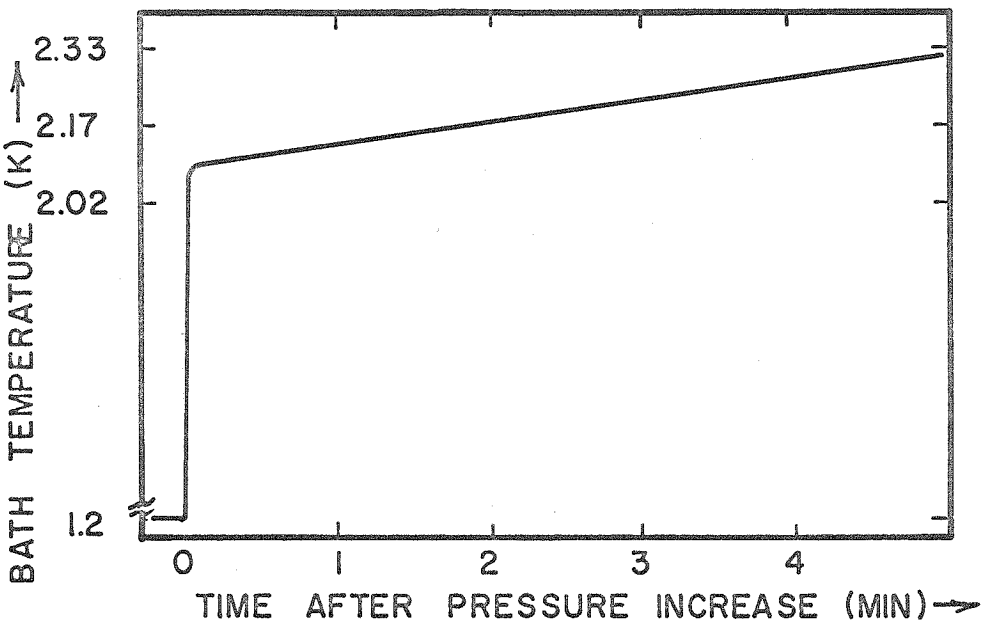

FIGURE 15. Bath temperature change with time when pressurizing to one atmosphere, for a thermometer 12 cm below the liquid surface. Dewar pressure reached one atmosphere at 20 sec.

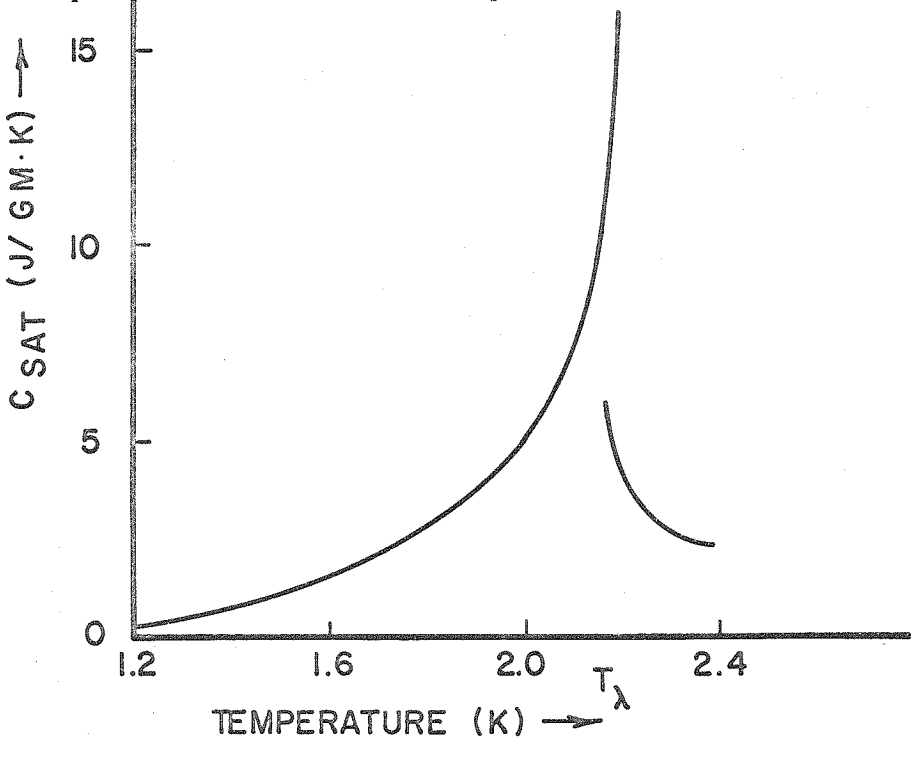

FIGURE 16. Specific heat of He^4 under the saturated vapor pressure.

increases with pressure, this procedure should suppress boiling as the spph enters the liquid.

Measurements of temperature in the liquid phase during overpressure.

Figure 17 is a schematic diagram of the apparatus. The thermometers were two Speer 100 Ω, 1/2 watt carbon resistors. These were attached to a stainless steel tube which could be positioned at any height in the dewar. The resistors were calibrated against the He^4 vapor pressure curve between 1.2 and 4.2 K. Resistance was measured with a low power input a.c. Wheatstone bridge built by John Wallace of the Low Temperature Physics Laboratory. With this bridge the resistors could be monitored at powers of 10^{-6} to 10^{-7} watts, so that self-heating of the resistors was minimized. Helium gas for the pressure increase was obtained from a helium storage dewar. Liquid helium was transferred from the storage dewar, through 6 feet of tygon tubing, into the experimental cryostat. This helium entered the cryostat as warm gas at about 8 C (281 K).

The warming curves of the liquid helium were made by pumping the bath to an equilibrium temperature of about 1.2 K. The resistance bridge was then adjusted to balance at 2.17 K and the pump valve closed. At time zero helium gas was transferred into the dewar and the dewar pressure rose to one atmosphere within 20-30 seconds. The liquid helium temperature rose as shown in

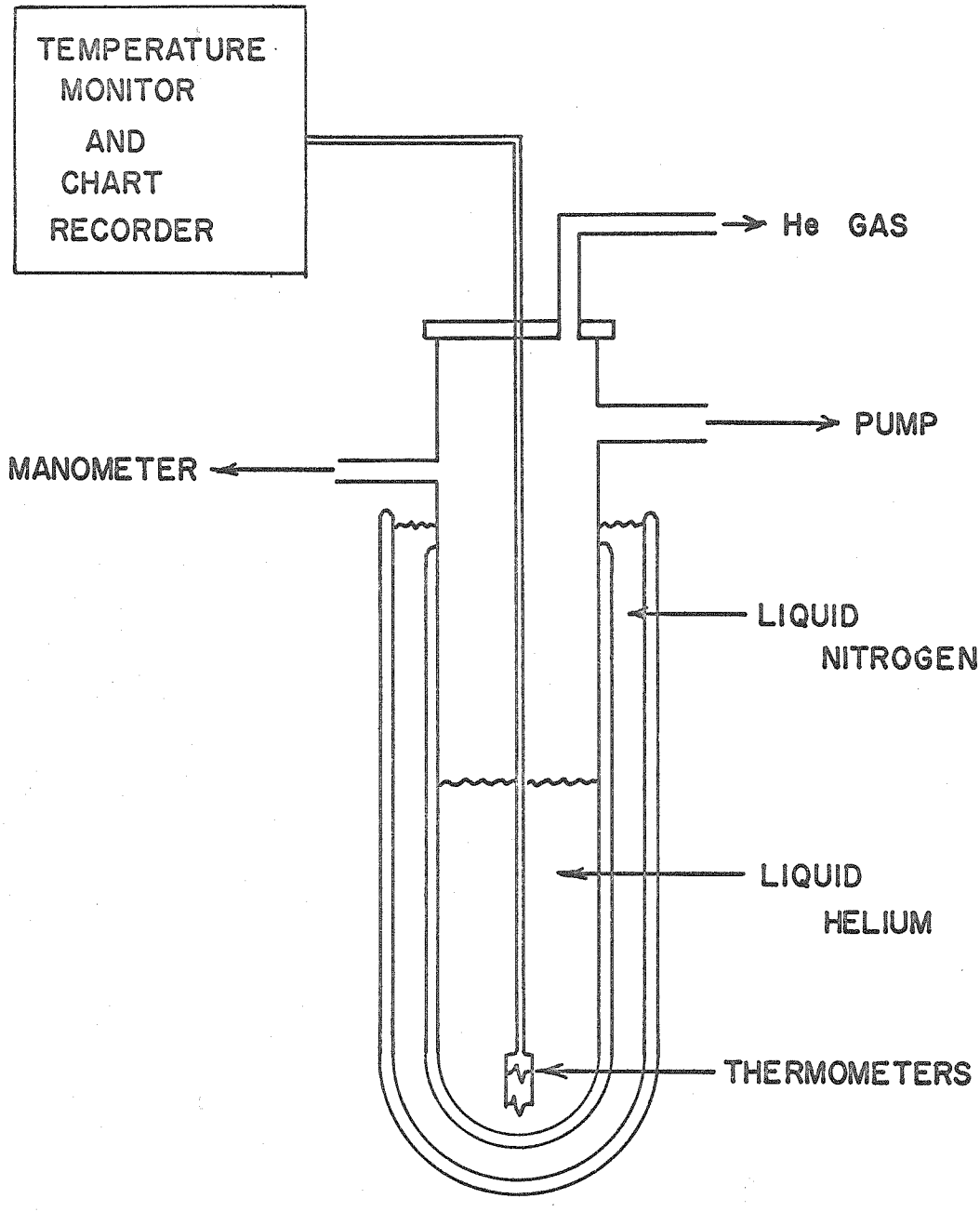

FIGURE 17. Overpressure apparatus.

figure 15. (The initial 1.2 K line is off scale in the figure.) Since the gas entering the dewar cools, contracts, and condenses, the gas transfer must be continued until all the liquid has reached 4.2 K (the normal boiling point) if the dewar pressure is to remain at one atmosphere.

D. Heat pulse experiments.

Most of the engineering data on critical heat transfer to liquid He II are for steady state conditions. In the case of a spph entering the liquid, the heat flux is transient and the critical heat flux may be different.

To estimate this transient heat flux we consider the cooling of an infinite circular cylinder of radius R. If k, ρ, and c_p are independent of temperature, if there is no phase transition, and if there is no thermal impedance at the surface of the cylinder (infinite heat sink), the temperature distribution within the cylinder is

$$T(r,t) - T_\infty = 2(T_o - T_\infty) \sum_{n=1}^{\infty} \frac{J_o(\lambda_n r)}{\lambda_n R\, J_1(\lambda_n R)}\, e^{-\kappa\lambda_n^2 t} \qquad (27)$$

where T_∞ is the bath temperature, T_o is the initial temperature of the cylinder, $\kappa = k/\rho c_p$, $J_o(\lambda_n r)$ and $J_1(\lambda_n R)$ are Bessel

functions and the λ_n are roots of the equation

$$J_o(\lambda R) = 0 \tag{28}$$

The slowest time constant of the cooling is $1/(\lambda_1)^2 = 3.3$ msec, and the initial cooling rate is $2(T_o - T)(\lambda_1)^2 = 1.8 \times 10^5$ K/sec. This initial cooling rate for the cylinder is fast enough to produce vitreous water according to the various estimates of chapter 1.

If there is a thermal boundary impedance, the rate of heat transfer from the surface, A, is expressed in terms of the heat transfer coefficient, h. Thus

$$q = Ah(T_{cyl} - T_\infty), \tag{29}$$

and the temperature of the cylinder is

$$T(r,t) - T_\infty = 2Bi\left(T_o - T_\infty\right) \sum \frac{J_o\left(\beta_n r\right)}{\left(\beta_n^2 R^2 + Bi^2\right) J_o\left(\beta_n R\right)} e^{-\kappa\beta_n^2 t} \tag{30}$$

where $Bi = hR/k$ is a measure of the impedance at the surface, and the β_n are the roots of the equation.

$$-\beta_n R\, J_1\left(\beta_n R\right) + Bi\, J_o\left(\beta_n R\right) = 0 \tag{31}$$

The worst possible case we may consider is film boiling in liquid He I. The heat transfer coefficient, h, is .03 w/cm^2 K in He I at large temperature differences (Frederking et al., 1965).

The slowest time constant of this system is then $1/\kappa(\beta_1)^2$ = .36 sec, and the initial cooling rate is 2 Bi $(T_o - T)$ $(\beta_1)^2$ = 45 K/sec which is much too slow for electron microscopic work. Thus we expect a spph to cool exponentially with an initial rate and time constant somewhere between these extremes. A model experiment was set up to estimate the time constant for spph cooling and to find the optimal conditions for heat transfer from the spph to the liquid. Once the optimal conditions were found and the critical heat flux was estimated, we planned to freeze spphs under these conditions. The experiments were not completed, but sufficient experiments were done to estimate the time constant for spph cooling at between 1 and 5 msec and to find that 1.9 - 2.0 K is indeed the optimal temperature, and that boiling is reduced and possibly suppressed during a transient pressure increase.

Estimate of the time constant for spph cooling.

The object of this experiment was to estimate the time constant for spph cooling at any temperature and pressure of the liquid by varying the transient cooling of a model spph until the noise and

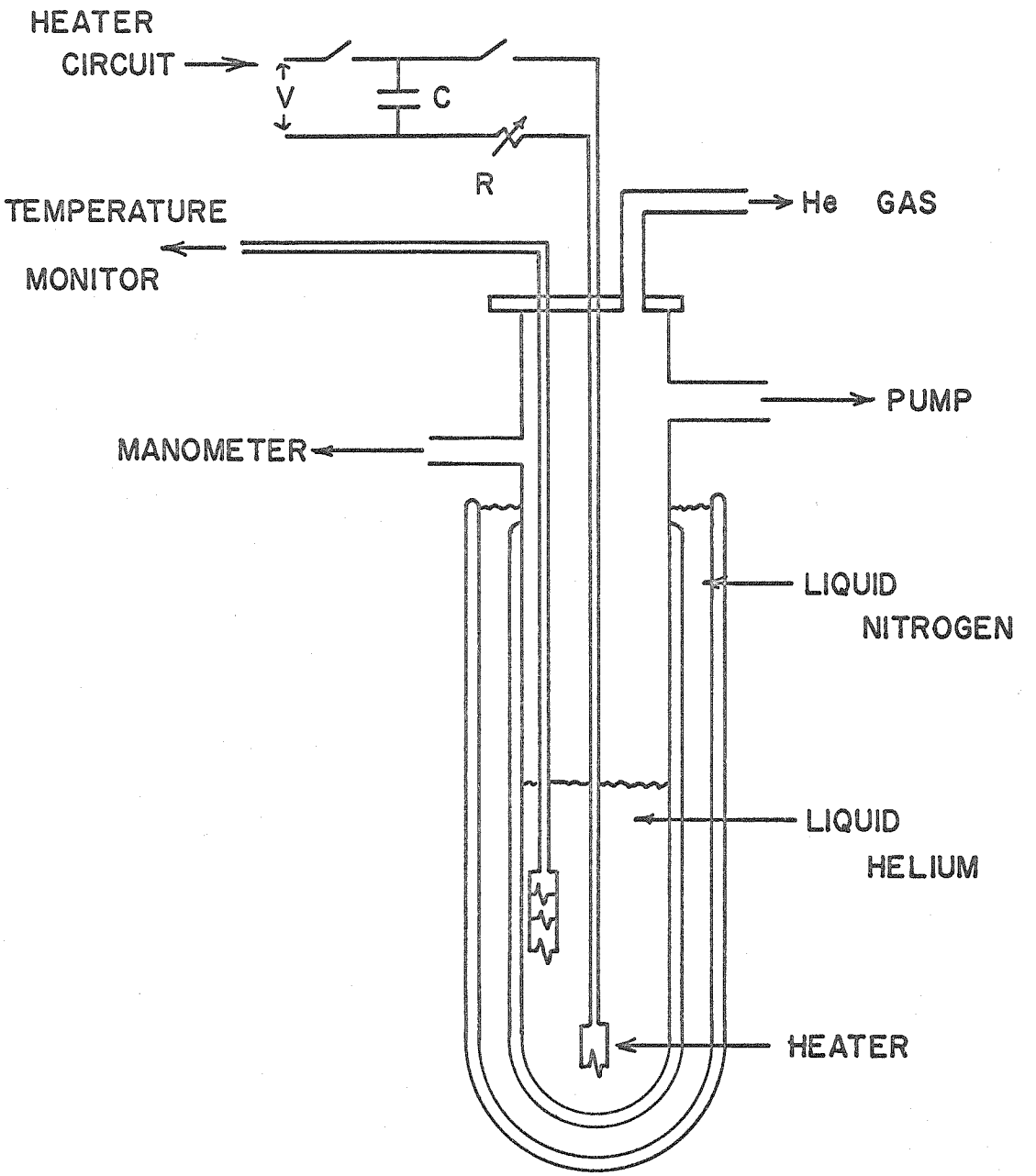

FIGURE 18. Heat pulse apparatus.

boiling were as that for the real spph. The variables in this experiment were: temperature, and pressure of the liquid helium, depth of the model in the bath, energy dissipated by the model, E, and the time constant for this energy dissipation, τ.

The heat pulse experiments were done with the apparatus shown in figures 18 and 19. The heater (model spph) is a stationary, horizontal, 2 cm length of Evanohm wire (94 μ diameter, resistance about 6Ω) obtained from Wilbur B. Driver Co., Newark, N. J. Heating is done with a simple RC circuit. The current pulse through the wire is

$$\frac{V}{R_h} e^{-t/RC} \tag{32}$$

where V is the voltage across the capacitor, C, R_h is the wire heater resistance, R is the total circuit resistance, and t is the time. Heating in the wire is approximately

$$\frac{V^2}{R_h} e^{-2t/Rc} \tag{33}$$

I have estimated that the heater temperature rises vary rapidly (on the order of microseconds) to 30-150 K and then as a result of interplay between supply and loss, falls with conduction of the heat away into the bath. The time constant of this decrease is RC/2

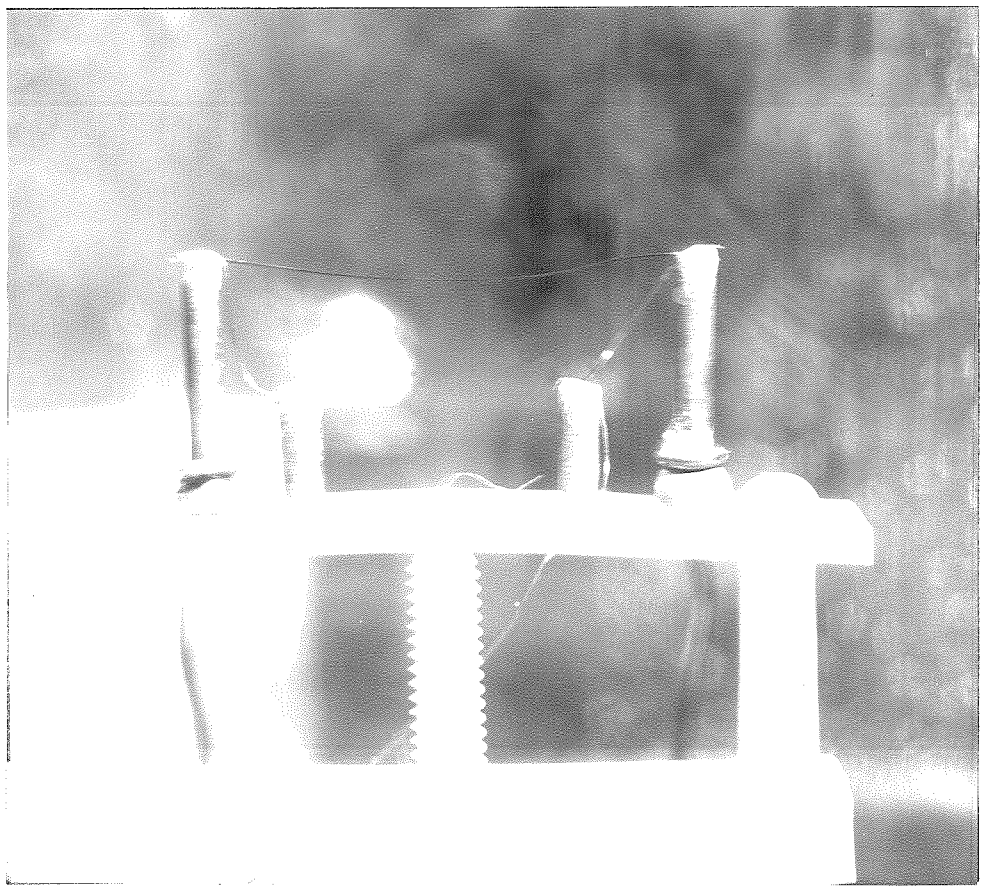

FIGURE 19. Heater wire in liquid helium II both at 1.2 K.

if heat transfer into the helium is ideal.

An approximate measure of the average energy dissipation (power per unit area) is E/A 3τ, where E is the energy, A is the wire surface area, and $\tau = RC/2$ is the time constant. (95% of the energy is dissipated within 3 time constants.) At any given temperature of the bath the value of the energy dissipation at which noise is heard or bubbles are seen, increases with τ. It also increases with temperature. The approximate value of the dissipation for which noise was heard for one wire is given in figure 20. The last four values (τ = 3.5-5 msec) are for an energy of .15 joules which is the approximate thermal energy content of a 2 cm spph. The 5 msec value is a minimum estimate because no sound was heard.

The depth effect is very small at this temperature, as observed by Lemieux and Leonard (1968). An overpressure of 40 Torr increased the point at .6 msec. For a second, similar wire the power at which sound occurred approximately tripled but bubbles were visible around this wire at the lower power densities. The boiling mode (with or without noise) must be strongly dependent on the condition of the wire surface.

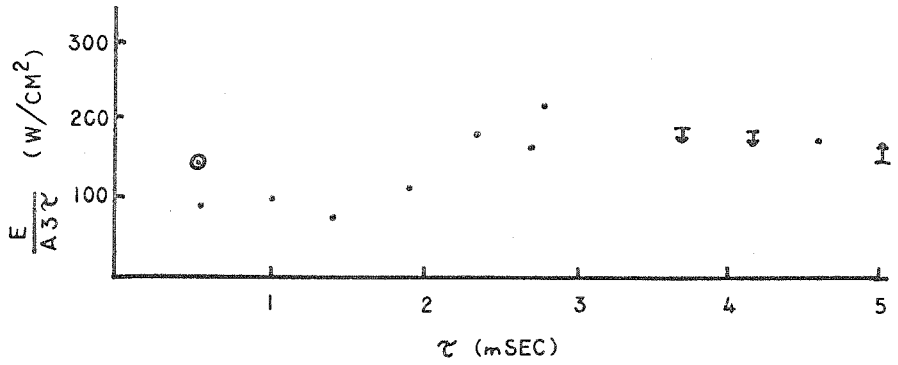

FIGURE 20. Power at which sound is heard for wire heater in liquid He II at 1.23 K. The point ⊙ is for an excess pressure of 20 Torr.

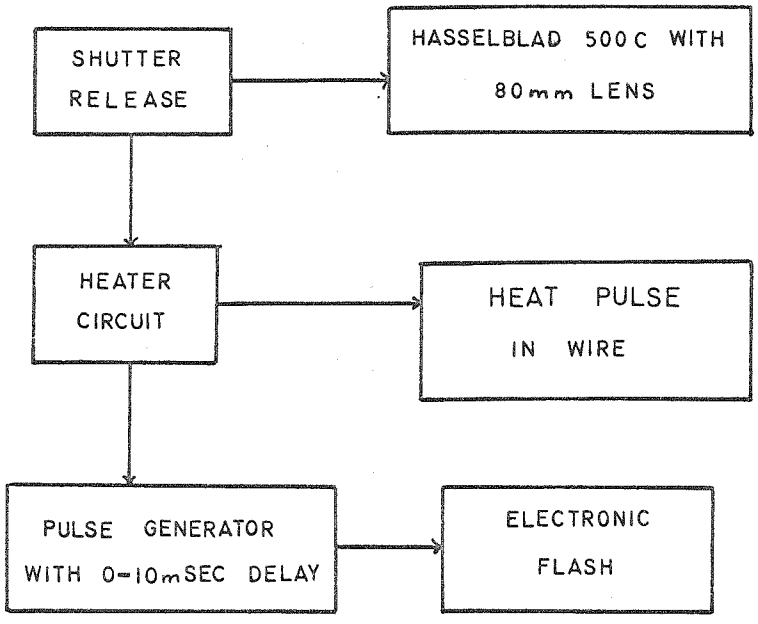

FIGURE 21. Block diagram of the apparatus used to take pictures of the heat pulse.

Time course of the boiling.

To better estimate the time constant for cooling of a spph, τ_s, pictures were taken of the boiling around the wire as it progressed at various temperatures and pressures. Two such sequences are shown in figures 22 and 23 for heat pulses at 1.5 and 1.9 K. The time constant for both pulses is τ = .6 msec, the pressure is the saturation vapor pressure, and the pictures were taken at 0, 1, 5, and 10 msec after the start of the pulse. The boiling film develops within milliseconds and lasts for at least 10 msec. The exact duration of the boiling is not known because longer time delays were not possible with the equipment used (figure 21). The film becomes more stable as the bath temperature is increased to 1.9-2.0 K. At 1.9-2.0 K the film is uniform and its thickness is probably determined by the heat flux. Rinderer and Haenseler (1960) found that the film thickness around a heated wire was proportional to the temperature difference between the bath and the wire. The data are consistent with the idea of a fixed, maximum heat flux at the gas-He II boundary.

Changing the time constant from .6 to 2.7 msec did not affect the boiling pattern appreciably. However, increasing the pressure to 40 Torr caused the film to be replaced with a fine haze (figure 24a,b) and may have suppressed it entirely when the time

constant was increased to 2.7 (figure 24c). Presumably the haze represents small bubbles and turbulent fluid, so that the heat transfer should be increased in either case. The heat fluxes used in these experiments as measured by the parameter E/A 3τ, are much larger than those used in the steady state experiments.

I had hoped to compare these pictures and others with pictures of spphs entering the helium. Apparatus problems have prevented my getting such pictures. Experiments to follow the temperature of the heater wire and to observe the boiling at times up to 100 msec were planned but never completed.

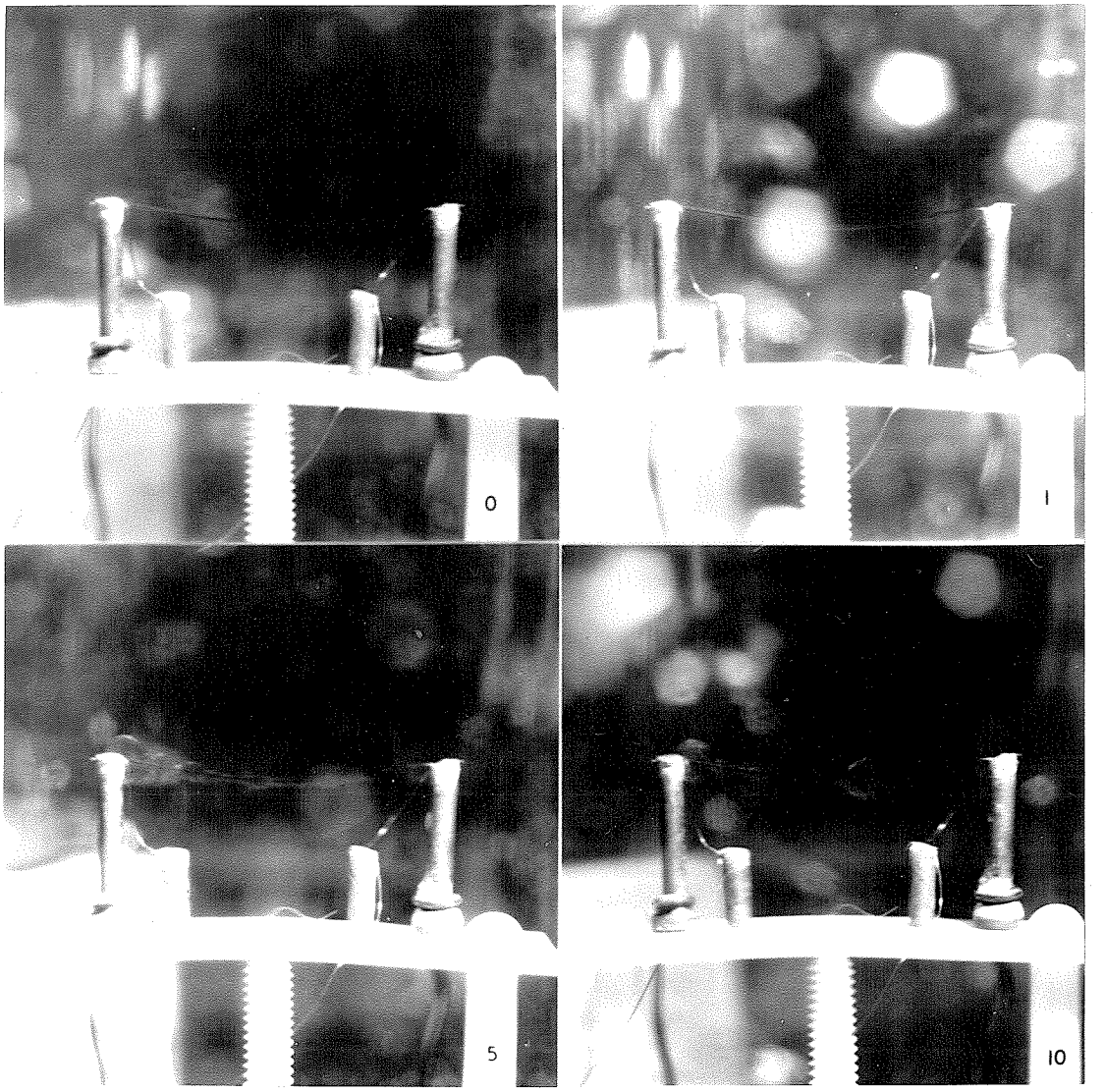

FIGURE 22. Development of the boiling film at 1.5 K. Pictures at 0, 1, 5, and 10 msec after the beginning of the pulse. Pulse time constant = .6 msec.

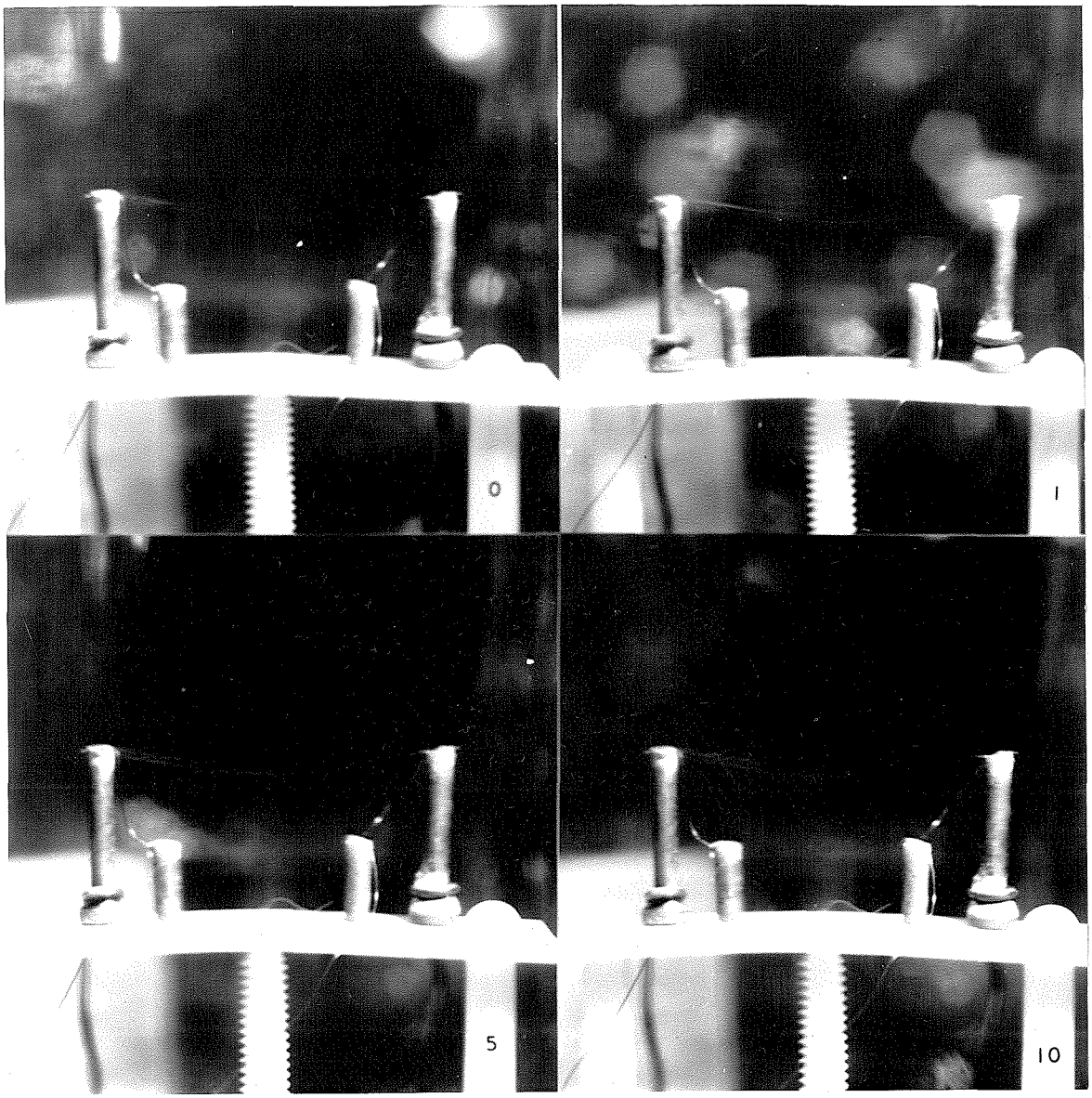

FIGURE 23. Development of the boiling film at 1.9 K. Pictures at 0, 1, 5, and 10 msec after the beginning of the pulse. Pulse time constant = .6 msec.

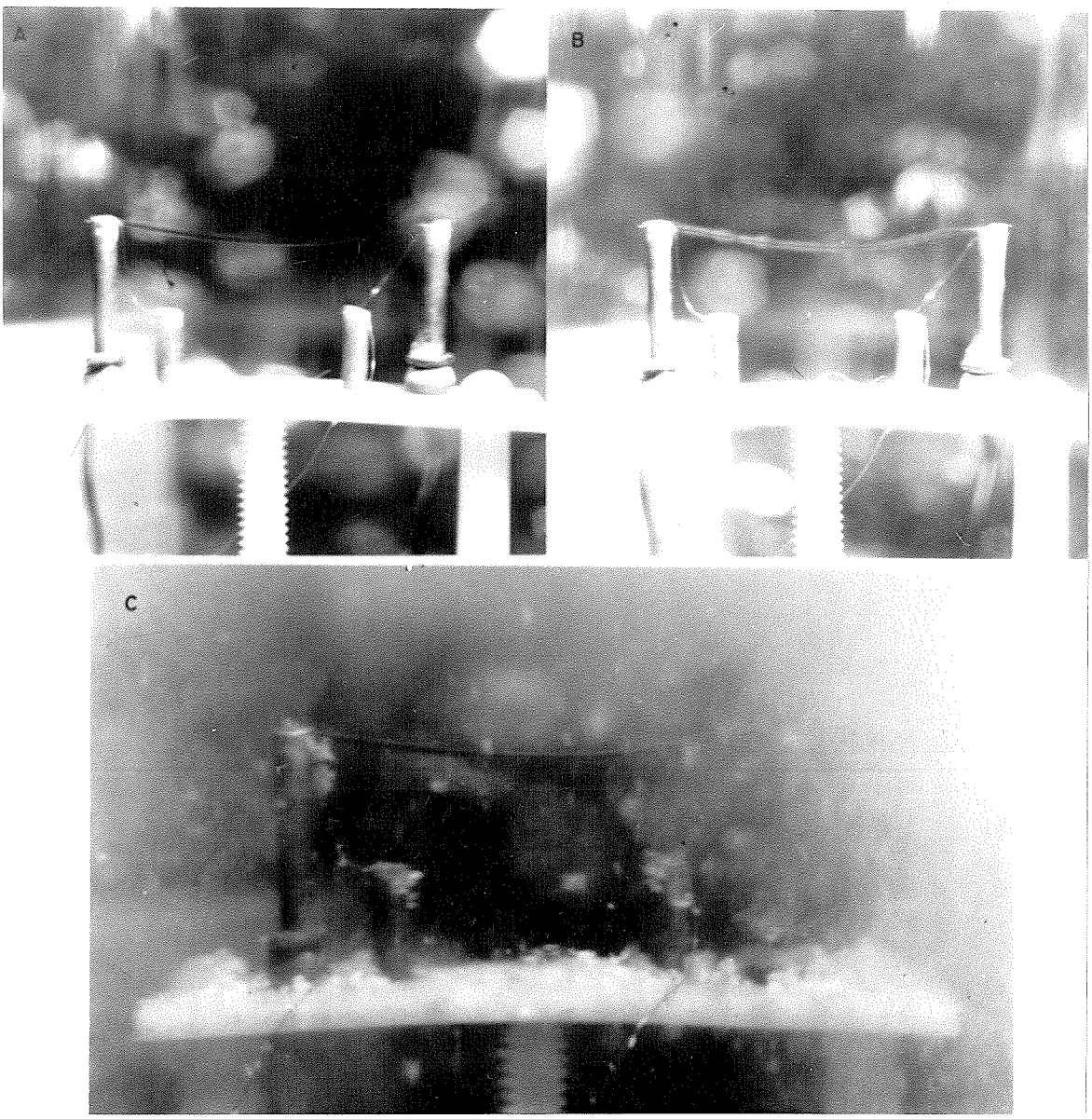

FIGURE 24. Comparison of the boiling film at 2 K and 1 msec after the beginning of the pulse at a) the saturation vapor pressure (23.8 Torr) and b) overpressured (40 Torr); c) shows the boiling film at 5 msec and 40 Torr for a pulse time constant of 2.7 msec.

Chapter 3

FREEZING EXPERIMENTS AND THE ULTRASTRUCTURE OF PHYCOMYCES SPORANGIOPHORES

The freezing of Phycomyces spphs has followed a basic theme with numerous variations. The subsequent preparatory procedures for electron microscopy have differed radically. These include two methods of freeze-substitution with concurrent chemical fixation, and freeze-etching.

Development of the freezing apparatus.

I needed a simple way of transferring spphs quickly from room temperature and atmospheric pressure into superfluid helium at low pressure. After checking that a spph can indeed survive for several minutes at low pressures or in a helium atmosphere, a small demountable vacuum chamber was built to go on top of the helium dewar system. Within this chamber the spph is attached to an iron filing with vaseline and the filing is suspended from an electromagnet (figure 25). Mounted thus, the spph can be released at will by turning off the magnet. If the filing becomes magnetized, it is released by reversing the magnetic field. The soft iron core of the electromagnet has a thin coating of Krylon (acrylic plastic about 0.1 mm thick) to attenuate any residual fields. Power leads for this magnet are #38 formvar coated copper wires which are threaded

through the bottom o-ring seal of this chamber. A hole in the bottom on the chamber (bottom flange) leads to the helium dewar. This hole has a rotating, sliding seal, hereafter referred to as a "trap door." A cut-off Nalgene beaker rests at the bottom of the helium dewar. Most spphs which enter the dewar through the trap door fall into this cup. It is hung from the bottom flange by three cotton threads, so that it can be removed from the dewar easily.

Basic procedure.

A spph is mounted on the electromagnet and positioned over the trap door. The chamber is then reassembled, the air in the chamber is exchanged for helium gas and the pressure adjusted to match that in the helium dewar. Then the trap door is opened; the spph is released into the helium dewar, and the trap door is closed. The chamber is refilled with air and disassembled to load the next spph.

After all the spphs have been frozen and the helium dewar has warmed sufficiently, the bottom flange is raised to lift the cup and spphs out of the helium dewar. Then the cup and spphs are transferred to a nitrogen dewar and stored under liquid nitrogen.

Variations on the basic procedure.

1. Originally the helium was continuously pumped to reach an equilibrium pressure of 1 Torr (which corresponds to 1.25 K), then the pump was shut off and the helium bath allowed to warm just before

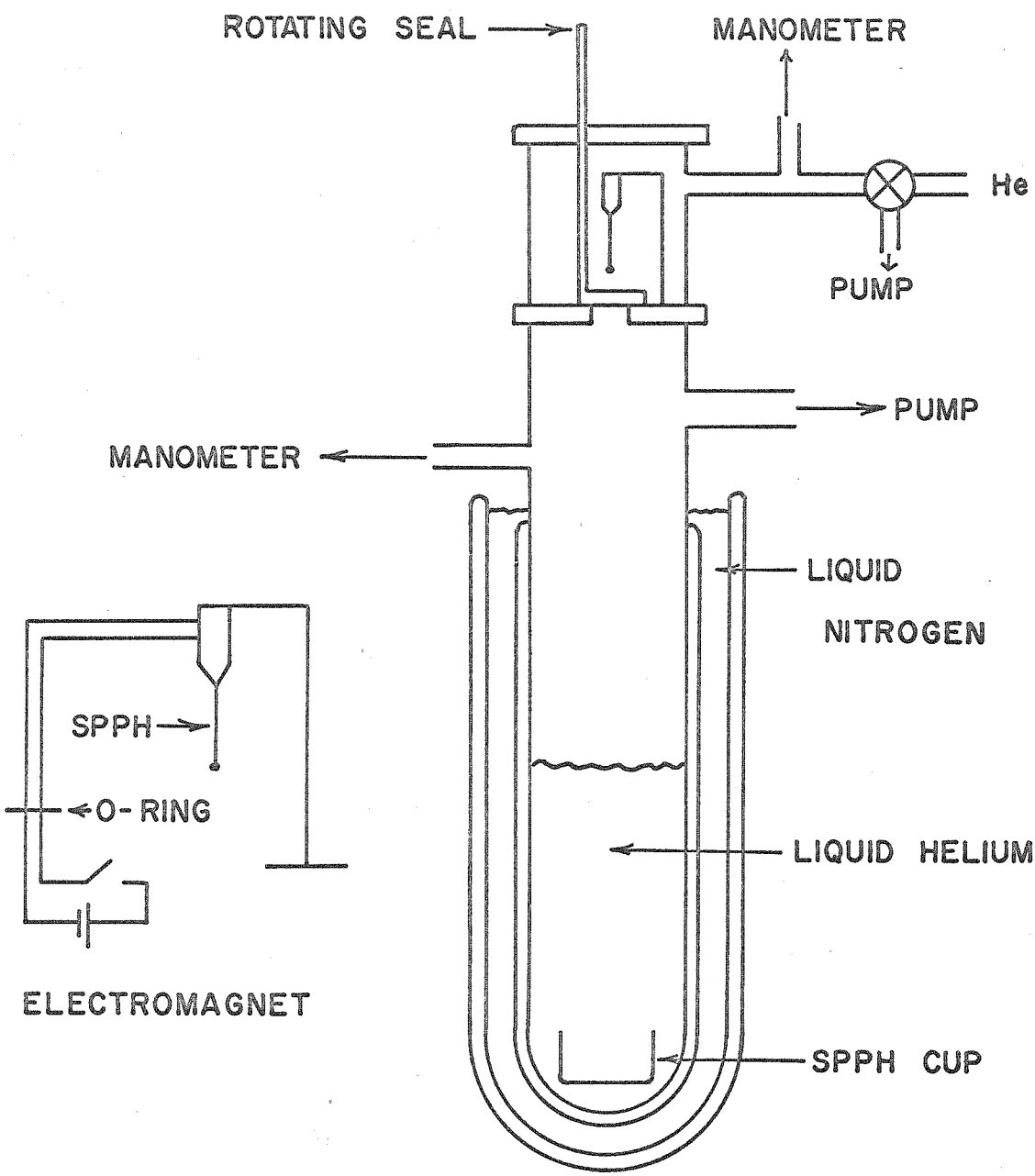

FIGURE 25. Original freezing apparatus. Insert shows a spph attached to the electromagnet by an iron filing.

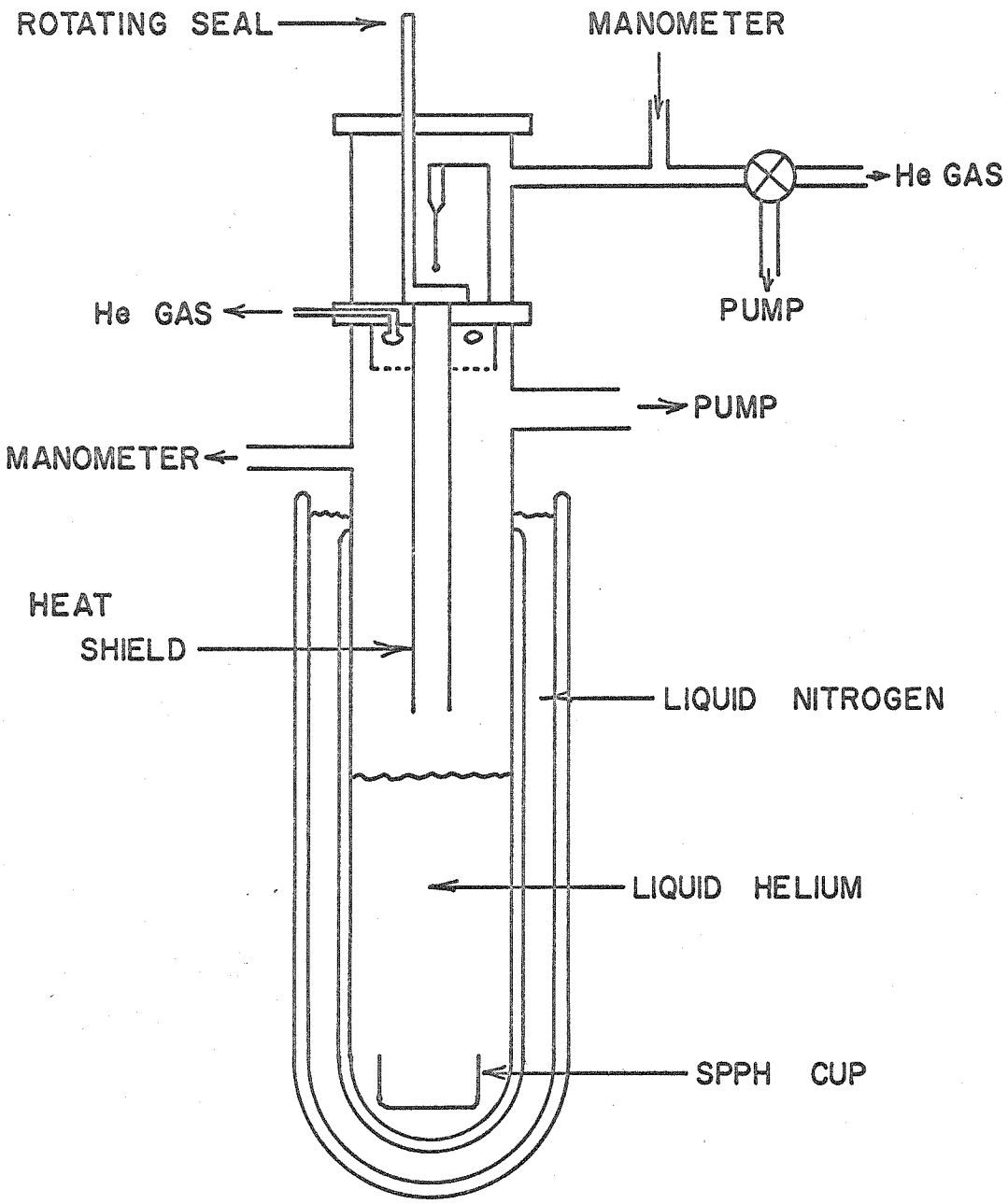

FIGURE 26. Freezing apparatus including overpressure flange and spph heat shield. See figure 14 for details of overpressure flange and heat shield.

and during the spph drop. We thought that the helium bath would rapidly warm to about 1.9 K. However the first "overpressure" experiments showed that the heat leak into the bath is very small (about 300 mwatts) so that the temperature rise is only .02 K/min at 1.9 K. Consequently, in later experiments the equilibrium bath pressure was adjusted to about 17.5 Torr (1.9 K) before the pump was shut off.

2. Transfer of the cup and spphs from the helium dewar to a nitrogen dewar has been done several ways:

a) the cup, full of helium is lifted and transferred to a liquid nitrogen storage dewar;

b) the cup, full of helium, is lifted to the neck of the helium dewar, or to the height of the nitrogen dewar surrounding the helium dewar, liquid nitrogen is poured into the cup which is then transferred;

c) the cup is partially filled with solid nitrogen before the experiment is started; after the spphs have been dropped, the helium is boiled off and the nitrogen is melted, then the cup is lifted and transferred;

d) liquid nitrogen is poured into the helium dewar on top of the cup and spphs; after the nitrogen has melted, the cup is lifted and transferred.

In case a), the helium may boil off before the transfer is completed. In case b), the added nitrogen may freeze the cup into the dewar at some height above the bottom of the helium dewar. In case c), the nitrogen must be cooled to liquid helium temperature. First the nitrogen is cooled to 50 K by pumping on it. Then the dewar is filled with helium gas and the liquid helium transferred immediately. About one liter of liquid helium must be transferred into the helium dewar and then boiled off to cool 50 cc of nitrogen from 50 K to 4 K. In case d), the liquid nitrogen must be poured into the dewar just before the last of the helium boils off. Any spphs that have stuck to the spph heat shield and frozen slowly may be swept into the cup at the bottom of the dewar. Basically, d) is the lazy man's version of c).

3. In one case the spphs were mounted in a sealed tube, lowered about 16 cm into the helium dewar, and shot into the liquid. The spring gun used is a variation on one designed by Marko Zalokar (1966). This procedure was used in a freeze-substitution experiment. The gun was not entirely satisfactory. Unless the spph is released cleanly and uniformly from the clamp, it tumbles and sticks to some part of the gun. The clamp release is not dependable. Further this method of release does not affect the spph heat loss to the helium gas appreciably but it could be used with specimens which can not survive the reduced pressure of the demountable vacuum chamber.

4. As discussed in chapters 1 and 2, the critical heat transfer rate may be increased by applying an additional gas pressure above the liquid. Since this helium gas contracts on cooling and some of it condenses into the liquid, large quantities of gas must be added to the dewar to maintain a supersaturated condition. Gary Brown and Paul Demotakis designed a gas inlet chamber which mixes the turbulent gas thoroughly before it enters the dewar. This chamber is below the spph chamber and the gas entering the dewar does not disturb the spph on the magnet or during its fall into the liquid (figure 26). Some details of this inlet nozzle are shown in figure 14, page 51.

The bath is brought to equilibrium at 1.2 K and the trap door is opened. Helium gas is forced into the dewar through the nozzle. When the pressure in the dewar reaches 40 Torr, the spph is released, the gas valve is closed, and the bath is pumped down to 1.2 K again.

5. The spph heat shield described in chapter 2 is attached to the overpressure flange. After the gas inside the heat shield has been warmed to 250 K or more the freezing is done as described in #4.

Freeze-substitution technique.

Fernandez-Moran first used freeze-substitution for electron microscopy in 1956 (Fernandez-Moran, 1957). He claimed that freeze-substitution in glycerol at -50 C was better than freeze-drying.

His work was followed by that of Bullivant (1960, 1962) who froze retinal rods and pancreas in He II without any cryoprotective agents. Later Bullivant switched to propane cooled with liquid nitrogen as a coolant and heavy glycerination (60%) of the tissue prior to freezing. He dehydrated the tissue with ethanol at -75 C for two weeks and then embedded it in the cold (below 0 C). All these preparations show some crystal damage and shrinkage which is probably due to the pretreatment with glycerol.

Rebhun (1965) investigated many coolants and found propane (or Freon 22) cooled with liquid nitrogen to be the best. He froze and substituted invertebrate eggs at -79 to -85 C in acetone or ethanol-acetone + 1% OsO_4 for two weeks. Embedding was at room temperature. The samples were reputed to turn brown due to reaction with the osmium at low temperatures. Malhotra found that the osmium was inactive until the tissue was warmed to -25 C (personal communication). Rebhun concluded that artifacts are inevitable and that good freezing requires glycerination or drying to inhibit the ice crystallization.

van Harreveld (van Harreveld and Crowell, 1964) has freeze-substituted various nervous system tissues and finds that two days at -85 C in acetone plus 2% OsO_4 is usually sufficient for substitution of animal tissues. Specimens are slowly warmed to room temperature and embedded.

Freeze-substitution of spphs.

Most of the freeze-substitution work reported in this thesis was carried out in Dr. van Harreveld's laboratory. Primary fixation (freezing in helium) and secondary fixation (2% OsO_4 in acetone during substitution) are summarized in table 3. The spphs were usually broken into 1/2 cm lengths and substituted with 2% OsO_4 in acetone at -85 C for 4 to 7 days. Thereafter, they were warmed (-25 C for 3 or more hours, 0 C for 3 or more hours) to room temperature, rinsed in absolute acetone, transferred to propylene oxide, and infiltrated with Epon. The Epon embedding followed the procedure of Luft or Spurr (Sjøstrand, 1967) with the following changes: 0.15 cc benzyldimethylamide per 10 cc Epon were used as the activator for the Spurr Epon; the dehydration and curing sequences were altered to those given in table 2. The cured blocks were cut with an LKB Ultratome and glass knives. Gold or silver sections were collected on parlodion coated copper grids which had been stabilized with a carbon film. They were stained with saturated, aqueous uranyl acetate (Watson, 1958) and lead citrate (Reynolds, 1963), and examined with a Phillips EM 200 electron microscope operated at 60 kv.

Spphs embedded in Spurr's Epon were easier to section than those embedded in Luft Epon and the plastic did not pull away from the sections during cutting. One set of blocks made with Spurr Epon did not cure properly. The Epon was uneven in hardness and fractured

Luft Epon:

5 rinses in absolute acetone (15 min)
2 rinses in propylene oxide (15 min)
1:1 :: Epon:propylene oxide (2 hours)
2:1 :: Epon:propylene oxide (overnight)
transfer to pure Epon in trays (beds)
cure: 37 C (overnight)
45 C (several hours, optional)
60 C (2-3 days)

Spurr epon:

3 rinses in absolute acetone (15 min)
2 rinses in propylene oxide (30-60 min)
1:1 :: Epon:propylene oxide (overnight)
transfer to pure Epon (15-30 min)
transfer to pure Epon in gelatin capsules (overnight)
cure: 37 C (2 days)
45 C (2 days)
50 C (2-3 days)
room temperature (2 days)

Vestopal:

2 rinses in 3:1 :: ethanol: methanol (20 min)
2 rinses in absolute ethanol (15 min)
4:1 :: ethanol:propylene oxide (20 min)
3:2 :: ethanol:propylene oxide (20 min)
1:1 :: ethanol:propylene oxide (15 min)
2:3 :: ethanol:propylene oxide (20 min)
1:4 :: ethanol:propylene oxide (20 min)
3 rinses in propylene oxide (15 min)
(the spphs may be left in the third rinse at 4 C)
1:2 :: Vestopal:propylene oxide and evaporate propylene oxide in a dry atmosphere (1 day)
transfer to pure Vestopal in gelatin capsules (overnight)
cure: 60 C (2 days)

TABLE 2. Embedding procedures.

badly. Sections cut from these blocks spread out on the water surface of the trough behind the glass knife and became extremely thin. The cause of this unsatisfactory curing of the plastic is unknown.

Thornton (1968) found that propylene oxide damaged the cytoplasm of chemically fixed spphs. Nothing was done about this possibility as such damage has not been observed in this laboratory.

Freeze-substitution of stage I spphs.

In collaboration with Marko Zalokar, two sets of stage I spphs were frozen and then substituted using a procedure which has been described in some detail (Zalokar, 1966). Spphs (previously frozen in helium) were placed in a small, open vial containing liquid nitrogen. The vial was then placed in the bottom of a test tube; a funnel containing the frozen substitution medium was set into the test tube above the vial, and the entire assembly was capped. The test tube (temperature about 80 K) was then frozen into an isobutyl alcohol bath which was cooled to its melting temperature (-110 C) with liquid nitrogen. The alcohol bath was surrounded by a dewar full of dry ice (-78.5 C). When the test tube warmed to -110 C the substitution medium (one part eutectic mixture of ethanol and methanol containing uranyl acetate, one part acrolein) melted and flowed into the vial containing the spphs. The dewar full of dry ice

and its entire contents were covered and placed in a deep freeze for 2 - 3 days (-15 C), then it was transferred to a refrigerator (4 C) overnight, and finally the test tube and vial were warmed to room temperature for rinsing and embedding. After rinsing, the spphs were transferred to propylene oxide and embedded in Vestopal. Spphs were infiltrated with a dilute solution of Vestopal in propylene oxide and then the solvent was evaporated in a dry atmosphere. Sectioning and staining procedures were the same as for the other freeze-substituted spphs. The embedding sequence is given in table 2.

The spphs of the first set were full of uniformly sized ice crystals. Those of the second set, which were shot into the liquid helium with the spring gun, also contained ice crystals but the preservation is somewhat better, comparable with some OsO_4 fixed spphs (Peat and Banbury, 1967).

Freeze-etch technique.

This low temperature replica technique was first employed by Hall in 1950. After subliming some surface ice from a frozen suspension of silver halide particles he made a shadowed metal replica of the frozen surface. In 1957 Steere applied the method to suspensions of virus particles. The frozen specimens were cut

with a cold scalpel before insertion into a vacuum evaporator for sublimation and replication. Haggis (1961) improved the technique by cleaving blood smear specimens in the vacuum evaporator just before replication. This procedure prevents contamination of the cold surface by water vapor and organic molecules (Steere, 1969b).

Little use was made of the technique until Moor et al. (1961) presented their excellent micrographs of glycerinated, frozen yeast cells. These results and the then recent work of Fernandez-Moran (1960) on freezing revived interest in the technique, so that a number of these elaborate apparatuses are now in use. The apparatus includes a cold ultramicrotome to cleave the specimen within a high vacuum evaporator. With this machine it is possible to remove a series of thin slices from the specimen. After a smooth surface is obtained, it is etched by warming the specimen to -100 C for a few seconds in a vacuum of 5×10^{-5} to 10^{-6} Torr. This treatment removes a few hundred Angstroms of ice by sublimation. The specimen is recooled to nearly liquid nitrogen temperature and a carbon-platimum shadowed, carbon backed replica is made by evaporation. After warming, the tissue specimen is floated on various aqueous solutions and the tissue dissolved away from the chemically inert replica (see figure 29).

Unfortunately, this apparatus is expensive. Therefore, several attempts have been made to produce replicas with simpler, less expensive apparatus. Steere (1969a) has developed a small

vacuum chamber incorporating sample cooling and a cold remotely controlled scalpel. Bullivant and Ames (1966) developed several simpler methods for making replicas of frozen, fractured specimens with no etching. McAlear and Kreutziger (1967) redesigned Bullivant's cold metal block containing the specimen and a knife to include ports for making the carbon-platinum replica and etching, using either light or joule heating to raise the specimen temperature to about -100 C. Such a device may be used in any vacuum evaporator and produces replicas comparable to those of the more complicated machines. Its major disadvantage is that only one cut can be made through the specimen.[1] The surface left after the first fracture is much rougher than one obtained after multiple cuts and the replica of such a surface is much more fragile and tends to fragment (Marot and Stoeckenius, 1970). The device described in this thesis is a modification of the McAlear and Kreutziger device. The latter device had developed out of a collaboration of Bullivant and McAlear.

---

[1]The cooled microtome of the Moor device permits many cuts to be made. In practice a number of shallow cuts are made after the initial fracture and when a visually smooth surface has been obtained a replica of the specimen is made.

Freeze-etching of spphs.

Figure 27 shows the replica device used with phycomyces. The top half contains a knife holder and razor blade, a port for shadowing the cleaved spph, and a port for evaporating a carbon support film onto the replica. The bottom half contains a spring loaded, vee-shaped grove for holding the spph, a carbon resistance thermometer, and a heater. The device is made of stainless steel which has a large thermal capacity so that the temperature of the device rises slowly to 150 K (figure 28).

Spphs to be replicated are stored under liquid nitrogen in small aluminum boxes. They are transferred to an aluminum loading block which holds the bottom half of the replica device (figure 27) and placed in the vee clamp of the device. The replica device is then assembled, removed from the liquid nitrogen, and immediately placed in a vacuum evaporator. When the pressure in the evaporator reaches 5×10^{-5} Torr, the top of the device is rotated to cut the spph and to align the shadowing and support film ports with their respective electrodes. At this point in the procedure the spph may be warmed to -100 C and "etched" for several seconds. This was not done with the specimens presented in this thesis. Thus they might be called freeze-cleaved, not freeze-etched, however, the generic term has been used. Etching was omitted because of the uncertainties involved in warming unglycerinated

specimens above the glass temperature. In fact, considerable care was taken to keep the spphs below the glass temperature in order to prevent recrystallization. The cleaved specimens show most of the detail of standard freeze-etch preparations (Bullivant and Ames, 1966) and etching need only be done to reveal special details of membranes and other structures (Branton, 1966).

Replica formation.

The cleaved spphs were shadowed with carbon-platinum pellets obtained from Ladd, Inc., and the carbon support film was made with .040 x 5/16 inch carbon rods obtained from the same company. The distances of these electrodes from the specimen and the arrangement of the replica device in the vacuum evaporator are shown in figure 30.

After the replica was made, the device was removed from the vacuum evaporator. The cold, bottom half of the vee-clamp, with the replica and part of the spph attached to the replica, was removed for closer inspection to a spot dish under a dissecting microscope. (The subsequent progress of the replica during all cleaning and mounting procedures was followed with this dissecting microscope.) The spph and attached replica were then transferred to a depression in the spot dish containing water and one or two drops of 1% detergent. The detergent is used to keep the replica from

FIGURE 27. Freeze-etch replica device:

a) view of the top and bottom halves of the device showing the knife, shadowing port, vee-groove, and clamp. The knife is inclined at 20°.

b) device in basin which is filled with liquid nitrogen during transfer of spphs from the small aluminum boxes into the vee-clamp.

A

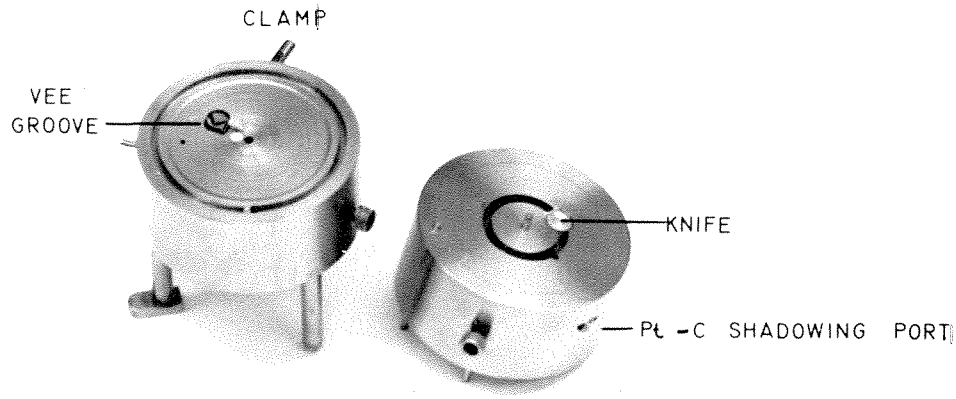

ONE INCH

B

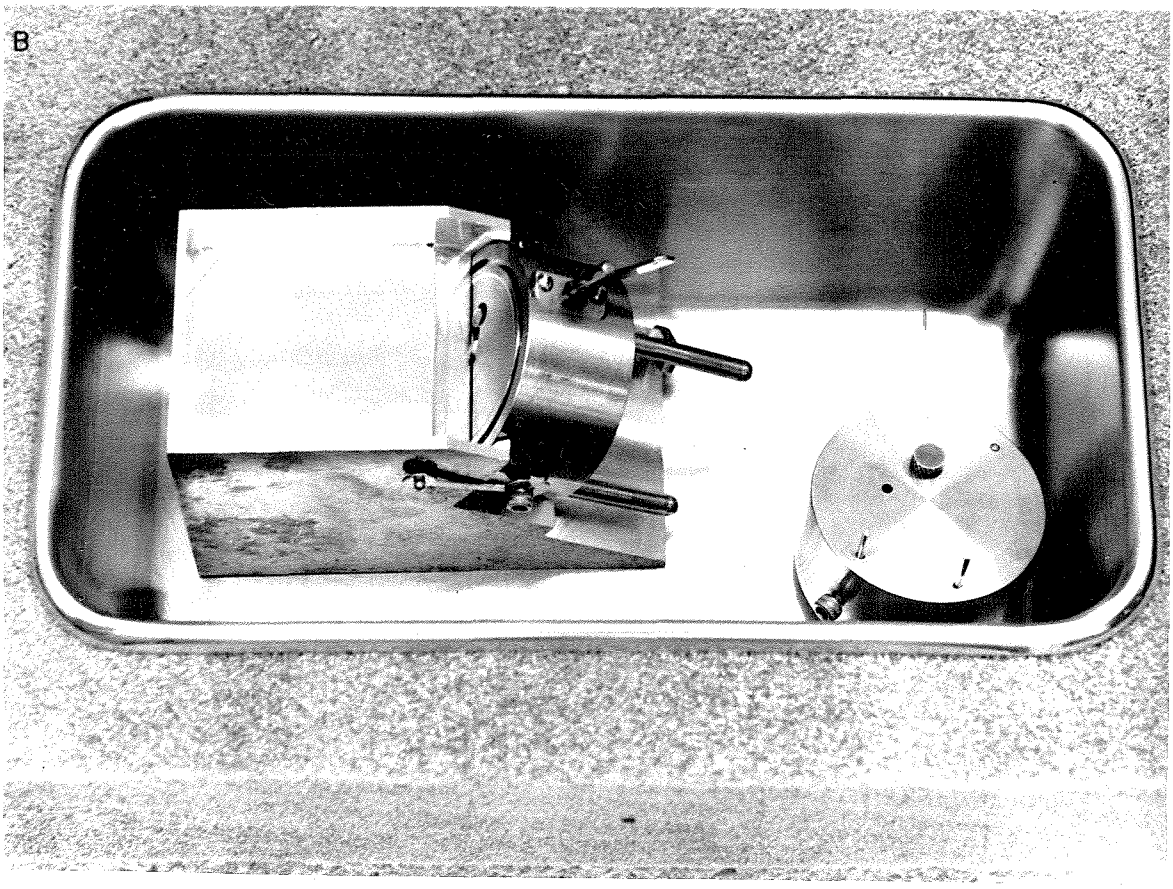

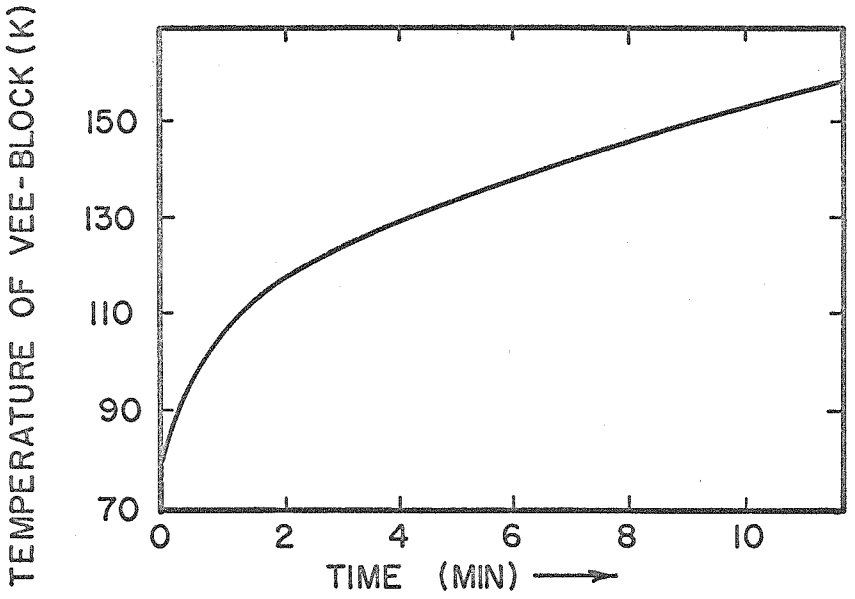

FIGURE 28. Warming curve for the stainless steel replica device in air: temperature of the vee-clamp as a function of the time after removal of the device from liquid nitrogen.

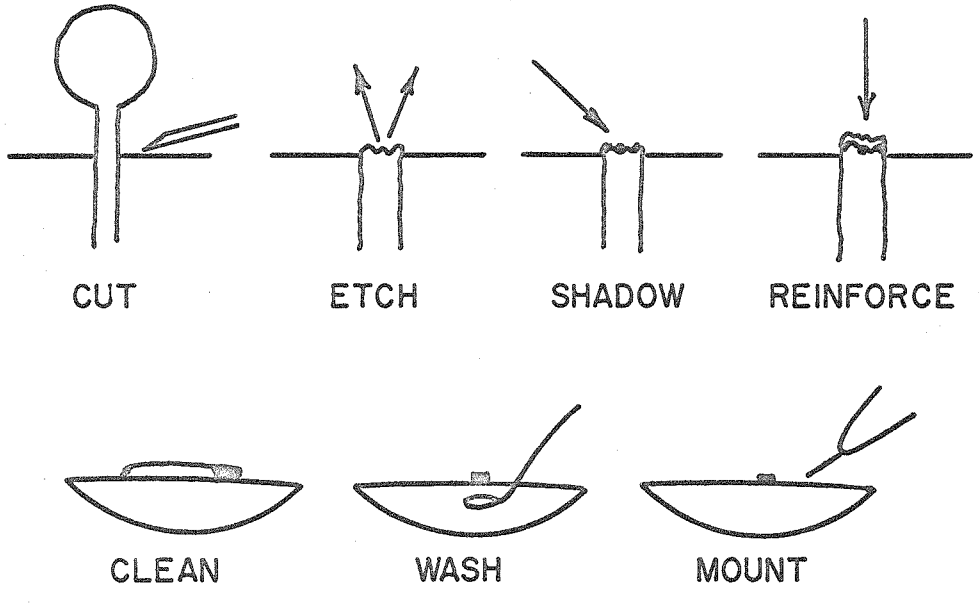

FIGURE 29. Freeze-etching.

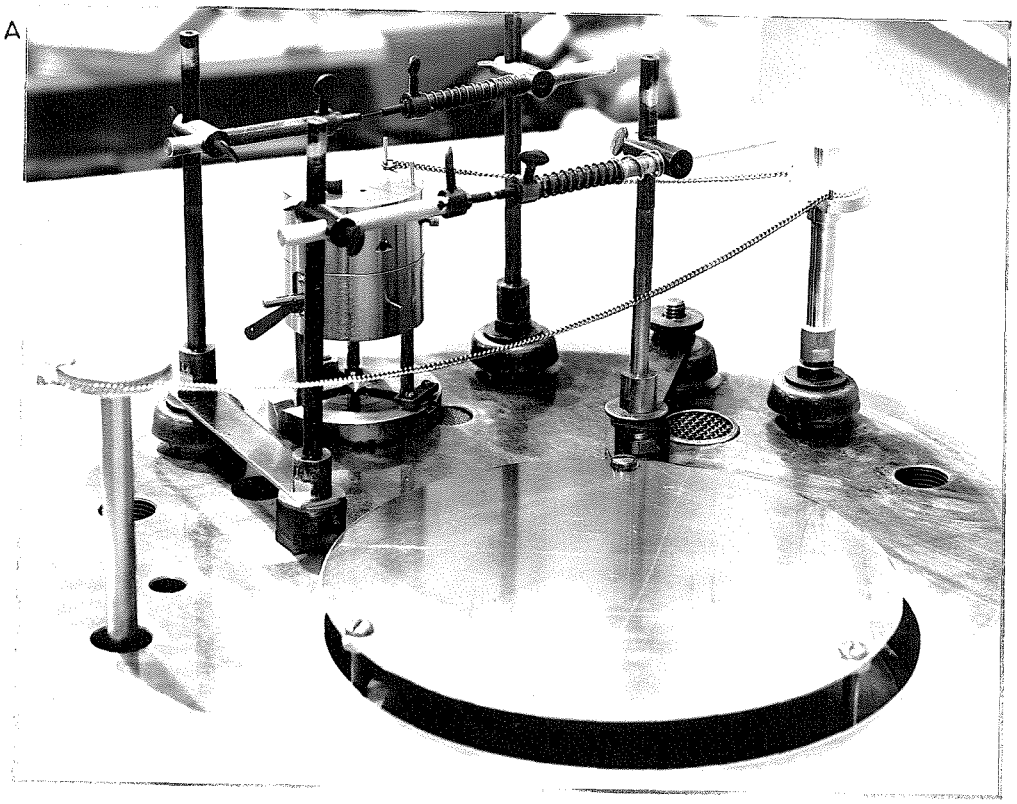

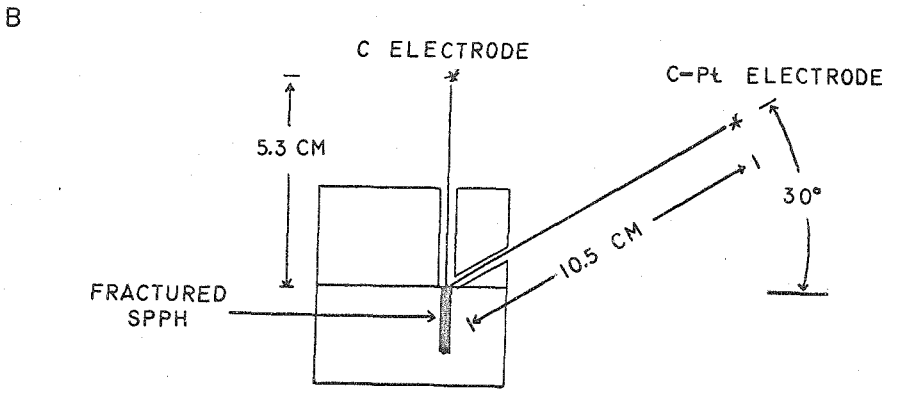

FIGURE 30. Stainless steel replica device set up inside the vacuum evaporator. a) photograph of the set up showing the electrodes, the C-Pt shadowing port and C backing film port within the device, and the rotating shaft and chain for rotating the top of the device to fracture the spph and align the ports with the electrodes; b) diagram showing the relevant dimensions.

disintegrating as it is floated on the water surface (Anderson, 1956).

Cleaning the replica.

Cleaning is one of the major problems of freeze-etching because it must be thorough but gentle so as not to break up the replica. In the case of spphs, nitric acid, sulfuric acid, hydrochloric acid, phosphoric acid, Purex bleach, 10 N NaOH, concentrated KOH, chloroform:methanol, ethanol, and chitinase have been tried in various combinations and at various temperatures. Purex followed by concentrated sulfuric acid has been used to clean replicas of spphs frozen in liquid nitrogen, but it has not been successful in cleaning replicas of spphs frozen in liquid helium II. Hot, concentrated phosphoric acid is also effective in cleaning replicas of liquid nitrogen frozen spphs. Presumably replicas of specimens with few or no ice crystals are harder to clean (Oscar Kreutziger, personal communication).

The following cleaning sequence was finally worked out: several drops of 50% chromic acid are added to the weak detergent solution on which the replica and spph float. This solution is left for several hours at room temperature. Five or ten more drops of acid are added and after another hour the spph plus replica is transferred to 50% chromic acid with a platinum loop. Again the replica is

left for several hours at room temperature. Then the solution is heated to 75 C for 12 or more hours. After the solution has cooled at room temperature it is diluted by allowing the acid to adsorb water (chromic acid is deliquescent), and apparently clean pieces of replica are transferred to water and picked up on bare copper electron microscope grids (300 or 400 mesh size). The copper grids are wetted by dipping them in ethanol and then water just before picking up the replica from the water surface. Pieces of replica which are still attached to spph cuticle or cell wall are transferred to NaOH or 70% chromic acid for further cleaning, at 75 C. Thorough cleaning of the replica usually requires treatment with 70% chromic acid at 75 C for several hours.

If the replica becomes wet and sinks into the cleaning solution (an unfortunate but not infrequent occurrence), it may be transferred from solution to solution with a small glass ladle. In such cases it is usually necessary to "blow" the replica off the bottom of the spot dish with a small glass blow pipe and then catch it in the ladle as it settles through the liquid. If less extreme cleaning methods are used, the replica can usually be floated on the surface of the aqueous solution.

The dissecting microscope is inclined at 6° to the vertical and illumination is with a small fluorescent lamp. With this system the liquid surface may be viewed in reflected or diffuse light.

Thus pieces of replica can be distinguished from small particles of dirt, which are always present, by looking for objects which reflect light strongly but are light gray in transmitted light (see figure 31 for a picture of the cleaning set up). Such extreme measures are not necessary if the replicas are large and stable, but they aid retrieval of the replica if it is thin and fragments.

Electron micrographs.

The results of the various freezing experiments are given in table 3; although there is extensive ice crystal damage, some information may be gleaned from the micrographs. The various organelles are easily distinguishable and are seen in several groupings near the cell wall and the tonoplast. The cell wall is well preserved and shows a three part structure in the thin sections of freeze-substituted spphs.

Freeze-etching may yield considerable information about the membranous structures of the spph if ice crystal damage can be prevented. Several replicas of liquid nitrogen frozen spphs are presented here to illustrate the possibilities of this technique.

Ice crystal damage is less extensive in stage I spphs than in stage IV spphs. Presumably, this is related to the increased size of the central vacuole. The crystal size is uniform in

FIGURE 31. Equipment used to clean the replicas. Note the tilted microscope and small fluorescent lamp.

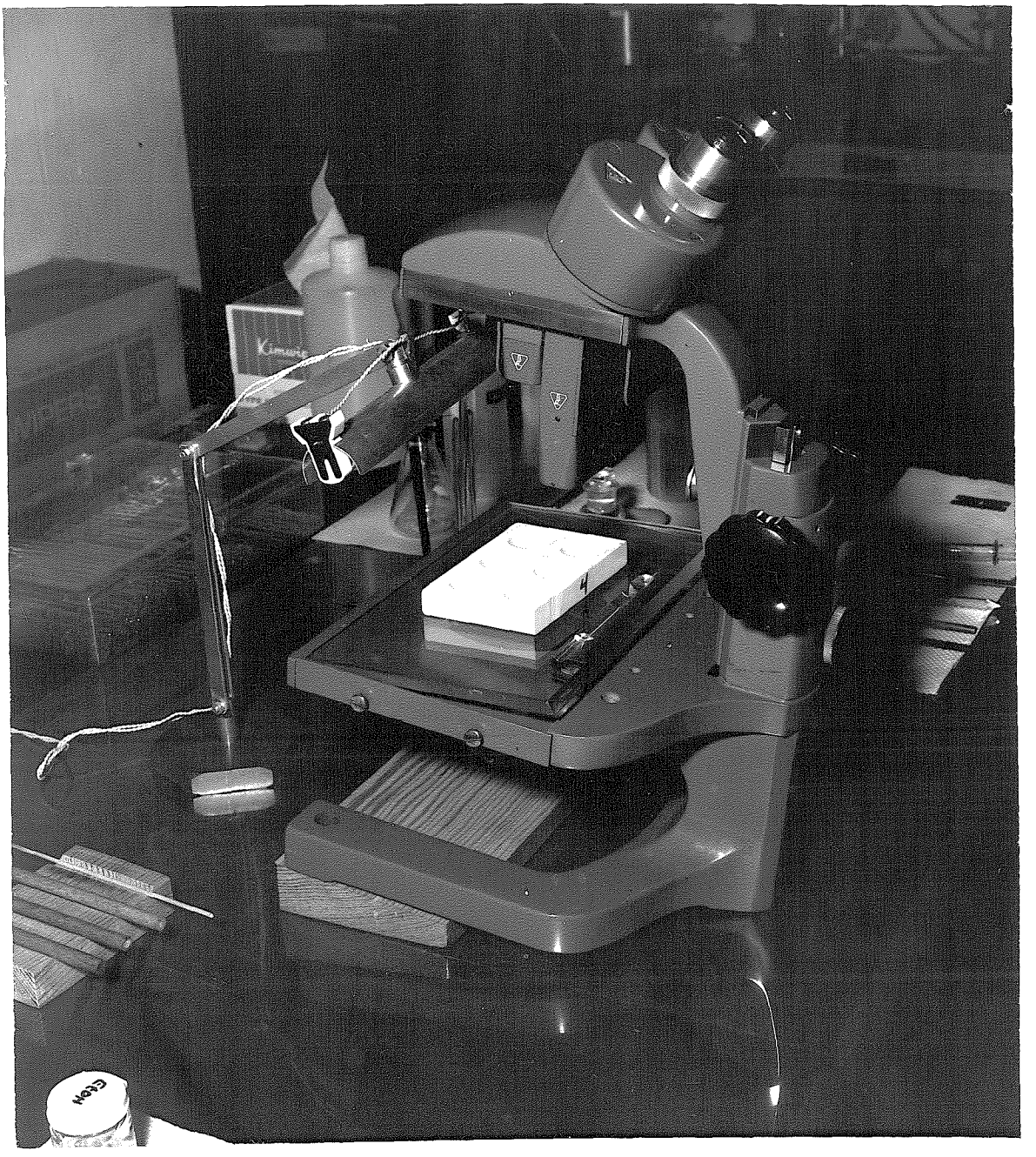
Kimaire

	Material	Primary fixation	Secondary fixation	Prep. for E.M.	Results
1.	stage IV's	frozen in He II at 1.2 K	substituted with 2% OsO_4 in acetone at -85 C for 4 days	embedded in Luft's Epon, sectioned, and stained	rather uniform ice crystals, 1-2 μ in size
2.	stage IV's	"	broken into .5 cm pieces and substituted for 7 days as in #1	"	similar to #1
3.	stage I's	"	done by Zalokar, probably as in #4	embedded in Vesto-pal, sectioned, and stained	"full of ice crystals" of rather uniform size
4.	stage I's	shot into He II at 1.2 K with spring gun	substituted with 50% acrolein in a eutectic mixture of ethanol-methanol plus uranyl acetate for 3 days	"	ice crystals, but smaller than those in stage IV's
5.	stage IV's	frozen in over-pressured He II	broken into .5 cm pieces and substituted for 6 days as in #1	embedded in Spurr's Epon, sectioned, and stained	size of ice crystals increases with distance from cell wall
6.	stage IV's	frozen in over-pressured HeIII using heat shield	broken into .5 cm pieces and substituted for 5 days as in #1	"	ice crystals less than 1 μ near cell wall

TABLE 3. a. Fixation procedures and results: freeze-substitution.

	Material	Primary fixation	Secondary fixation	Prep. for E. M.	Results
1.	stage II's stage IV's	frozen in He II at 1.9 K	none; may have warmed during transfer to liquid nitrogen	freeze-fracture replica	unidentifiable replicas, very dirty replicas, and replicas of the cuticle
2.	stage I's	frozen in over-pressured He II	"	"	"
3.	stage IV's	frozen in He II at 1.9 K	none	"	dirty replicas
4.	stage I's	frozen in over-pressured He II	none	"	"
5.	stage IV's	frozen in over-pressured He II using heat shield	none	"	dirty replicas, replicas of the cuticle, unidentifiable replicas

TABLE 3 (continued)

b. Fixation procedures and results: freeze-etching.

stage IV spphs frozen at 1.2 K. In spphs frozen at 2 K in over-pressured liquid He II the crystals are graduated in size (small near the wall and larger near the vacuole). In the case of large, uniform ice crystals, the organelles are dehydrated, severely squashed, and distorted. Such organelles show no internal ice crystals. If the crystals are graduated in size, the nucleus frequently show internal ice crystal damage.

Figure 32 is a survey micrograph of a stage IV spph. It shows the appearance of the growing zone after chemical fixation (5% acrolein plus 5% glutaraldehyde in cacodylate buffer at pH 7.0, as described by Zalokar (1969), postfixed in 1% OsO_4). There are numerous vacuoles and mitochondria in the groundplasm. Some of the small, spherical bodies are probably lipid droplets. The absence of glycogen granules may be due to section thickness and the low magnification.

Figure 33 shows a freeze-substituted stage I spph which was frozen in liquid helium II at 1.2 K and prepared for electron microscopy in collaboration with Marko Zalokar. The vesicular cytoplasm is presumably due to many small ice crystals. It is similar in appearance to micrographs of OsO_4 fixed spphs and the layers of endoplasmic reticulum and membranes and vesicles found by Zalokar (1969) in centrifuged spphs. Some of the empty spaces contained lipid before substitution. The dark spots may be glycogen.

Ice crystal damage is much more extensive in stage IV spphs as shown in figure 34. The ice crystals are quite small near the plasmalemma but grow in size as they approach the vacuole. The crystals within the vacuole are uniform in size and larger than those in the cytoplasm (2 or more μ depending on the preparation). The appearance of the cytoplasm near the columella (figure 35) is similar to that in the growing zone (figure 34) and contrasts strongly with the fixation of the sporangium just inside the columella. However, fixation within the sporangium can be excellent near the outer wall of the sporangium (figure 36). The groundplasm there looks the same as that seen with glutaraldehyde fixation (Malhotra, unpublished).

The cell wall itself is very well preserved by freeze-substitution and show a three layer structure (figures 37 and 38). The palisade structure of the outermost layer has not been reported before.

Figure 39 shows the state of preservation of mitochondria and nuclei after freeze-substitution, when ice crystal damage occurs. The organelles are dehydrated and displaced. The spph in figure 39a was frozen in liquid He II at 1.2 K. The organelles apparently dehydrated without interior ice crystal damage. The double membrane around the nucleus can be seen in several places. It appears to separate from the nucleus and extend out into the cytoplasm. Such

a proliferation of the nuclear envelope is the source of endoplasmic reticulum in several fungi (Hawker, 1965) and has been seen in Phycomyces before by Thornton (1966). The spphs pictured in 39b,c were frozen in liquid He II with an over-pressure of 80 Torr. There is ice crystal damage within the nuclei. Note that the mitochondrion in 39c is inside an autophagic vesicle (Thornton, 1968).

Figure 40 shows a cluster of organelles near the cell wall of a stage IV spph. There are several multivesicular bodies (Peat and Banbury, 1967). The lightly colored particles are probably lipid. Other particles with debris inside them may be autophagic vesicles. Figure 41a shows a group of endoplasmic cisternae near the vacuole. There are several mitochondria within the group. Similar things have been seen with chemical fixation (Thornton, 1968).

Figure 41b is a replica of a helium frozen spph. The upper portion of the picture is probably cuticle on the outside of the cell wall. The bottom may be plasmalemma with many pores (arrow). Most of the replicas retrieved for electron microscopy have been of cuticle or cell wall. This happens because the spph and the replica of the spph cross section tend to sink into the cleaning solutions as the spph dissolves, while the cuticle comes free and floats on the liquid surface. Figure 42 shows another such replica. The outer surface (right hand side of the figure) where

the cuticle has lifted off the wall, is much smoother than previously reported. Previous work on the structure of the cell wall has dealt with walls treated with acid or alkali (Frey-Wyssling and Mühlethaler, 1950; Roelofsen, 1951). Luckily, Roelofsen (1951) published one micrograph of a cuticle replica which made possible the identification of many replicas made with the freeze-etch technique employed here.

I have included several micrographs of a replica made of a stage I spph frozen in liquid nitrogen. (Many replicas of liquid nitrogen frozen spphs were made during the development of the freeze-etch apparatus and used to devise a suitable replica cleaning procedure for spphs.) This spph was full of ice crystals but the micrographs show the various organelles and illustrate the different perspective given by freeze-etching. Figure 43 shows spphs prepared by freeze-substitution and by freeze-etching. The detailed structure of the cytoplasm between the ice crystals is much better illustrated in the freeze-etch preparation. The replica also shows some details of the membrane structure of the organelles. Relief within the replica is considerable (several microns) so that one replica may contain as much information about an organelle as many serial sections. However, this relief also makes the replica fragile and is responsible for the many cracks in the micrograph. At higher magnification, the glycogen granules

within the cytoplasm are easily distinguished (figure 44b) and particles on the membrane surfaces can be seen. Apparently the fracture may be through the membrane itself or along the surface. The location is determined in part by the type of membrane and in part by the prefreezing treatment. The propensity of frozen material to fracture along or through membrane surfaces has led to considerable work on the structure of membranes using freeze-etching (Branton, 1966; Branton and Park, 1967; Northcote and Lewis, 1968; Staehelin, 1968; Fluck et al., 1969). The membrane of a possible mitochondrion at the top of figure 45 has fractured in two ways revealing two surfaces which may be the inside of the membrane and membrane surface bordering the cytoplasm. Presently, there are not enough data to distinguish the various surfaces and etching is required to properly identify them (Branton, 1966). Cross-sectional breaks through the organelles sometimes reveal an internal structure (figure 44). Mitochondria sometimes fracture along internal membranes and lipid particles frequently fracture to reveal layers (figure 45). The layered lipid particles in figure 45 are very similar to the lipid droplets in yeast (Moor and Mühlethaler, 1963). The crystalline array (F in figure 45) on one particle is ferritin which occurs in crystalline arrays on lipid droplets in Phycomyces (David, 1968).

Key to Abbreviations

CY	cytoplasm
F	lattice of particles, presumably ferritin
G	glycogen
I C	ice crystal
L	lipid particle
M	mitochondrion
M P	membrane with particles
M V	multivesicular body
N	nucleus
PL	plasmalemma
T	tonoplast
V	vesicle or multivesicular body
VAC	vacuole
W	cell wall

Lines in micrographs are 1 μ unless otherwise noted.

FIGURE 32. Transverse section through a stage IV spph fixed in acrolein plus glutaraldehyde.

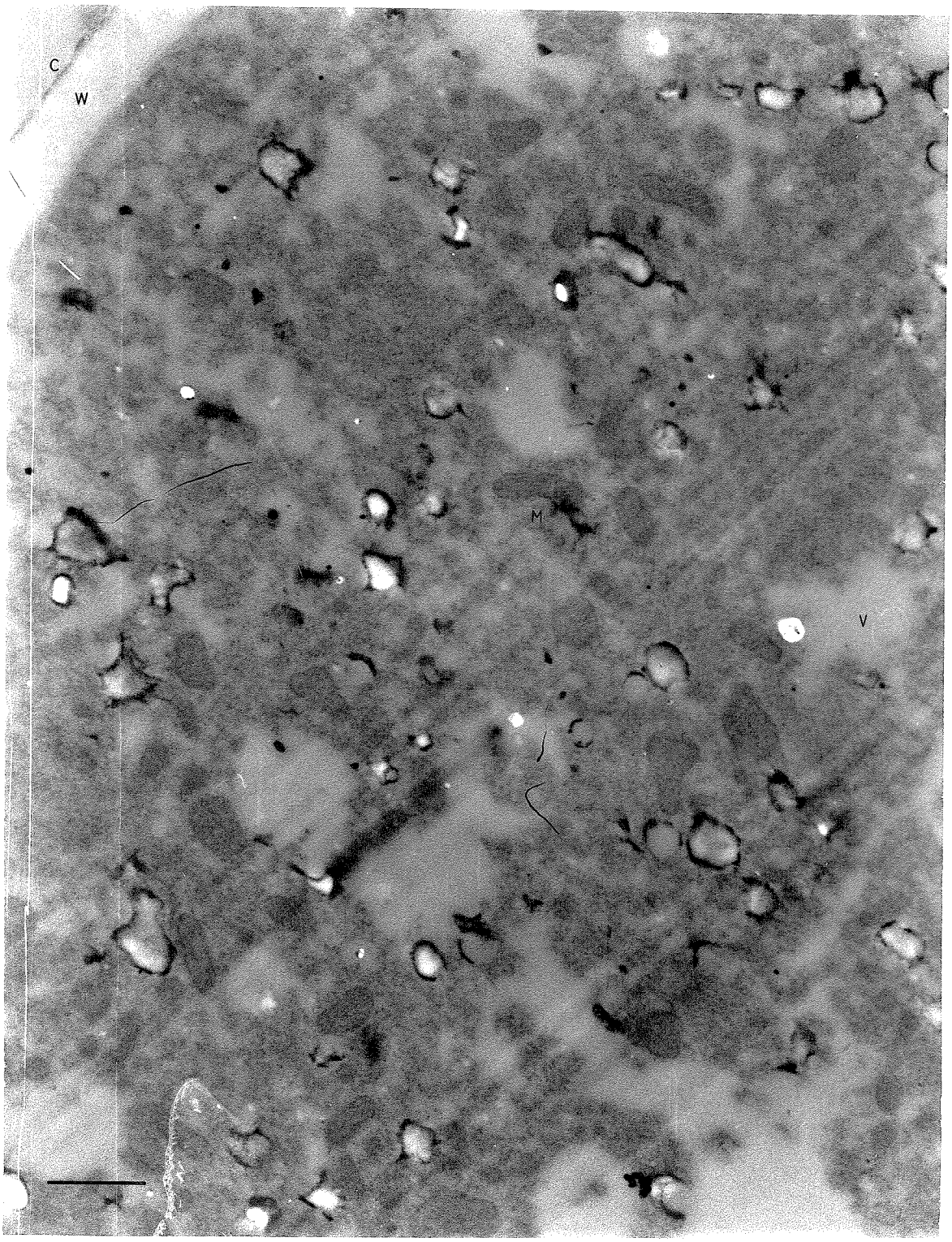
C
W
M
V

FIGURE 33. Transverse section through a stage I spph frozen in liquid He II at 1.2 K and substituted with alcohol and acrolein. Some of the medium sized holes contained lipid droplets before substitution.

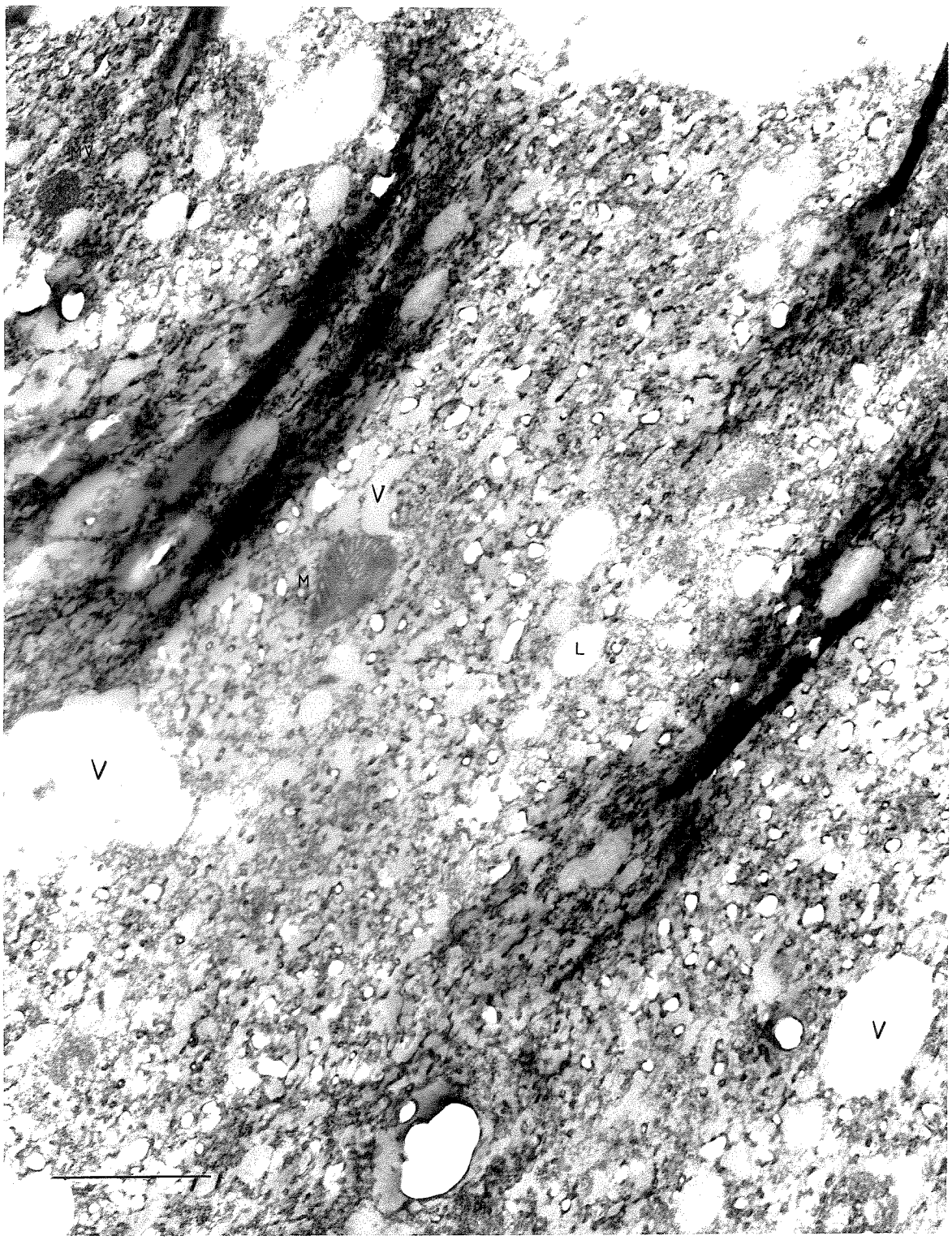
MY
V
M
L
V
V

FIGURE 34. Transverse section through a stage IV spph frozen in liquid He II with an overpressure of 80 Torr, and substituted with acetone at -85 C. Note the gradient in ice crystal size between the cell wall and the vacuole.

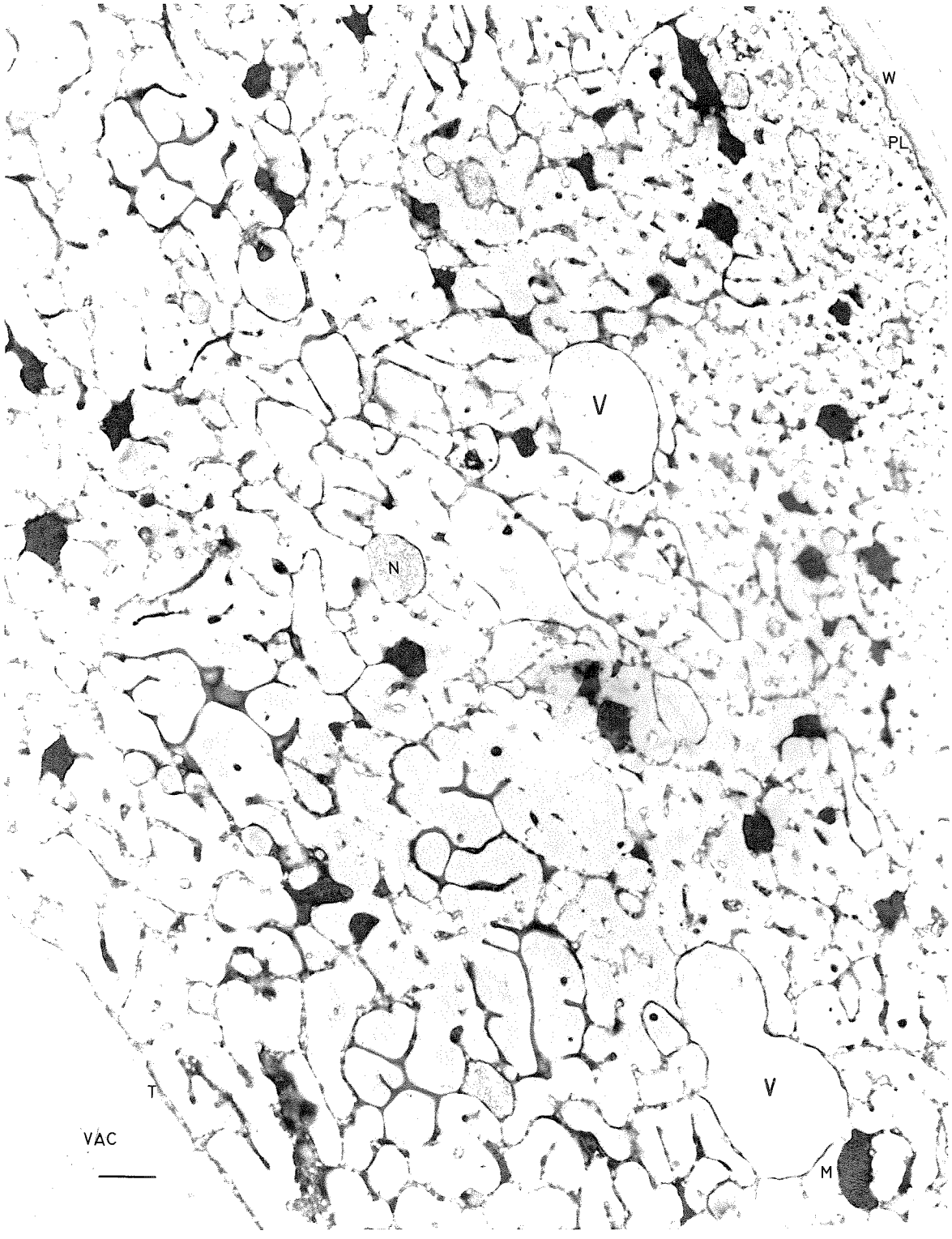
W
PL
V
N
V
T
VAC
M

FIGURE 35. Section through the columella of a stage IV spph (same preparation as figure 34). The same gradient in ice crystal size exists in the cytoplasm as in figure 34. The ice crystals in the sporangium are much larger.

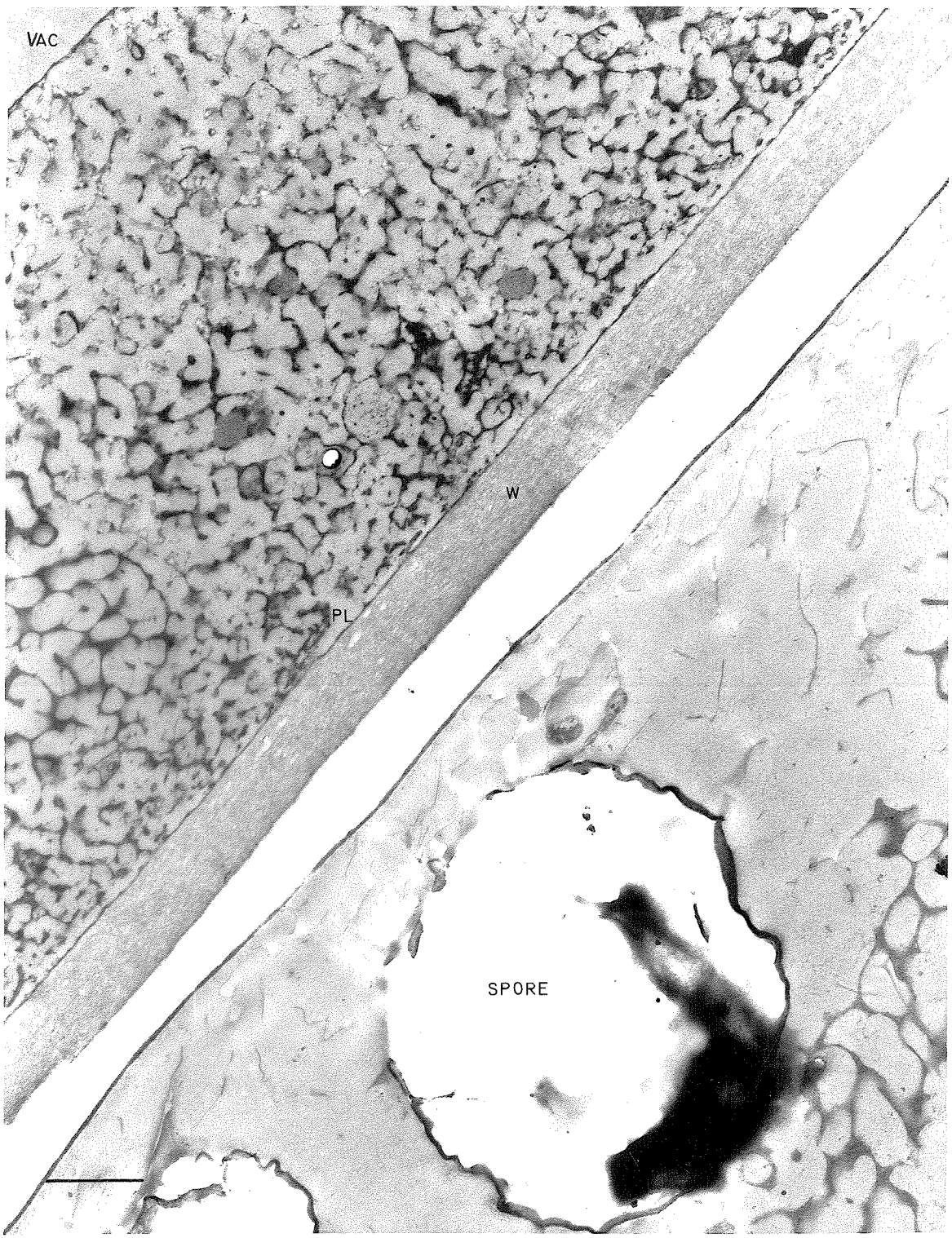
VAC
W
PL
SPORE

FIGURE 36. Same sporangium as shown in figure 35 but near the outer wall of the sporangium. The matrix between the spores is well preserved near the wall.

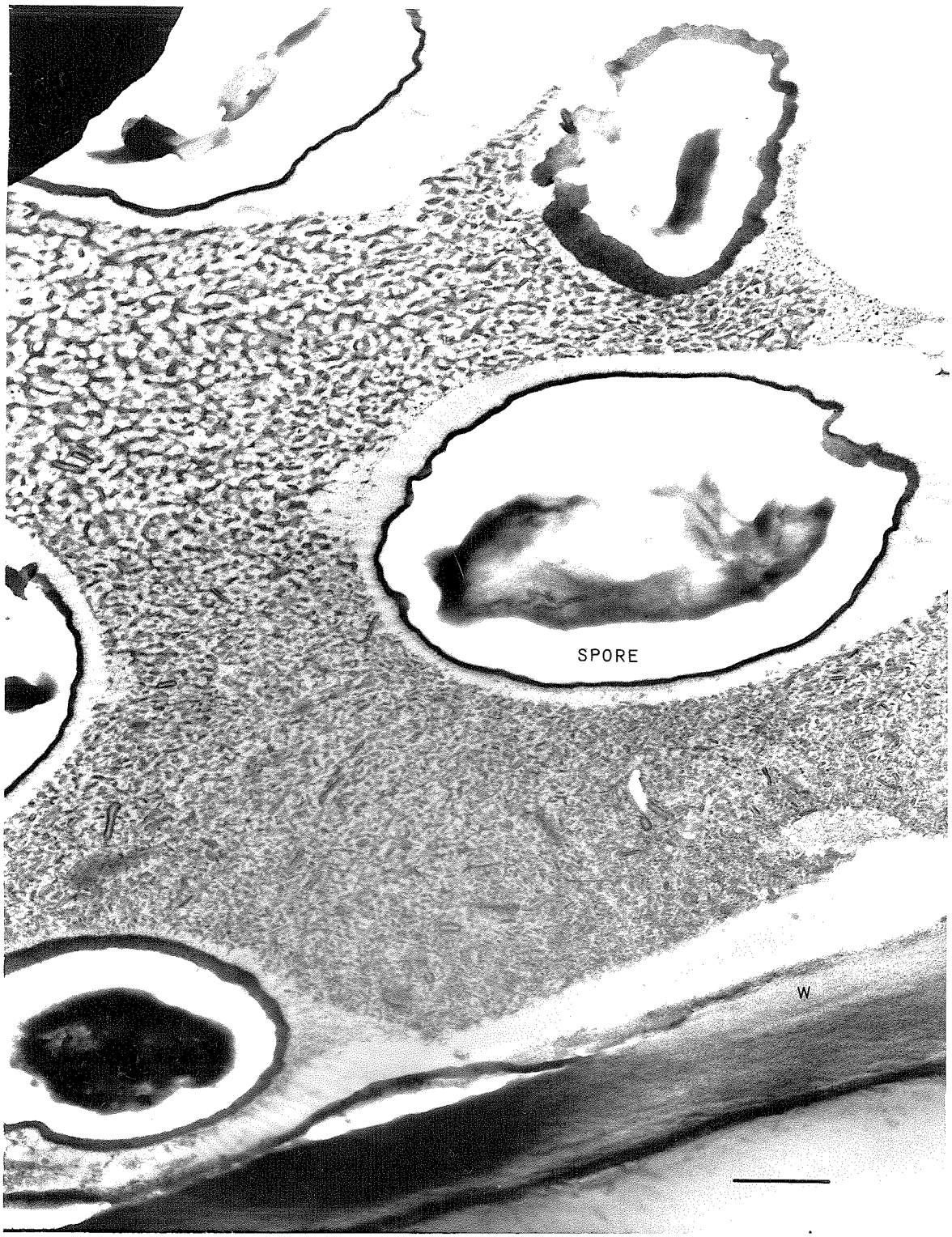
SPORE
W

FIGURE 37. Cell wall and plasmalemma of a stage IV spph frozen with overpressured helium. The wall has three layers. The outer, palisade structure (arrow) has not been seen before.

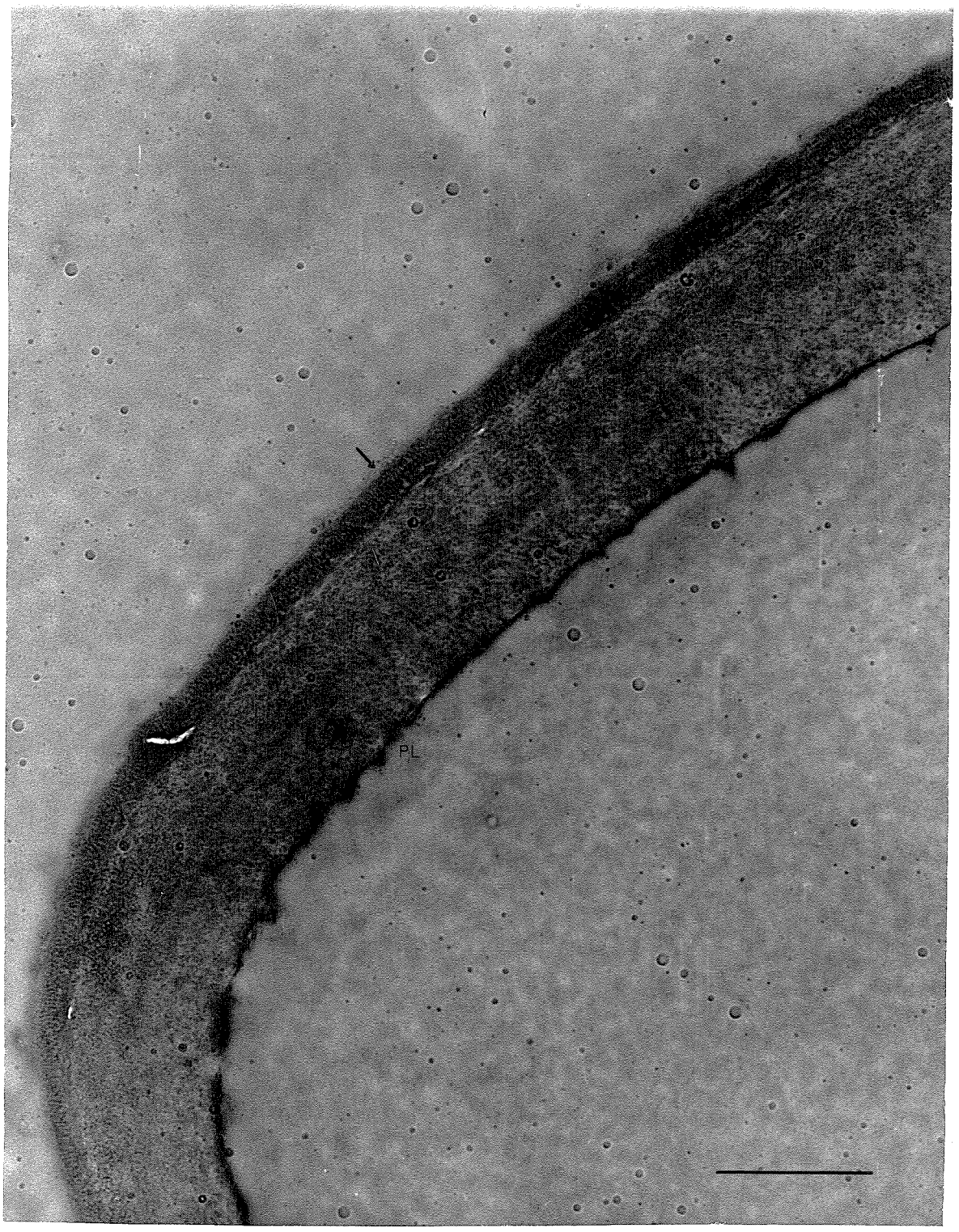
PL

FIGURE 38. Enlargement of figure 37 showing detail of wall and membrane.

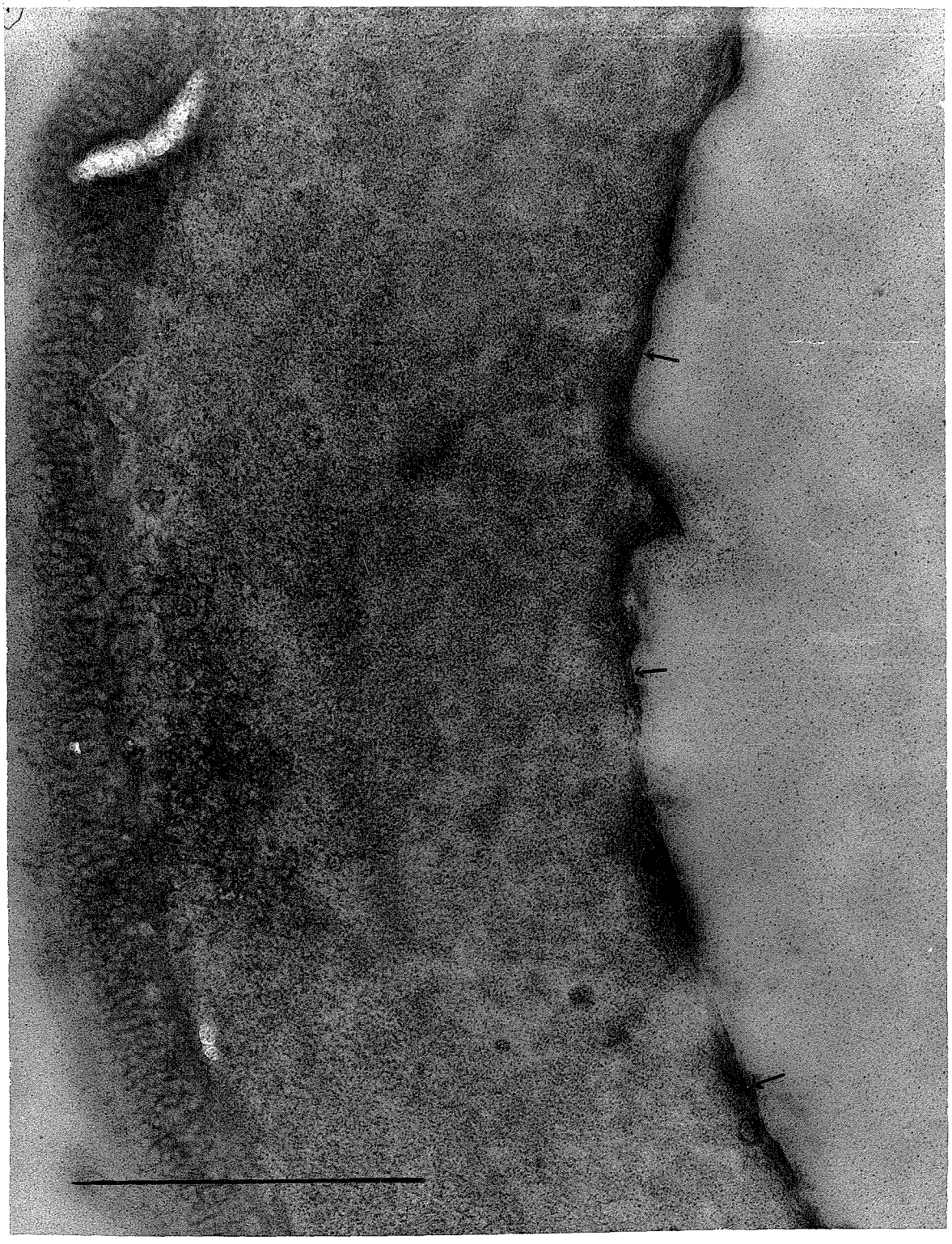

FIGURE 39. Organelles inside freeze-substituted spphs with ice crystal damage; a) spph frozen in liquid He II at 1.2 K. Organelles are dehydrated but show no internal crystal damage. Note the double membrane around the nucleus. b) and c) spph frozen in overpressured helium. The nuclei show internal ice crystal damage.


N
M
.1μ

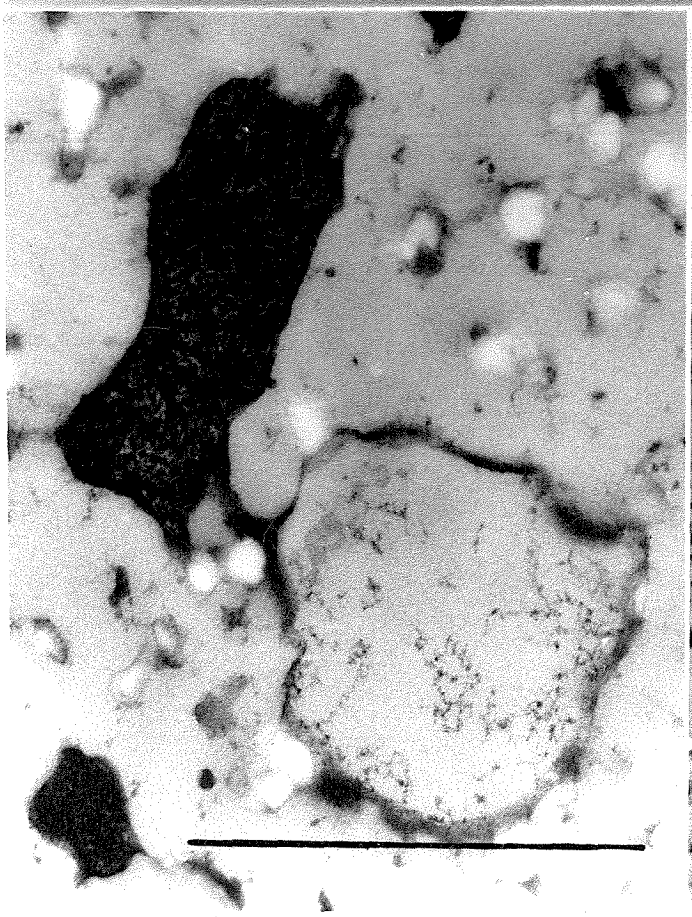


W
MV
L
N

FIGURE 40. A group of particles near the wall of a stage IV spph growing zone.

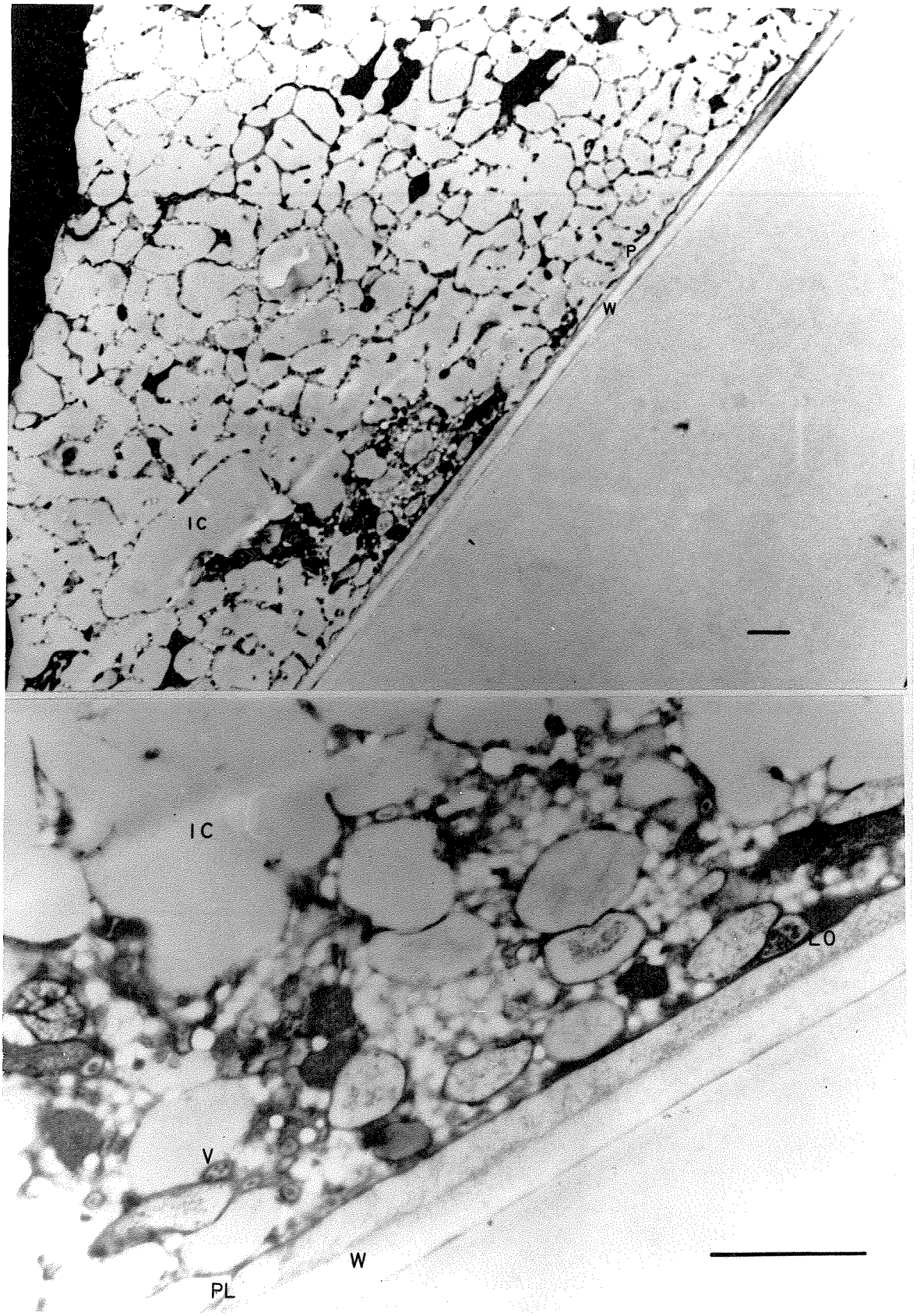
P
W
IC
IC
LO
V
W
PL

FIGURE 41. a) Endoplasmic cisternae near the vacuole of a stage IV spph. b) Replica of the wall of a helium frozen stage IV spph. The region at the bottom may be plasmalemma with pores (arrow).

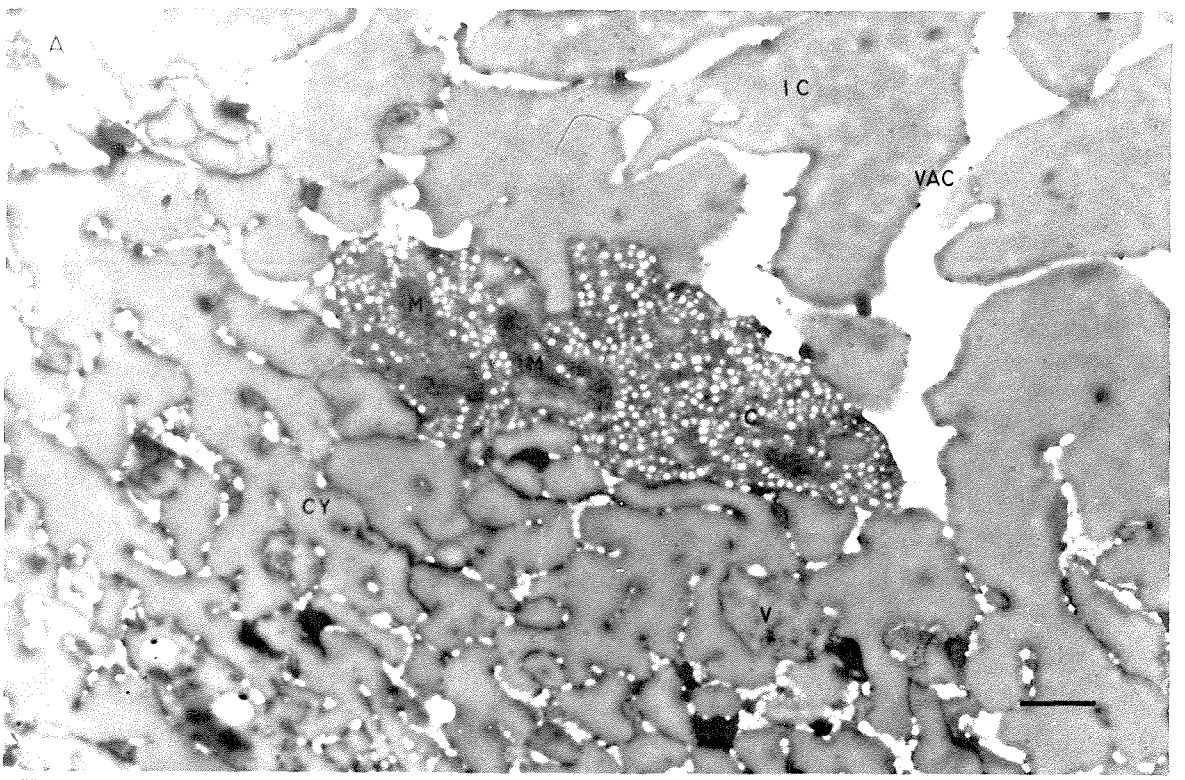
A
IC
VAC
M
M
C
CY
V

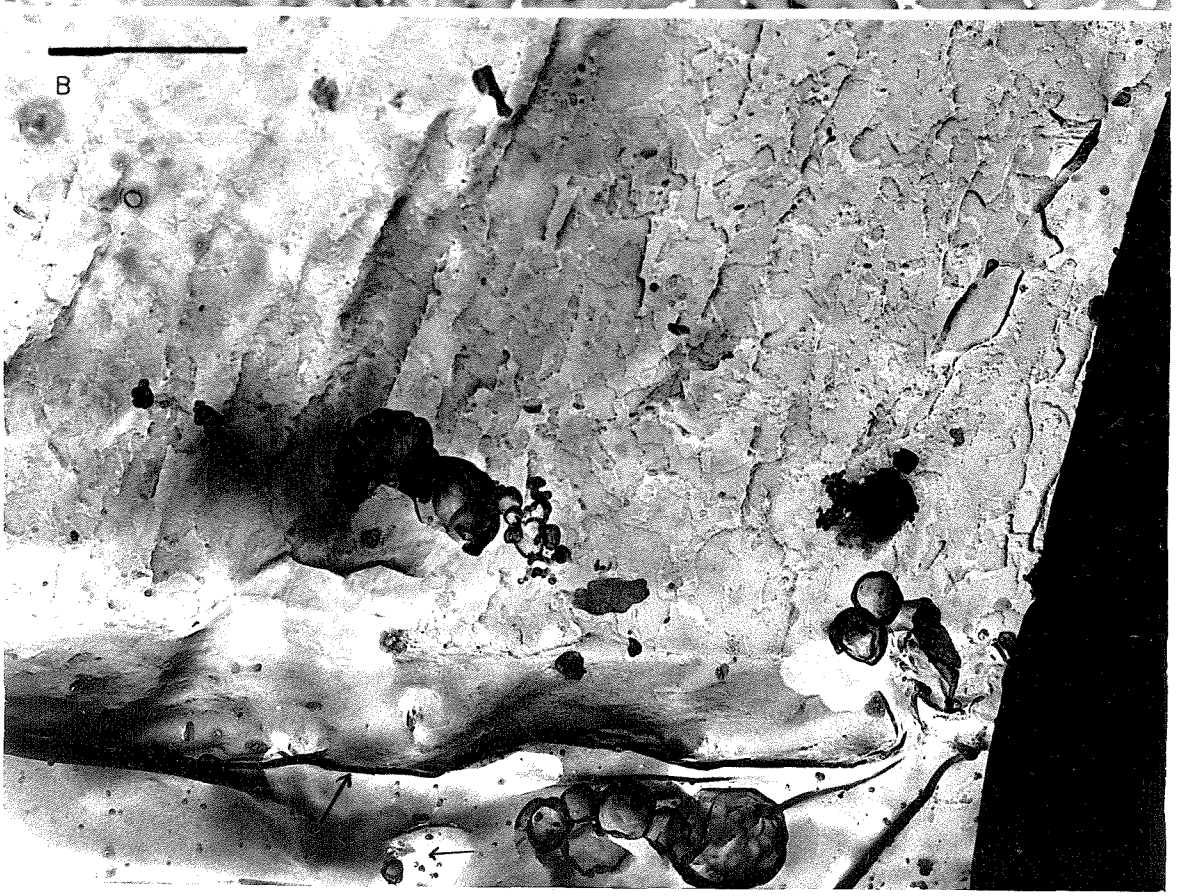
B
O

FIGURE 42. Replica of the wall of a helium frozen spph. The cuticle has lifted off the wall on the right.

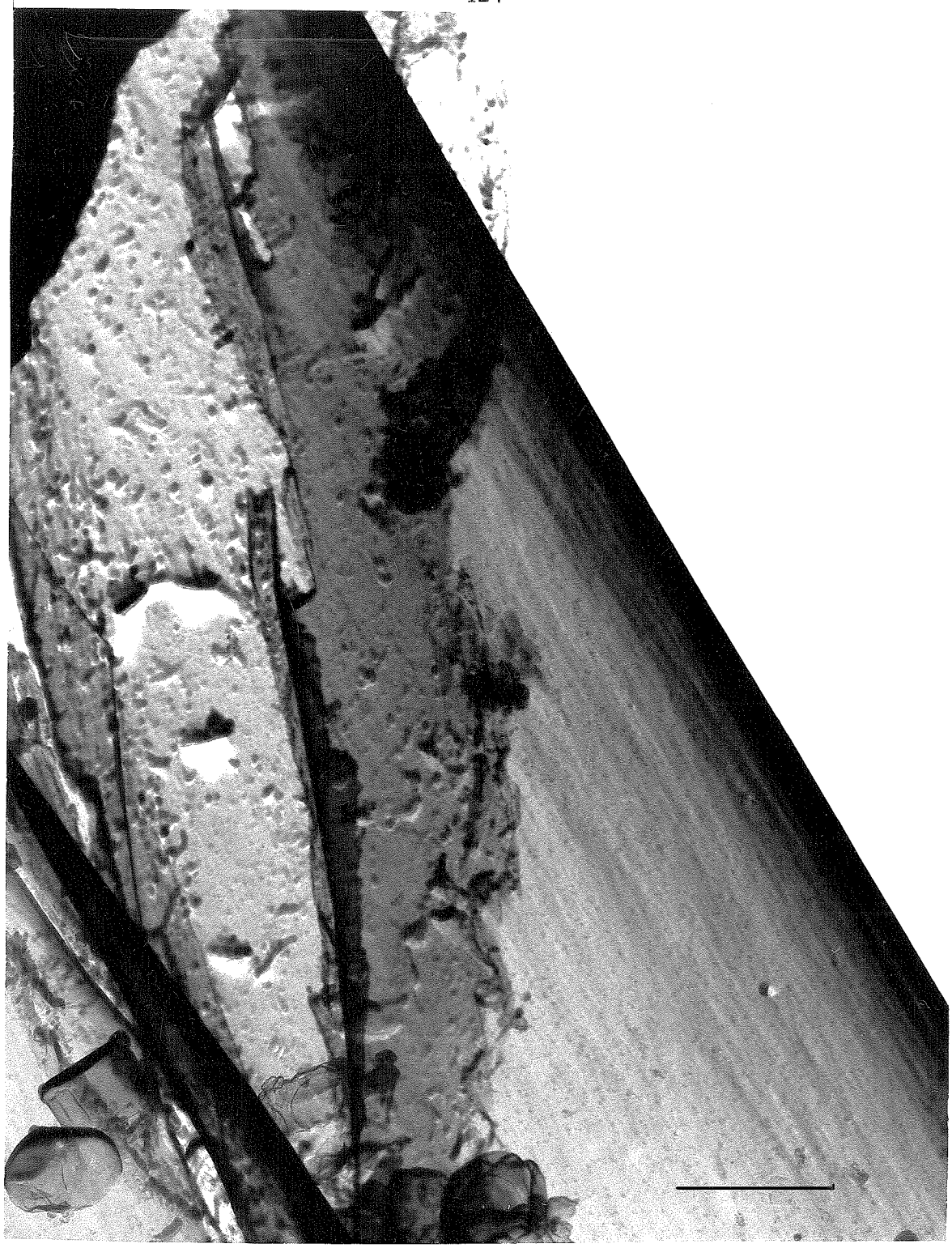

FIGURE 43. A comparison of freeze-substituted and freeze-etched micrographs: a) stage IV spph frozen in liquid He II at 1.2 K and substituted in acetone; b) stage IV spph frozen in liquid nitrogen and freeze-fracture replicated.

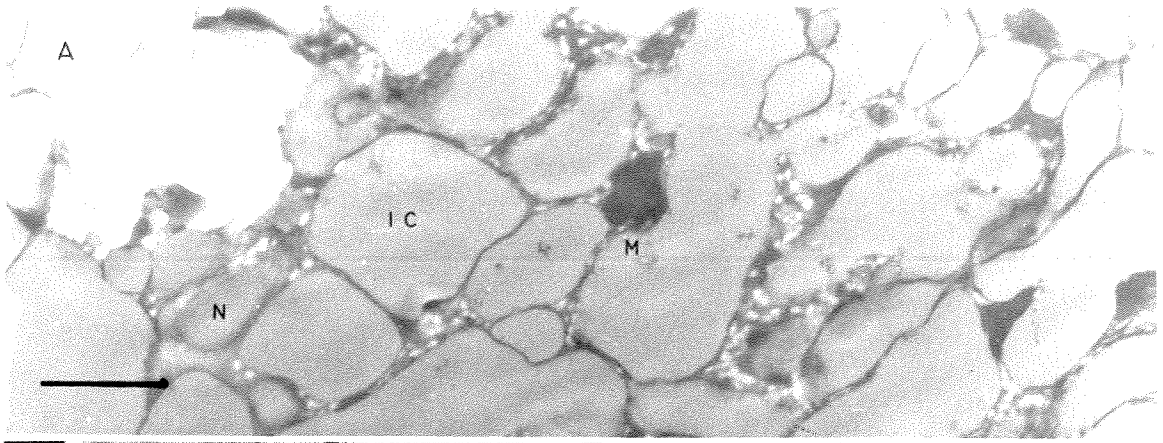
A
IC
M
N

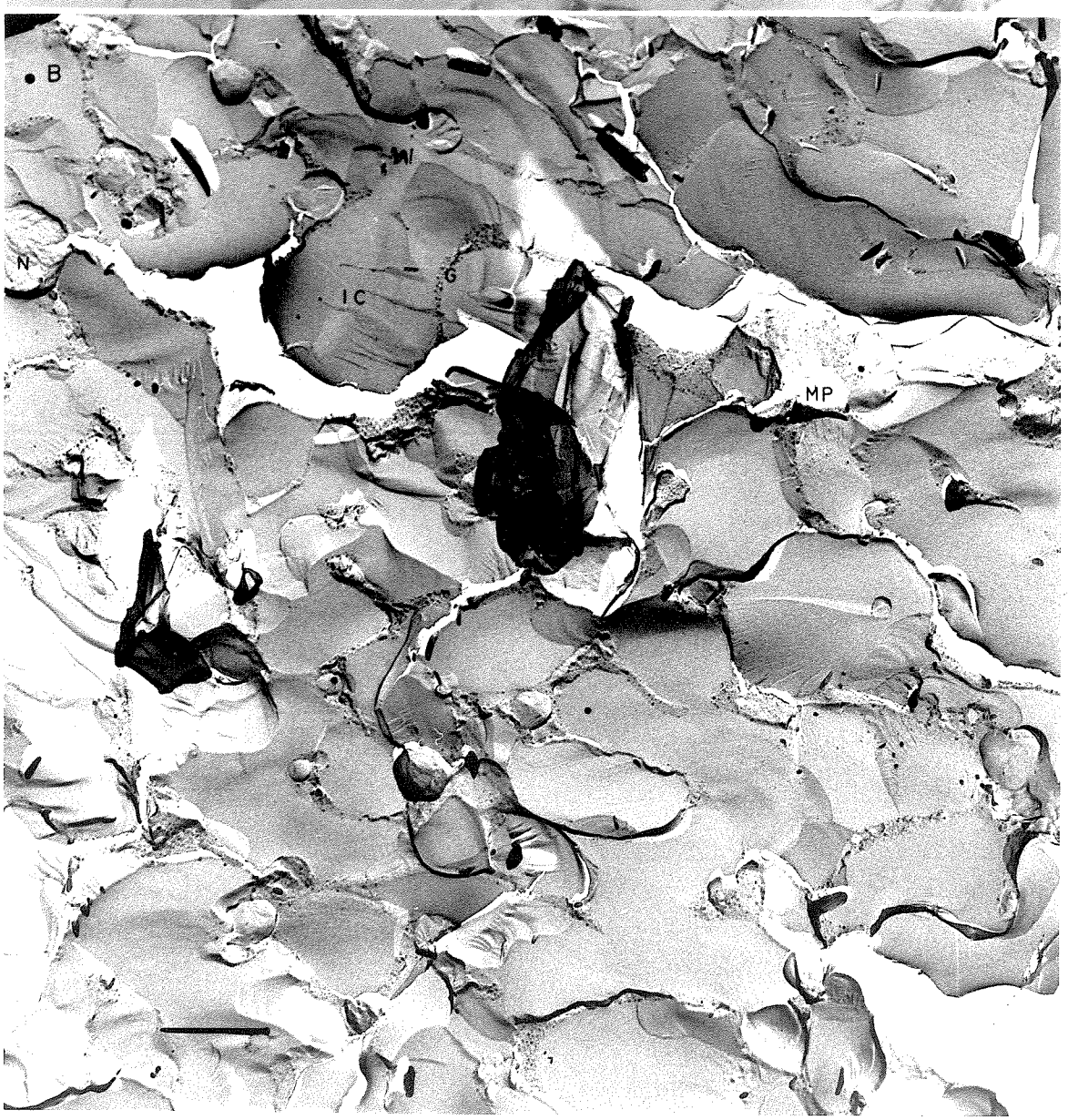
B
M
N
G
IC
MP

FIGURE 44. Organelles within a stage IV spph as shown by freeze-etching. Glycogen particles are easily seen in the cytoplasmic inclusions. Note the membrane surfaces on the various particles.

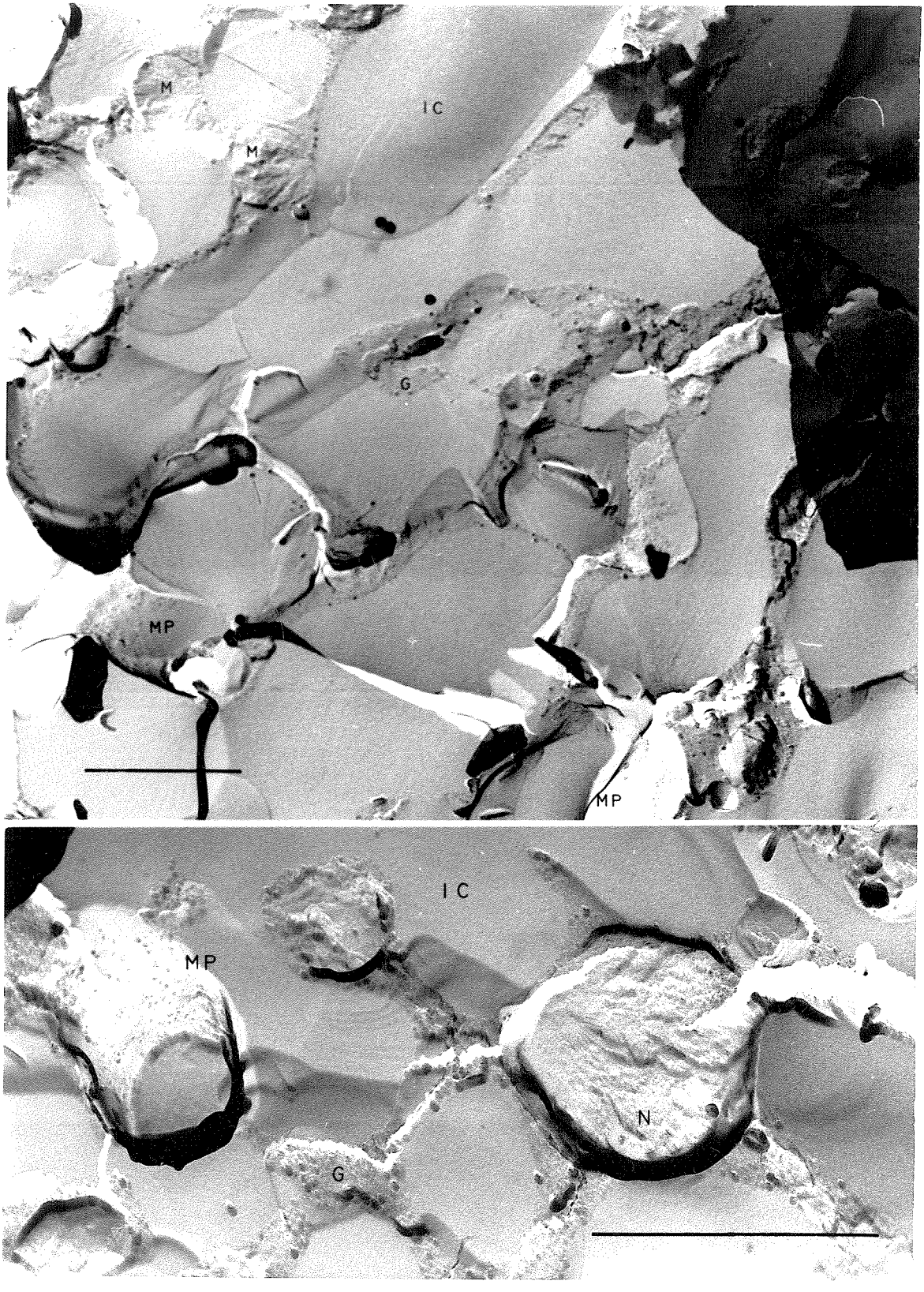
M
M
IC
G
MP
MP
IC
MP
N
G

FIGURE 45. Lipid droplets and a mitochondrion as shown by freeze-etching. Two layers of the mitochondrial membrane are visible.


MP
M
IC
L
L

Chapter 4

CONCLUDING REMARKS

A review of the results.

The helium experiments showed that spph cooling in the gas can be avoided by using the heated tube, and that the critical heat flux at which boiling occurs in the liquid can be manipulated by changing the liquid temperature and pressure (overpressure). Optimal freezing should occur with a pressure of 40 Torr (or more) and a liquid temperature of about 2 K. At these pressures the gas that the spph falls through before reaching the liquid must be heated to avoid cooling the spph below 0 C.

In general, the results obtained to date are not satisfactory. Almost every preparation had ice crystals which differ in the various preparations in their size and spatial distribution.

Very few freeze-etch replicas have been recovered from the cleaning procedure and the majority of those recovered have been replicas of the cuticle or cell wall. Thus little has been learned from them about the cell's interior. Several replicas of spphs frozen in liquid nitrogen show the possibilities of freeze-etching of spphs if proper freezing and good recovery could be obtained.

Freeze-substitution has yielded good micrographs of the cell wall but not of much else. Ice crystal damage in the stage IV spphs

is extensive and leaves large "holes" and dehydrated organelles. Preservation of the stage I spphs is much better, even with less favorable freezing conditions (1.2 K He II), presumably because the central vacuole is much smaller in these spphs.

Discussion of the helium experiments.

The properties of the critical heat flux at which boiling occurs around stationary wire heaters may be explained, at least qualitatively, by the linear form of the Landau equations for He II plus the empirical Gorter-Mellink mutual friction terms which are added to account for the frictional forces within the liquid. Figure 7 at the end of chapter 1 shows the theoretical dependence of this critical heat flux on temperature, depth of the heater in the bath, and gas pressure above the liquid. The "depth effect" is most pronounced in the neighborhood of 1.9 - 2.0 K, and the critical heat flux increases as the heater wire diameter decreases. All these effects have been observed experimentally (Frederking and Haben, 1968).

Liquid He II may be pressurized with He^4 gas without immediately destroying the quantum fluid. In fact, most of the liquid remains in the form of non-equilibrium He II for several minutes. This state of affairs is brought about by the logarithmic singularity in the specific heat of liquid He^4 at the λ - point and by the

relatively poor thermal conductivity of the He I phase. Thus as heat is supplied to the liquid by the gas above it, the liquid warms to about 2 K. A thin layer of liquid at the surface warms to T_λ (2.172 K) and immediately changes phase. This insulating layer then limits the rate at which heat reaches the remaining He II and slows the propagation of the phase change He II → He I down into the bulk liquid. This slow phase change makes it possible to increase the gas pressure and thus the critical heat transfer rate when freezing spphs.

Pictures of the boiling of He II around a heater wire during large heat flux transients show that the nature of the boiling, once the critical heat transfer rate is exceeded, is changed by increasing the gas pressure. As the pressure is increased the thickness of the boiling film decreases since its size is determined by the critical heat flux to the liquid, and the film becomes a fine haze (presumably) of small bubbles and turbulent liquid.

Discussion of the freezing experiments.

The source of the ice crystals which plague these experiments may be sought either in the initial freezing, or in the warming for substitution or replication, or in the substitution or replication processes themselves.

Crystal formation during freezing.

During the initial freezing high temperature gradients exist within the spph. If the surface can be held at 2 K, there is a temperature gradient of 300 K in .0025 cm (1.2×10^5 K/cm). Since the center of the spph cools much more slowly than the outer cytoplasm, some crystallization may occur in the vacuole. If the latent heat of this crystallization can be conducted out to the surface of the spph and transferred to the coolant as rapidly as it is generated, the spph will continue to cool until it reaches the glass temperature of the remaining liquid and crystallization ceases. If not, the entire spph will warm and crystallization will go to completion (Stephenson, 1956).

In the latter case, ice crystals will be approximately uniform in size and their size will be determined, in part, by the cytoplasm which occupies the interstitial spaces between ice crystals. This cytoplasm forms a barrier to further crystal growth. Such a situation might account for the uniform crystals within the cytoplasm of stage IV spphs frozen in liquid He II at 1.2 K and for the slightly larger, uniform crystals within the vacuole of such spphs.

In the former case of rapid or extremely rapid cooling, ice crystals still occur on freezing but their size will be determined by the temperature gradient within the spph (because the crystal

growth rate is proportional to the temperature) and by the time required to reach the temperature at which crystal growth ceases. This time depends on the cooling rate and increases as one approaches the center of the cell. Such a situation might account for the graduated ice crystal sizes observed in stage IV spphs frozen in overpressured liquid He II at 2 K.

Crystal formation during warming and during substitution.

During warming for substitution or replication temperature gradients again exist within the cell and if the temperature is high enough recrystallization may occur. Glasses of pure water recrystallize rapidly and completely near 140 K. Meryman (1957) has observed migratory recrystallization (crystal growth) of pure water to occur within minutes at 177 K (-96 C). Since spphs are warmed to higher temperatures for substitution, recrystallization may be expected to occur. Even though the crystal growth rate may be uniform throughout the cell, graduated ice crystal sizes are again expected because crystal growth will cease as the substitution fluid reaches the crystal and begins to dissolve it.

Crystal formation during freeze-etching and freeze-fracture.

While recrystallization may occur during freeze-etching which requires warming the specimen to about 170 K to sublime away ice,

recrystallization is not expected to occur during freeze-fracture replication because the temperature may be held to 140 K or lower. Thus freeze-fracture would constitute a critical test for the source of the ice crystals. Unfortunately, no clean replicas of well frozen (overpressured He II at 2 K with a heat shield in the gas above the liquid) spphs exist.

Sources of the ice crystals.

Tentatively, the sources of the ice crystals are assigned as follows: Poor freezing of stage IV spphs in liquid He II at 1.2 K is attributed to initial poor freezing in the liquid. The heat transfer properties of the liquid at this temperature are not favorable and it was not our original intention to use this particular temperature. Poor freezing of stage IV spphs in overpressured He II is attributed to the large latent heat of crystallization in the vacuole which distorts the temperature gradient within the cytoplasm and prevents the formation of a thin layer (1 to 10 μ) of well frozen cytoplasm near the cell wall. The relatively small ice crystals in the stage I spph frozen in liquid He II at 1.2 K is attributed to the poor choice of freezing conditions. It may be possible to obtain good fixation of stage I spphs if they are frozen in overpressured He II using the heat shield. The conclusions await substantiation by freeze-fracture experiments

or by freeze-substitution experiments with other tissues. Undoubtedly, spphs are very difficult to freeze well. Very few tissues have frozen well without some form of ice crystal inhibitor. Success seems to depend on relationships between cell water and proteins which are not yet understood. Within tissues that can be frozen well without protective agents there are frequently cells which have frozen well next to cells that have not.

Suggestions.

If any further work is done on the problem of freezing spphs in liquid He II, the freezing should be done with the overpressured liquid as described in chapter 3 using the spph heat shield, and the spphs should be young stage I's which are not highly vacuolated. Emphasis should be on obtaining freeze-fracture replicas, since these might pin-point the question of recrystallization. Freeze-substitution should also be tried as these experiments yield considerably more information per spph frozen. (You may make only 2 or 3 replicas from a frozen spph but a nearly infinite number of serial sections.)

I tend to think that the ice crystals in the spphs formed during freezing and that recrystallization has not been our problem. Quite possibly the Phycomyces spph is inherently unfreezeable without ice crystal formation. Other biological materials (bacteria, spores,

etc.) may give more rewarding results with the procedures worked out here.

Appendix

FREEZE-SUBSTITUTION OF A COCKROACH GANGLION FROZEN IN LIQUID HELIUM II

As a test of the freezing in overpressured liquid helium II, a set of cockroach ganglia were frozen and then substituted with 2% OsO_4 in acetone at -85 C for two days. These ganglia have been prepared previously by freeze-substitution and are known to substitute well (Dafny and van Harreveld). The experiment was carried out with the help of Drs. Nachum Dafny and Anthonie van Harreveld.

The cockroach has six small (about .2 mm diameter) abdominal ganglia connected by double commissures (connectives) both sheathed in a neural lamella. The array is about .5 cm long. The ganglia were dissected out of the cockroach and tied to a thin glass rod (.3mm diameter, 1 cm long). An iron filing had been epoxyed to this rod so that the ganglia could be suspended from the electromagnet inside the demountable chamber above the helium cryostat. The filing was carefully dried before suspending it from the electromagnet, but the ganglia and rod were bathed in Ringer's solution until then. This procedure should minimize the drying of the tissue that occurs during pump down of the demountable chamber and during the free fall of the ganglia into the liquid helium. The ganglia were frozen and substituted in the same manner as were the spphs described in chapter 3. After substitution

the individual ganglia were removed from the glass rod and embedded in Spurr's Epon. Two ganglia with some connective tissue were sectioned and studied with the electron microscope. The first was full of ice crystals. The second contained ice crystals, but a thin region 1.5 to 2 microns thick at the surface of the tissue was well preserved. Figure 46 shows a portion of the connective tissue associated with the second ganglion.

FIGURE 46. Cross section through a connective of a cockroach abdominal ganglion showing nerve fibers in the undamaged portion of the tissue. Spaces left by ice crystals appear on the left.

BIBLIOGRAPHY

1. Anderson, T. F. (1951). Techniques for the preservation of three-dimensional structure in preparing specimens for the electron microscope. Trans. N. Y. Acad. Sci. (2) 13, 130.

2. _____ (1956). Electron microscopy of microorganisms, p. 178. In G. Oster and A. W. Pollister (eds.), Physical Techniques in Biological Research, Vol. 3, Academic Press, New York.

3. Bergman, K., P. V. Burke, E. Cerda-Olmedo, C. N. David, M. Delbrück, K. Foster, E. W. Goodell, M. Heisenberg, G. Meissner, M. Zalokar, D. S. Dennison, and W. Shropshire, Jr. (1969). Phycomyces. Bacteriol. Rev. 33, 99.

4. Branton, D. (1966). Fracture faces of frozen membranes. Proc. Natl. Acad. Sci. U. S. 55, 1048.

5. Branton, D., and R. B. Park (1967). Subunits in chloroplast lamellae, J. Ultrastruct. Res. 19, 283.

6. Broadwell, J. E., and H. W. Liepmann (1969). Local boiling and cavitation in heat-induced counterflow of He II. Phys. Fluids 12, 1533.

7. Bullivant, S. (1960). The staining of thin sections of mouse pancreas prepared by the Fernandez-Moran helium II freeze-substitution method. J. Biophys. and Biochem. Cytol. 8, 639.

8. Bullivant, S. (1962). Consideration of membranes and associated structures after cryofixation. In S. S. Breese Jr. (ed.), Electron Microscopy, Vol. 2, abstract R-2, Academic Press, New York.

9. _____ (1965). Freeze substitution and supporting techniques. Laboratory Invest. 14 (No. 6, Pt. 2), 1178.

10. Bullivant, S., and A. Ames, 3rd (1966). A simple freeze-fracture replication method for electron microscopy. J. Cell. Biol. 29, 435.

11. Castle, E. S. (1942). Spiral growth and the reversal of spiraling in Phycomyces, and their bearing on primary wall structure. Am. J. Botany 29, 664.

12. Coulter, D. M., A. C. Leonard, and J. G. Pike (1968). Heat transportvisualization in helium II using focused shadow-graph and schlieren techniques. In K. D. Timmerhaus (ed.), Advances in Cryogenic Engineering 13, 640.

13. David, C. N. (1968). Ferritin in the fungus Phycomyces. Ph.D. Thesis, California Institute of Technology.

14. Dennison, D. S. (1959). Gallic acid in Phycomyces sporangiophores. Nature 184, 2036.

15. Fernandez-Moran, H. (1950). Electron microscope observations on the structure of the myelinated nerve fiber sheath. Exptl. Cell Res. 1, 143.

16. _____ (1957). Electron microscopy of nervous tissue, p. 1. In D. Richter (ed.), Metabolism of the Nervous System, Pergamon Press, New York.

17. _____(1959). Cryofixation and supplementary low-temperature preparation techniques applied to the study of tissue ultrastructure. J. Appl. Phys. 30, 2038.

18. _____ (1960). Low-temperature preparation techniques for electron microscopy of biological specimens based on rapid freezing with liquid helium II. Ann. N. Y. Acad. Sci. 85, 689.

19. Fletcher, L. S., D. G. Briggs, and R. H. Page (1970). A review of heat transfer in separated and reattached flows. Am. Inst. Aeronautics and Astronautics paper to be published.

20. Fluck, D. J., A. F. Henson, and D. Chapman (1969). The structure of dilute lecithin-water systems revealed by freeze-etching and electron microscopy. J. Ultrastruct. Res. 29, 416.

21. Frederking, T. H. K. (1968). Thermal transport phenomena at liquid helium II temperatures. Chem. Eng. Progress Symposium Series #87, 64, 21.

22. Frederking, T. H. K., R. C. Chapman, and S. Wang (1965). Heat transport and fluid motion during cooldown of single bodies to low temperatures. In K. D. Timmerhaus (ed.), Advances in Cryogenic Engineering 10, 353.

23. Frederking, T. H. K., and R. L. Haben (1968). Maximum low temperature dissipation rates of single horizontal cylinders in liquid helium II. Cryogenics 8, 32.

24. Frey-Wyssling, A., and K. Mühlethaler (1950). Der submikroskopishe Feinbau von Chitinzellwanden, Vierteljahrsschr. Naturforsch. Ges. Zurich 95, 45.

25. Glauert, M. B., and M. J. Lighthill (1955). The axisymmetric boundary layer on a long thin cylinder. Proc. Roy. Soc. London A230, 188.

26. Haggis, G. M. (1961). Electron microscope replicas from the surface of a fracture through frozen cells. J. Biophysic. and Biochem. Cytol. 9, 841.

27. Hall, C. E. (1950). A low temperature replica method for electron microscopy. J. Appl. Physics 21, 61.

28. Hawker, L. E. (1965). Fine structure of fungi as revealed by electron microscopy. Biol. Reviews (Camb.) 40, 52.

29. Kreger, D. R. (1954). Observations on cell wall of yeasts and some other fungi by x-ray diffraction and solubility tests. Biochim. Biophys. Acta 13, 1.

30. Landau, L. (1941). The theory of superfluidity of helium II. J. Phys. USSR 5, 71. Reprinted in I. M. Khalatinkov, Introduction to the Theory of Superfluidity, Benjamin, New York (1965).

31. Lemieux, G. P., and A. C. Leonard (1968). Maximum and minimum heat flux in helium II for a 76.2 μ diameter horizontal wire at depths of immersion up to 70 centimeters. In K. D. Timmerhaus (ed.), Advances in Cryogenic Engineering 13, 624.

32. Liepmann, H. W. (1958). A simple derivation of Lighthill's heat transfer formula. J. Fluid Mech. 3, 357.

33. Marot, I., and W. Stoeckenius (1970). A comparison of two freeze-fracturing techniques (Abstr.). J. Ultrastruct. Res. 30, 241.

34. McAlear, J. H., and G. O. Kreutziger (1967). Freeze etching with radiant energy in a simple cold block device. Proc. Electron Microscope Soc. Meeting 25, 116.

35. McLean, J. D. (1960). Fixation of plat tissue. 4th Intern. Conf. Electron Microscopy, Berlin, 1958, 2, 27.

36. Menz, L. J., and B. Luyet (1961). An electron microscope study of the distribution of ice in single muscle fibers frozen rapidly. Biodynamica 8, 261.

37. Meryman, H. T. (1957). Physical limitations of the rapid freezing method. Proc. Roy. Soc. London B 147, 452.

38. Moor, H., and K. Muhlethaler (1963). Fine structure in frozen-etched yeast cells. J. Cell Biol. 17, 609.

39. Moor, H., K. Muhlethaler, M. Waldner, and A. Frey-Wyssling (1961). A new freezing-ultramicrotome. J. Biophys. and Biochem. Cytol. 10, 1.

40. Moore, R. T., and J. H. McAlear (1961). Fine structure of Mycota. 5 Lomasomes - previously uncharacterized hyphal structures. Mycologia 53, 194.

41. Northcote, D. H., and D. R. Lewis (1968). Freeze-etched surfaces of membranes and organelles in the cells of pea root tips. J. Cell Sci. 3, 199.

42. Pease, D. C. (1967). The preservation of tissue fine structure during rapid freezing. J. Ultrastruct. Res. 21, 98.

43. Peat, A., and G. H. Banbury (1967). Ultrastructure, protoplasmic streaming, growth and tropisms of Phycomyces sporangiophores. I. General introduction. II. The ultrastructure of the growing zone. New Phytologist 66, 475.

44. Pryde, J. A., and G. O. Jones (1952). Properties of vitreous water. Nature 170, 685.

45. Rayfield, G. W., and F. Reif (1963). Evidence for the creation and motion of quantized vortex rings in superfluid helium. Phys. Rev. Letters 11, 305.

46. Rayfield, G. S., and F. Reif (1964). Quantized vortex rings in superfluid helium. Phys. Rev. 136, A 1194.

47. Rebhun, L. I. (1965). Freeze-substitution: fine structure as a function of water concentration in cells. Federation Proc. 24 (Suppl. 15), S-217.

48. Reynolds, E. S. (1963). The use of lead citrate at high pH as an electron-opaque stain in electron microscopy. J. Cell Biol. 17, 208.

49. Rinderer, L., and F. Haenseler (1960). In M. Jul and A. M. Jul (eds.), Progress in Refrigeration Science Technology, Vol. 1, 243, Proc. of the 10th Internat. Cong. of Refrigeration, Pergamon Press, New York.

50. Roelofsen, P. A. (1951). Cell wall structure in the growth-zone of Phycomyces sporangiophores. II. Double refraction and electron microscopy. Biochim. Biophys. Acta 6, 357.

51. Seban, R. A., and G. L. Caldwell (1968). The effect of a spherical protuberance on local heat transfer to a turbulent boundary layer. Trans. A. S. M. E., J. Heat Transfer 90, 408.

52. Shepley, L. C., and A. B. Bestul (1963). Deuterium isotope effect on glass transformation temperatures of aqueous inorganic solutions. J. Chem. Phys. 39, 680.

53. Sjøstrand, F. S. (1967). Electron Microscopy of Cells and Tissues, Vol. L, Instrumentation and Techniques. Academic Press, New York.

54. Sjøstrand, F. S., and R. F. Baker (1958). Fixation by freeze-drying for electron microscopy of tissue cells. J. Ultrastruct. Res. 1, 239.

55. Staehelin, L. A. (1968). The interpretation of freeze-etched artifical and biological membranes. J. Ultrastruc. Res. 22, 326.

56. Staronka, L. (1939). Formation of an amorphous (vitreous) modification of water by condensation of vapor at low temperature. Roczn. Chem. 19, 201.

57. Steere, R. L. (1957). Electron microscopy of structural detail in frozen biological specimens. J. Biophys. and Biochem. Cytol. 3, 46.

58. _____ (1969a). Freeze-etching simplified. Cryobiology 5, 306.

59. _____ (1969b). Freeze-etching and direct observation of freezing damage. Cryobiology 6, 137.

60. Stephenson, J. L. (1956). Ice crystal growth during the rapid freezing of tissues. J. Biophysic. and Biochem. Cytol. 2 (Suppl. 2), 45.

61. Tanford, C. (1961). Physical Chemistry of Macromolecules, p. 327, Wiley, New York.

62. Thornton, R. M. (1966). A comparative study of phototropism in Phycomyces and Avena. Ph.D. Thesis, Harvard University.

63. _____ (1968). The fine structure of Phycomyces. I. Autophagic vesicles. J. Ultrastruct. Res. 21, 269.

64. van Harreveld, A., and J. Crowell (1964). Electron microscopy after rapid freezing on a metal surface and substitution fixation. Anat. Rec. 149, 381.

65. Watson, M. L. (1958). Staining of tissue sections for electron microscopy with heavy metals. J. Biophysic. and Biochem. Cytol. 4, 475.

66. Winkel, P., A. Broese van Groenou, and C. J. Gorter (1955). On the heat conduction in liquid helium II. Physica 21, 345.

67. Wolken, J. J. (1969). Microspectrophotometry and the photoreceptor of Phycomyces I. J. Cell Biol. 43, 354.

68. Zalokar, M. (1966). A simple freeze-substitution method for electron microscopy. J. Ultrastruct. Res. 15, 469.

69. _____ (1969). Intracellular centrifugal separation of organelles in Phycomyces. J. Cell Biol. 41, 494.